

---

Electronic Thesis and Dissertation Repository

---

8-15-2018 10:00 AM

## Behavioural and Anatomical Effects of Unilateral Injection of Botulinum Neurotoxin A in the Entopeduncular Nucleus of a Parkinsonian Rat Model

Adrianna Tsang  
*The University of Western Ontario*

Supervisor  
Jog, Mandar S.  
*The University of Western Ontario* Co-Supervisor  
Rajakumar, Nagalingam  
*The University of Western Ontario*

Graduate Program in Physiology and Pharmacology  
A thesis submitted in partial fulfillment of the requirements for the degree in Master of Science  
© Adrianna Tsang 2018

Follow this and additional works at: <https://ir.lib.uwo.ca/etd>



Part of the [Behavioral Neurobiology Commons](#)

---

### Recommended Citation

Tsang, Adrianna, "Behavioural and Anatomical Effects of Unilateral Injection of Botulinum Neurotoxin A in the Entopeduncular Nucleus of a Parkinsonian Rat Model" (2018). *Electronic Thesis and Dissertation Repository*. 5531.

<https://ir.lib.uwo.ca/etd/5531>

This Dissertation/Thesis is brought to you for free and open access by Scholarship@Western. It has been accepted for inclusion in Electronic Thesis and Dissertation Repository by an authorized administrator of Scholarship@Western. For more information, please contact [wlsadmin@uwo.ca](mailto:wlsadmin@uwo.ca).

## Abstract

Loss of dopamine in Parkinson's disease is associated with glutamatergic hyperactivity of the subthalamic nucleus. Pharmacological and electrical therapies aimed to suppress this overactivity favourably alleviate parkinsonian motor symptoms. No study has explored the potential of botulinum neurotoxin A in the central nervous system beyond cholinergic blockage despite evidence of its ability to inhibit glutamate release. Thus, the present study investigated the effect of selective suppression of hyperactive glutamatergic input from the subthalamic nucleus to the entopeduncular nucleus by botulinum neurotoxin A in a parkinsonian model. Unilateral 6-hydroxydopamine lesioned rodents received microinfusions of botulinum neurotoxin A or vehicle into the ipsilateral entopeduncular nucleus, and their mobility was assessed using the CatWalk apparatus. Administration of a single dose of botulinum neurotoxin A (0.5 ng) significantly improved the rotational asymmetry and dynamic gait abnormalities, suggesting a potential use of intracerebral botulinum neurotoxin A to produce effective neuromodulation in the parkinsonian brain.

## Keywords

Parkinson's disease, botulinum neurotoxin A, 6-hydroxydopamine, entopeduncular nucleus, subthalamic nucleus, gait, CatWalk

## Abbreviations

6-OHDA	6 hydroxydopamine
BG	basal ganglia
BoNT	botulinum neurotoxin
BSA	bovine serum albumin
ChAT	choline acetyltransferase
CPu	caudate putamen
DBS	deep brain stimulation
EPN	entopeduncular nucleus
GABA	$\gamma$ -amino-butyric acid
GAD67	glutamate decarboxylase 67 kDa
GFAP	glial fibrillary acidic protein
GPe	external globus pallidus
GPi	internal globus pallidus
Hc	carboxy-terminal of the heavy chain
H <sub>N</sub>	amino-terminal of the heavy chain
IP	intraperitoneal
L chain	light chain
L-DOPA	L-3,4-dihydroxyphenylalanine
LF	left front
LH	left hind
LRRK2	leucine-rich repeat kinase 2
MFB	medial forebrain bundle
MLR	mesencephalic locomotor region
MPTP	1-methyl-4-phenyl-1,2,3,6-tetrahydropyridine
MSN	medium spiny neuron
PB	phosphate buffer
PBS	phosphate buffered saline
PD	Parkinson's disease
PPN	pedunculopontine nucleus
RF	right front

RH	right hind
ROS	reactive oxidative species
SC	subcutaneous
SNAP-25	synaptosomal-associated protein 25
SNARE	soluble <i>N</i> -ethylmaleimide-sensitive factor attachment protein
SNpc	substantia nigra pars compacta
SNpr	substantia nigra pars reticulata
STN	subthalamic nucleus
SV2	synaptic vesicle protein 2
TH	tyrosine hydroxylase
vGluT2	vesicular glutamate transporter 2

## Acknowledgements

First and foremost, I would like to express my profound gratitude to my supervisors, Dr. Mandar Jog and Dr. Nagalingam Rajakumar. Guided by your unrivaled dedication and passion for science, thank you, Dr. Jog, for the opportunity to think innovatively and for the motivation to drive science forward. Likewise, thank you, Dr. Rajakumar, for your unparalleled extensive knowledge in every field of science, along with your unwavering patience and sympathetic guidance.

In addition to my mentors, I would like to extend my appreciation to my advisory committee: Dr. Rommel Tirona, Dr. Brian Allman and Dr. Walter Rushlow. Thank you for your time, effort and invaluable scientific insight.

My heartfelt thanks also goes to all my fellow labmates at the Movement Disorders Centre for their continued encouragement and stimulating discussions. I will cherish all the countless memories and laughter we shared over the last few years.

Last but not least, I would like to offer my sincerest thanks to my family and friends. To my mom and dad, your fortitude and sacrifices will remain my inspiration throughout my life. To my siblings, I am privileged to be surrounded by such remarkable and supportive role models. And to my best friend, you rock, never change. This thesis stands as a testament to all the unconditional love and encouragement.

Thank you.

# Table of Contents

Abstract .....	i
Keywords .....	i
Abbreviations .....	ii
Acknowledgements .....	iv
Table of Contents .....	v
List of Tables .....	ix
List of Figures .....	x
List of Appendices .....	xii
Chapter 1 .....	1
1 Introduction .....	1
1.1 Parkinson's Disease .....	1
1.1.1 Overview .....	1
1.1.2 Pathology .....	2
1.1.3 Aetiology .....	3
1.1.4 Symptoms .....	3
1.1.5 Treatment .....	5
1.2 Neural Circuitry Involved in Parkinson's Disease .....	6
1.2.1 Overview of Basal Ganglia Circuitry .....	6
1.2.2 Changes in Basal Ganglia Circuitry in Parkinson's Disease .....	9
1.3 Animal Models of Parkinson's Disease .....	11
1.3.1 Common Animal Models .....	11
1.3.2 Overview of 6-OHDA .....	13
1.3.3 6-OHDA Lesion of the MFB .....	14
1.4 Gait Dysfunction in Parkinson's Disease .....	17

1.4.1	Overview.....	17
1.4.2	Gait Assessment Tools for Animal Models.....	19
1.4.3	Gait Changes in the 6-OHDA Model of Parkinson’s Disease.....	20
1.5	Botulinum Neurotoxins.....	21
1.5.1	Overview and Mechanism.....	21
1.5.2	BoNT-A Effects in Non-Cholinergic Systems.....	22
1.5.3	Use of BoNT-A for Parkinson’s Disease.....	24
1.6	Rationale.....	25
1.6.1	Overview.....	25
1.6.2	Hypothesis.....	27
1.6.3	Objectives.....	27
1.6.4	Predictions.....	27
Chapter 2	.....	29
2	Materials and Methods.....	29
2.1	Experimental Animals.....	29
2.2	6-OHDA Lesioning of the MFB.....	31
2.3	BoNT-A Injection at the EPN.....	31
2.4	Behavioural Tests.....	32
2.4.1	Apomorphine-Induced Rotation Test.....	32
2.4.2	CatWalk Studies.....	32
2.5	Perfusion and Tissue Collection.....	33
2.6	Immunohistochemistry.....	33
2.6.1	Immunofluorescence Staining.....	33
2.6.2	TH Staining.....	34
2.6.3	Microscopy.....	35
2.7	Statistical Analysis.....	36

Chapter 3.....	37
3 Results.....	37
3.1 Results of the Apomorphine Rotation Test.....	37
3.2 Results of the CatWalk Apparatus.....	40
3.2.1 Changes in Average Speed.....	40
3.2.2 Changes in Body Speed Variation.....	42
3.2.3 Changes in Cadence.....	44
3.2.4 Changes in Stand.....	46
3.2.5 Changes in Swing.....	48
3.2.6 Changes in Step Cycle.....	50
3.2.7 Changes in Duty Cycle.....	52
3.2.8 Changes in Single Stance.....	54
3.2.9 Changes in Initial Dual Stance.....	56
3.2.10 Changes in Terminal Dual Stance.....	58
3.2.11 Changes in Swing Speed.....	60
3.2.12 Changes in Stride Length.....	62
3.2.13 Changes in Max Contact Area.....	64
3.2.14 Changes in Mean Intensity.....	66
3.2.15 Changes in Walking Pattern.....	68
3.2.16 Summary of CatWalk Results.....	69
3.3 Results of Immunohistochemical Staining.....	70
3.3.1 Verification of 6-OHDA Lesion.....	70
3.3.2 BoNT-A Selectively Targets Glutamatergic Terminals.....	71
3.3.3 Effects of BoNT-A Injection are Non-Permanent.....	73
3.3.4 BoNT-A Infusion Elicits a Small Immune Response.....	75



Chapter 4.....	77
4 Discussion .....	77
4.1 Safety of Central BoNT-A Injection.....	77
4.2 Selectivity of Central BoNT-A Injection.....	78
4.3 Changes in Basal Ganglia Circuitry Following BoNT-A: Rotational Behaviour..	80
4.4 Changes in Basal Ganglia Circuitry Following BoNT-A: Locomotion .....	81
4.5 Effect of BoNT-A on Specific Gait Parameters .....	83
4.5.1 Changes in Gait Parameters Following 6-OHDA Lesioning.....	83
4.5.2 Dynamic Gait Parameters Affected by BoNT-A .....	84
4.5.3 Static Gait Parameters Unaffected by BoNT-A.....	85
4.5.4 BoNT-A versus Other Interventions in 6-OHDA Rodents.....	86
4.5.5 Putting It All Together: BG Involvement in Locomotion .....	88
4.6 Conclusion .....	89
4.6.1 Significance.....	89
4.6.2 Limitations .....	90
4.6.3 Future Directions .....	92
References.....	93
Appendices.....	115
Curriculum Vitae .....	117

## List of Tables

Table 1 – Definition of Gait Parameters .....	20
Table 2 – List of Primary Antibodies for Immunostaining.....	35
Table 3 – Summary of CatWalk Results.....	69

## List of Figures

Figure 1 – BG circuitry in normal and parkinsonian states .....	10
Figure 2 – Experimental timeline .....	29
Figure 3 – Experimental animal groups.....	30
Figure 4 – Apomorphine-induced rotation of hemi-PD rats treated with BoNT-A.....	39
Figure 5 – Average speed of hemi-PD rats treated with BoNT-A.....	41
Figure 6 – Body speed variation of hemi-PD rats treated with BoNT-A .....	43
Figure 7 – Cadence of hemi-PD rats treated with BoNT-A.....	45
Figure 8 – Stand of hemi-PD rats treated with BoNT-A .....	47
Figure 9 – Swing of hemi-PD rats treated with BoNT-A .....	49
Figure 10 – Step cycle of hemi-PD rats treated with BoNT-A.....	51
Figure 11 – Duty cycle of hemi-PD rats treated with BoNT-A.....	53
Figure 12 – Single stance of hemi-PD rats treated with BoNT-A .....	55
Figure 13 – Initial dual stance of hemi-PD rats treated with BoNT-A.....	57
Figure 14 – Terminal dual stance of hemi-PD rats treated with BoNT-A.....	59
Figure 15 – Swing speed of hemi-PD rats treated with BoNT-A .....	61
Figure 16 – Stride length of hemi-PD rats treated with BoNT-A.....	63
Figure 17 – Max contact area of hemi-PD rats treated with BoNT-A.....	65
Figure 18 – Mean intensity of hemi-PD rats treated with BoNT-A .....	67
Figure 19 – Walking pattern of hemi-PD rats treated with BoNT-A .....	68

Figure 20 – 6-OHDA lesioning of the MFB .....	70
Figure 21 – Immunostaining of synaptic markers at the EPN .....	72
Figure 22 – Effect of BoNT-A on synaptic markers at various timepoints .....	74
Figure 23 – GFAP expression in lesioned animals treated with BoNT-A or vehicle.....	76
Figure 24 – BG circuitry in parkinsonian states following BoNT-A injection.....	82

## List of Appendices

Appendix 1 – Animal Use Protocol Approval .....	115
Appendix 2 – Sample of Raw CatWalk Data .....	116
Appendix 3 – Stereotaxic Surgery Coordinates.....	116

# Chapter 1

## 1 Introduction

Parkinson's disease is a common neurodegenerative disorder, which is associated with a spectrum of motor and cognitive symptoms unique to each individual. Despite tremendous breakthroughs in research to understand the complexity of this disease, many key questions remain unanswered. The exact cause of Parkinson's disease is still unknown and although various treatments exist for symptomatic relief, there is currently no cure.

This chapter aims to provide a general overview of Parkinson's disease, outline the neural circuitry involved in this disorder, highlight common parkinsonian animal models used in research, and introduce the potential of botulinum neurotoxin as a novel therapeutic.

## 1.1 Parkinson's Disease

### 1.1.1 Overview

Parkinson's disease (PD) is a progressive neurodegenerative disease characterized by the loss of dopaminergic neurons in the substantia nigra pars compacta (SNpc). This complex disorder was first medically described by its prominent motor abnormalities by James Parkinson in 1817 (Parkinson, 2002). Over 50 years later, Jean-Martin Charcot further described and refined the cardinal symptoms of PD (Goetz, 2011). The chief parkinsonian motor symptoms are bradykinesia, resting tremor, rigidity, and postural instability.

Currently, PD is the second most common neurodegenerative disorder after Alzheimer's disease. It is estimated that PD affects over 7 million individuals globally and about 1% of the population over 60 years of age (De Lau et al., 2006). Furthermore, it is expected that the prevalence of PD will more than double by 2030 (Dorsey et al., 2007). In Canada, PD affects over 100 000 people and 85% of those diagnosed are over 65 years old (Parkinson Society Canada, 2003). Due to the chronic and progressive nature of the disease, patients often experience gradual complications and a reduced quality of life. This leads to an

escalating economic burden on patients, society and the healthcare system (Whetten-Goldstein, 1997). Accordingly, it is estimated that the total annual cost of PD in North America will exceed \$50 billion by 2040 (Findley, 2007). With an aging population and growing economic burden, there is an ongoing need to research the mechanisms underlying the pathogenesis of PD and to identify novel management and treatment options.

### **1.1.2 Pathology**

The main pathological hallmark of PD is the death of neuromelanin-pigmented dopaminergic neurons in the substantia nigra, with predominant loss in the lateroventral component of the pars compacta. At the onset of motor symptoms, it is estimated that there is a 68% dopaminergic loss in the lateroventral region, a 48% neuronal loss in the whole nigra and an 80% loss of axon terminals at the striatum (Fearnley & Lee, 1991; Bernheimer et al., 1973). This neuronal death is accompanied by the appearance of intraneuronal inclusions called Lewy bodies in distinct areas of the brain. Lewy bodies are abnormal proteinaceous inclusions containing aggregates of  $\alpha$ -synuclein and other neurofilamentous proteins (Spillantini et al., 1997; Baba et al., 1998). The distribution of these Lewy bodies is used to classify the degree of sporadic PD pathology (Braak, 2003; Braak, 2006). Based on Braak staging, the earliest pathological changes occur in the dorsal motor nucleus of the vagus and olfactory bulb (Stages 1 and 2). As the disease advances, pathological changes are observed in the substantia nigra, areas of the midbrain and basal forebrain (Stages 3 and 4) until finally, the neocortex is affected (Stages 5 and 6). This classification helps to elucidate the progression of PD symptoms from early olfactory dysfunction (Stages 1 and 2) to motor deficits (Stages 3 and 4) and ultimately, to cognitive impairments in advanced stages (Stages 5 and 6). The formation of Lewy bodies is one of the major proposed theories underlying neuronal death in idiopathic PD, yet the exact mechanistic cascade is unknown (Gibb & Lees, 1988). Other leading pathological factors include mitochondrial dysfunction, increased oxidative stress, disruption of autophagy, and activation of microglia (Lin & Beal, 2006; Narendra, Tanaka, Suen, & Youle, 2008; Glass, Saijo, Winner, Marchetto, & Cage, 2010).

### **1.1.3 Aetiology**

Although the cause of PD is not yet known, both genetic and environmental factors have been associated to an increased risk of disease development. While majority of cases of PD are idiopathic, approximately 5-15% of cases are associated to familial mutations in specific autosomal genes (Lesage & Brice, 2008). Amongst the many PD-related genes that have been identified, the most extensively studied genes are SNCA (codes for  $\alpha$ -synuclein) and leucine-rich repeat kinase 2 (LRRK2; codes for dardarin), which are transmitted in an autosomal-dominant inheritance pattern (Polymeropoulos et al., 1997; Simon-Sanchez et al., 2009; Lesage & Brice, 2008). While the discovery of PD-linked genes has tremendously furthered the field of PD research, the clear majority of PD cases cannot be solely attributed to genetic factors. This suggests a multifactorial aetiology, which includes an environment contribution as well.

There are numerous environmental risk factors that have been thought to contribute to the aforementioned pathological mechanisms underlying PD (Goldman, 2014). Of the many potential environmental factors, in vitro, animal and epidemiological studies most strongly support a link with exposure to pesticides and heavy metals. Implicated pesticides include rotenone, paraquat and organochlorine compounds (Cannon et al., 2009; McCormack et al., 2002; Tanner et al., 2011; Elbaz et al., 2009). Dysregulated iron homeostasis and augmented exposure to manganese are also implicated in PD aetiology (Dexter et al., 1989; Coon et al., 1989, Aschner et al., 2009). Other environmental factors, such as head injuries and pollution may also contribute to an increased risk of PD (Goldman, 2014).

Although the role of both genetic and environmental factors to development of PD is not fully understood, it is evident that their contribution is linked to the mechanistic pathways underlying PD pathogenesis.

### **1.1.4 Symptoms**

Although PD is generally thought of as a disorder of movement, it is associated with both motor and non-motor symptoms. The cardinal motor symptoms of PD are bradykinesia, resting tremor, rigidity, and postural instability (Jankovic, 2008).



Bradykinesia is characterized as the slowness of voluntary movement due to a progressive reduction in speed and amplitude of continuous activity (Berardelli, Rothwell, Thompson, & Hallett, 2001). Classically, bradykinesia is the most characteristic feature of PD and a hallmark of basal ganglia disorders. It encompasses dysfunction in all aspects of motor control, from planning to initiation to execution of movement (Cooper, Sagar, Tidswell, & Jordan, 1994). Initial indicators include slowness in performing daily tasks that require fine motor control and slower reaction times. Other manifestations present as impaired swallowing, dysarthria, hypomimia, and reduced arm swing while walking (Jankovic, 2008).

Tremor is the most common and apparent symptom of PD (Jankovic, 2008). It refers to the alternating contraction and relaxation of agonist and antagonist muscles. Characteristically, tremor occurs at a frequency between 4 to 6 Hz during rest and appears in a unilateral manner at a distal part of the limb. The occurrence of rest tremor is variable amongst PD patients with approximately 70% of patients reporting tremor at disease onset and at least 75% of patients affected by tremor at some point in disease (Hughes, Daniel, Blankson, & Lees, 1993).

Rigidity refers to an increased stiffness and resistance to limb movement due to the excessive and sustained contraction of muscles (Jankovic, 2008). It may present in a uniform or ratchet-like manner and most often occurs asymmetrically. Increased muscle tone at the neck and trunk leads to axial rigidity, which often results in postural deformities that appear more frequently at early stages of PD (Ashour & Jankovic, 2006). As the disease progresses, rigidity typically spreads distally to the face and extremities, ultimately resulting in a reduction in the ability to move.

Postural instability usually manifests at late stages of PD due to the loss of postural reflexes and impaired balance (Jankovic, 2008). This symptom along with freezing of gait contributes significantly to an increased frequency of falls (Williams, Watt, & Lees, 2006).

In addition to these four cardinal motor symptoms of PD, other motor impairments include gait abnormalities, bulbar dysfunction, and neuro-ophthalmological disturbances (Bloem, Harusdorff, Visser, & Giladi, 2004; Hunker, Abbs, & Barlow, 1982; Biousse, Skibell,

Watts, Loupe, Drews-Botsch, & Newman, 2004). Gait dysfunction in PD will be discussed in detail in Chapter 1.4.

Non-motor symptoms of PD are also common and can even present prior to the aforementioned motor symptoms (Poewe, 2008). These include autonomic dysfunction, neuropsychiatric disturbances (changes in mood, cognition and behaviour), and sensory and sleep abnormalities.

### **1.1.5 Treatment**

As there is no cure for PD, current treatment strategies focus on providing symptomatic relief by medications and/or surgery. Most interventions only treat certain symptoms of the disease but have not been shown to slow the rate of progression of PD nor have been confirmed as displaying neuroprotective, neurorescuing or neurorestorative effects (National Collaborating Centre for Chronic Conditions, 2006). Typically, medications act by either replenishing dopamine levels in the brain or mimicking the effects of dopamine. The gold standard symptomatic therapy for PD is L-3,4-dihydroxyphenylalanine (levodopa or L-DOPA), a dopamine precursor (Parkinson Study Group, 2004). After crossing the blood-brain barrier, levodopa is readily converted into dopamine by aromatic L-amino acid decarboxylase (Rahman, Toshiharu, & Takeshi, 1981). Typically, levodopa is given with a peripheral dopamine decarboxylase inhibitor to block peripheral conversion of levodopa to dopamine. At earlier stages of disease, treatment with levodopa improves many motor symptoms of PD, including bradykinesia, rigidity and tremor, but there is a decrease in effectiveness as the disease progresses (Parkinson Study Group, 2004). Additionally, long-term levodopa therapy may lead to the development of complications, such as dyskinesias and motor fluctuations (Rascol et al., 2000, Marsden & Parkes, 1977).

When complications arise that cannot be satisfactorily controlled by medical therapy, surgical interventions, such as lesioning of affected areas or deep brain stimulation (DBS) are available. Although creation of lesions at the internal globus pallidus (GPi) or subthalamic nucleus (STN) provides some benefits to patients, it includes the risk of inducing neurological deficits, particularly with bilateral procedures (Hariz, 2000).

Alternatively, DBS of these same brain targets mirrors the effect of a lesion without deliberately causing damage to the brain (Benabid, Pollak, Louveau, Henry & De Rougemont, 1987). DBS is associated to an improvement in motor scores for patients with advanced PD while reducing dyskinesia and motor fluctuations (Deep-Brain Stimulation for Parkinson's Disease Study Group, 2001). However, the mechanism of action of DBS remains elusive with many proposed mechanisms. Furthermore, other caveats of DBS include its unavailability to people with cognitive or psychiatric problems and its inconclusive effect to improve speech, balance and aspects of gait (Bronstein et al., 2011).

Although medical and surgical interventions are available for the treatment of PD, they are each associated with their own advantages and disadvantages. There is a clear unmet need for exploring novel interventions that could be applied to many patients, offer novel neuromodulatory effects with an already understood mechanism and even target multiple affected sites within the brain.

## 1.2 Neural Circuitry Involved in Parkinson's Disease

### 1.2.1 Overview of Basal Ganglia Circuitry

The proper execution of voluntary movement requires the correct integration of sensory to motor information in the brain. This is accomplished by an intricate neural network, which includes the cerebral cortex, the motor thalamus and the basal ganglia (BG) nuclei (Albin Young, & Penney, 1989; Blandini, Nappi, Tassorelli, & Martignoni, 2000; DeLong & Whichmann, 2007). Overall, the BG play a crucial role at the centre of this looped circuit by modulating afferent information from the cortex to produce an efferent signal that returns through the thalamus back to the cortex (Obeso et al., 2008). A schematic overview of the BG circuitry in a normal state is presented in Figure 1 A.

The BG are located at the base of the telencephalon and comprise of multiple interconnected nuclei: the striatum (dorsal: caudate nucleus and putamen; ventral: nucleus accumbens and olfactory tubercle), the globus pallidus (internal [GPi] and external [GPe]),

the substantia nigra (pars compacta [SNpc] and pars reticulata [SNpr]) and the subthalamic nucleus (STN) (Blandini, 2000).

Of these structures, the striatum is the main input nucleus of the BG. The clear majority (approximately 95%) of neurons in the striatum are characterized as medium spiny neurons (MSNs) that release  $\gamma$ -amino-butyric acid (GABA) as a neurotransmitter (Kemp & Powell, 1971). These MSNs receive predominately glutamatergic projections from all cortical areas and then send projections to their main targets, the SNpr, GPi and GPe (Parent & Hazrati, 1995). In the rat, it is estimated that approximately 5000 glutamatergic inputs converge onto a single striatal MSN and then, 100 MSNs project onto each pallidal neuron (Obeso et al., 2008). Thus, this arrangement is in need of a precise filtering mechanism to select incoming and outgoing signals required to perform specific movements. This filtering activity is principally facilitated by dopamine (Bamford et al., 2004; Obeso et al., 2008). Accordingly, the striatum is also innervated by dopaminergic inputs originating in the SNpc (Beckstead, Domesick, & Nauta, 1993). Striatal neurons express D1 and/or D2 receptors, with majority of D1 receptors expressed by neurons projecting to the GPi and SNpr, while D2 receptors are expressed by neurons projecting to the GPe (Gerfen et al., 1995; Yung et al., 1995). Moreover, the incoming cortical projections to MSNs that express D1 receptors are relatively distinct from those that project to MSNs expressing D2 receptors, from cortical layer III versus layer V respectively (Lei, Jiao, Del Mar, & Reiner, 2004). It is generally accepted that this functional segregation of the inputs and outputs of the striatum has formed the basis for the direct and indirect pathway model of BG functional organization (Blandini et al., 2000).

In the direct pathway, dopamine exerts an excitatory role on striatal GABAergic neurons, which express dynorphin, substance P and D1 receptors. These D1 expressing striatal neurons project inhibitory information directly to the GPi and SNpr. The entopeduncular nucleus (EPN), which is the rat's equivalent to the human GPi, shares many histological and functional properties to the SNpr. Together, the GPi/EPN and SNpr are considered the main output nuclei of the BG (Blandini et al., 2000). They are populated by GABAergic neurons and send their inhibitory projections primarily to the ventral anterior and ventral lateral thalamic nuclei, which in turn project to the motor cortex (Parent & Hazrati, 1995).

In the indirect pathway, dopamine exerts an inhibitory role on striatal GABAergic neurons, containing enkephalin as a co-transmitter and expressing D2 receptors. These D2 expressing striatal neurons send their information indirectly to the output nuclei through a more complicated route involving the GPe and STN (Blandini et al., 2000). The GPe receives major afferent projections from the striatum (inhibitory GABAergic fibers) and the STN (excitatory glutamatergic fibers) (Parent & Hazrati, 1995). The inhibitory GPe then projects to many structures within the BG circuitry, including the STN, GPi/EPN, SNpr and SNpc (Parent & Hazrati, 1995). The STN is the only glutamatergic nucleus of the BG and sends its excitatory information primarily to the BG output nuclei, the GPi/EPN and SNpr, as well as reciprocally to the GPe and pedunculopontine nucleus (PPN) (Kita & Kitai, 1987). In addition to receiving information through the indirect pathway, the STN is also innervated by the motor cortex, thalamus and PPN (Canteras, Shammah-Lagnado, Silva, & Ricardo, 1990).

The functional consequence of this complex organization is that stimulation of the direct versus the indirect pathway results in opposite effects in the net outcome of the BG circuitry (Blandini et al., 2000). Activation of striatal GABAergic MSNs of the direct pathway leads to inhibition of GABAergic neurons of the output nuclei. This results in disinhibition or facilitation of the thalamus, due to the lack of inhibitory control by those output nuclei. Consequently, the thalamus sends its projections to the motor cortex to facilitate movement. On the contrary, activation of striatal GABAergic MSNs of the indirect pathway leads to inhibition of the GABAergic GPe and subsequent disinhibition of the glutamatergic STN. This results in increased excitatory outflow from the STN to the output nuclei, which ultimately enhances their inhibitory activity. Consequently, this contributes to greater inhibitory outflow to the thalamocortical motor centers to inhibit movement.

As mentioned before, dopamine serves as a crucial modulator at the centre of this complex network. Dopamine acts on D1 receptors to enhance the role of the direct pathway and on D2 receptors to inhibit the role of the indirect pathway. Therefore, in simplistic terms, the net effect of dopamine on the BG circuitry in a normal individual is to facilitate movement (Blandini et al., 2000).

### **1.2.2 Changes in Basal Ganglia Circuitry in Parkinson's Disease**

PD is characterized by the degeneration of dopaminergic neurons in the SNpc, which triggers a cascade of changes in BG circuitry (Albin et al., 1989). Present concepts of BG circuitry propose that the loss of dopaminergic denervation of the striatum in PD results in decreased excitation through the direct pathway and increased inhibition through the indirect pathway (Albin et al., 1989; Blandini et al., 2000). Together, this imbalance of these pathways contributes to enhanced inhibitory activity of the output nuclei. As a result, there is greater inhibitory outflow to the thalamocortical motor centers, which are then unable to facilitate movement. These alterations in BG circuitry underlie an array of PD motor symptoms such as tremor, rigidity, and bradykinesia (Obeso et al., 2008). An overview of changes in BG circuitry in PD is presented in Figure 1 B.

In more detail, the loss of dopamine acting on D1 receptors causes a decrease in activation of GABAergic MSNs of the direct pathway. This results in less inhibition on the GPi/EPN and SNpr, which in turn send inhibitory projections to the thalamus to inhibit movement. On the contrary, the loss of dopamine acting on D2 receptors causes an increase in activation of GABAergic MSNs of the indirect pathway. This results in more inhibition of the GPe, and subsequent disinhibition of the STN. Hence in PD, the STN is considered overactive due to its increased excitatory outflow to the output nuclei, the GPi/EPN and SNpr. This enhanced activation of these output nuclei results in greater inhibition to the ventral anterior and ventral lateral thalamic nuclei, which in turn fail to stimulate the motor cortex.

Thus, amongst this complicated network, it is evident that the STN, which is the only glutamatergic BG nuclei, plays a key role in the facilitation or inhibition of movement. It is well accepted that the loss of dopamine in PD causes the STN to become overactive, but this overactivity is not fully understood (Rodriguez, Obeso, & Olanow, 1998). As a result, there has been much focus on understanding the role of the STN in PD. Moreover, the STN has become a key target site for implementing interventions to treat and manage symptoms of PD, such as DBS. There is strong evidence that suggests that novel pharmacological or surgical therapies that are able to reduce STN neuronal overactivity or impair glutamate

transmission at its target structures, such as the GPi/EPN may be highly promising in the treatment of PD.

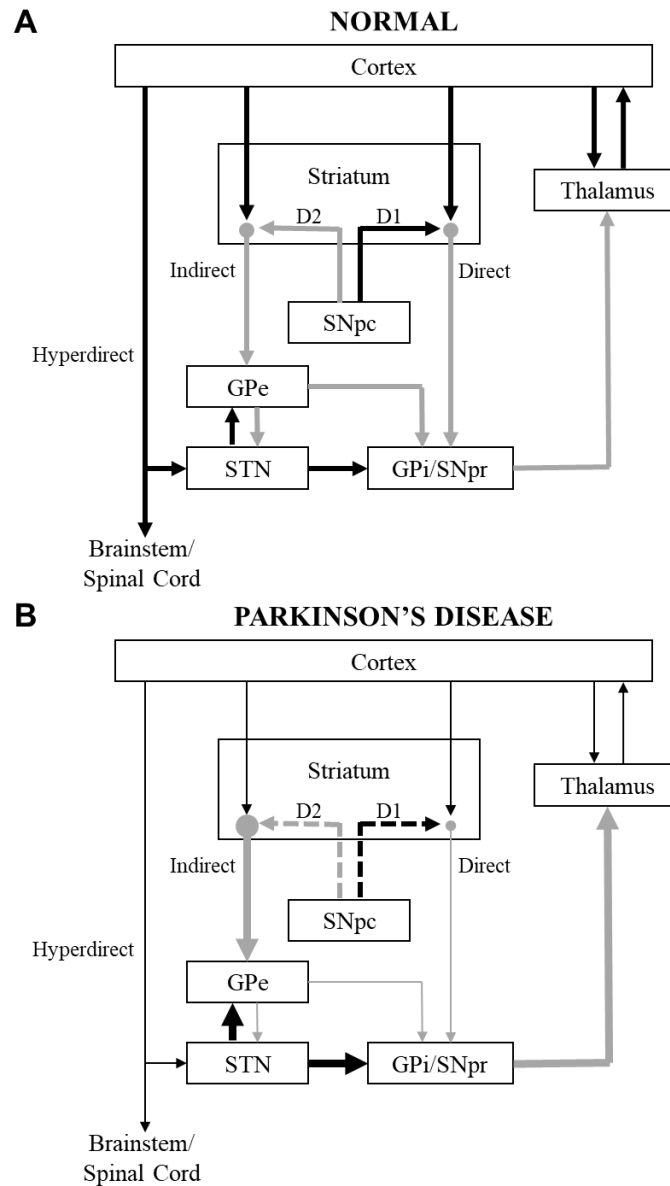


**Figure 1 – BG circuitry in normal and parkinsonian states**

Schematic diagram of the direct and indirect pathways of the BG circuitry in normal (A) and parkinsonian states (B). Black arrows represent excitatory projections and grey arrows represent inhibitory projections. The thickness of the arrows indicates changes in activity of specific connections in PD.

## 1.3 Animal Models of Parkinson's Disease

### 1.3.1 Common Animal Models

Over the past few decades, significant strides in clinical research and post-mortem studies medicine have contributed to a better understanding of PD. However, many important questions regarding the etiology, pathology and molecular biology of PD remain unanswered. While cell and tissue models are helpful in investigating the underlying molecular pathways, animal models offer deeper insight to understand the pathogenesis of PD and to test the potential of novel neuroprotective, neurorestorative or neuromodulatory interventions (Blesa & Przedborski, 2014). Classically, these animal models are grouped into two main categories: genetic or toxic models (Blesa, Phani, Jackson-Lewis, & Przedborski, 2012). Even though nearly all the hallmarks of PD can be mimicked by different experimental models, none of the currently available animal models fully phenocopy the human condition, as they lack some specific neuropathological and/or behavioural feature (Blesa & Przedborski, 2014). Thus, each model has certain strengths and weaknesses, which all must be considered when selecting the appropriate and optimal model for the question being asked.

The development of genetic animal models of PD has been more recently invigorated due to the identification of several PD-linked genes. Although the vast majority of PD cases are idiopathic, the use of overexpressed or knocked-out genes linked to PD in animals may help to reveal the cascade of molecular events underlying the death of dopaminergic neurons. Transgenic mice with mutations in  $\alpha$ -synuclein demonstrate some alterations in behaviour, but no consistent loss of dopaminergic neurons in the substantia nigra (Oaks, Frankfurt, Finkelstein, & Sidhu, 2013; van der Putten et al., 2000). Similarly, LRRK2 knock-out mice failed to reproduce the neuropathological features of PD and LRRK2 mutations knock-in mice did not demonstrate considerable striatal dopamine loss or sustained motor deficits (Hinkle et al., 2012; Tong et al., 2009; Ramonet et al., 2011). Other genetic models of PD-related genes, such as PINK1, Parkin and DJ-1 all failed to exhibit obvious behavioural changes or reduce nigrostriatal dopamine levels (Gispert et al., 2009; Itier et al., 2003; Goldberg et al., 2005). Thus, although transgenic or knock-out models



offer insight in evaluating the role of genetics in PD, they are insufficient in reproducing the neuronal degeneration associated with PD.

Neurotoxic models involve the use of compounds that can produce both reversible and irreversible effects (Blesa & Przedborski, 2014). Similar to genetic models, these toxin-based animal models each offer their own advantages and disadvantages. Some of the key benefits to neurotoxic models over genetic models are their ability to replicate the degeneration of the nigrostriatal pathway and to display motor abnormalities (Blesa et al., 2012). However, most of the neurotoxic models lack the characteristic PD proteinaceous inclusions called Lewy bodies (Forno, DeLanney, Irwin, & Langston, 1992). Of the toxin-based models, the most commonly used are the 6-hydroxydopamine (6-OHDA) rat model and the 1-methyl-4-phenyl-1,2,3,6-tetrahydropyridine (MPTP) primate model (Schober, 2004). MPTP is a lipophilic drug that can rapidly cross the blood-brain barrier and thus, it can be administered systemically, which makes it very desirable to researchers (Jackson-Lewis & Przedborski, 2007). After entering astrocytes of the brain, MPTP is activated to MPP<sup>+</sup> by the enzyme monoamine oxidase-B (Heikkila, Manzino, Cabbat, & Duvoisin, 1984). MPP<sup>+</sup> is then released from the glial cells and selectively picked up by dopaminergic neurons by the vesicular monoamine transporter 2 (Javitch, D'Amato, Strittmatter, & Snyder, 1985). In the neurons, MPP<sup>+</sup> inhibits complex 1 of the mitochondrial electron transport chain to reduce ATP production and increase reactive oxidative species (ROS) release, which leads to the death of the neurons (Tipton & Singer, 1993). Consequently, administration of MPTP is able to reproduce bilateral neuroanatomical and behavioural effects similar to that of the human PD condition (Langston, Langston, & Irwin, 1983; Bankiewicz, 1986). Despite being quite effective at mimicking the nigrostriatal loss of dopamine in primates, rats are much less susceptible to the adverse effects of MPTP (Chiueh et al., 1984). For that reason, the 6-OHDA model is the most frequently used and best-studied rodent model of PD. Due to its ability to reproduce both behavioural and neurodegenerative effects, the 6-OHDA model of PD is the chosen parkinsonian animal model that will be used to conduct this research project. The features of the 6-OHDA PD rat model will be explored in further detail in Chapter 1.3.3.

In addition to these commonly used neurotoxic models, there are pesticide and/or herbicide based PD animal models which utilize compounds such as paraquat and rotenone. The mechanism of paraquat is very similar to the ability of MPTP to deplete dopamine, but administration of paraquat can also induce significant increase of  $\alpha$ -synuclein in dopaminergic neurons of the substantia nigra (Brooks, Chadwick, Gelbard, Cory-Slechta, & Federoff, 1999; Manning-Bog et al., 2002). However, it fails to demonstrate clear motor deficits in rodents, which is why it was not chosen for this study. Administration of rotenone in rats also leads to the presence of  $\alpha$ -synuclein aggregation and mild behavioural changes (Betarbet et al., 2000; Cannon et al., 2009). However, the ability of rotenone to deplete dopamine remains uncertain and there is a very high rate of mortality associated to this model (Wu & Johnson, 2011; Ferrante, Schulz, Kowall, & Beal, 1997; Sherer, Kim, Betarbet, & Greenamyre, 2003).

Overall, based on the benefits and drawbacks of all the main neurotoxic animal models, the 6-OHDA model of PD is the best-suited system to study behavioural changes in rodents for this study.

### **1.3.2 Overview of 6-OHDA**

6-OHDA was first isolated over 50 years ago, and shortly after, its toxic effects on selective dopaminergic and noradrenergic terminals were demonstrated (Senoh & Witkop, 1959; Porter, Totaro, & Stone, 1963). 6-OHDA is a hydroxylated analogue of dopamine and it utilizes this similarity to exert its neurotoxic effects (Kostrzewa & Jacobowitz, 1974). As 6-OHDA does not cross the blood-brain barrier, it cannot be administered systemically when producing the PD model. Rather, it is injected directly into the brain by stereotaxic surgery (Ungerstedt, 1968). At the target brain region, 6-OHDA exploits the dopamine and noradrenaline reuptake transporters to enter the neurons where it can exert its neurotoxic effects (Storch, Ludolph, & Schwarz, 2004). In order to selectively destroy dopaminergic neurons and prevent uptake by noradrenergic terminals, a noradrenaline reuptake transporter blocker, such as desipramine, is often administered in conjunction with 6-OHDA when creating a PD model (Torres & Dunnett, 2012).

After entering a neuron, principally through the dopamine active transporter, 6-OHDA mediates its neurotoxic effects by generating oxidative stress and triggering mitochondrial dysfunction (Blum et al., 2001). Excessive formation of hydrogen peroxide, hydroxyl radicals and superoxide radicals occur via deamination of 6-OHDA by monoamine oxidase and/or auto-oxidation (Breese & Traylor, 1971; Heikkila & Cohen, 1972). Consequently, the build of oxidative stress reduces antioxidative capabilities of the neurons, exhausts phospholipids and impairs regulation of redox potentials (Kumar, Agarwal, & Seth, 1995; Shiraga, Pfeiffer, & Ebadi, 1993). 6-OHDA-generated ROS also leads to DNA damage and cytoskeleton disorganization (Bruchelt, Schraufstatter, Niethammer, & Cochrane; Davison, Legault, & Steele, 1986). Moreover, 6-OHDA targets complex I and IV of the mitochondrial electron chain in order to impair mitochondrial function (Glinka & Youdim, 1995). The combined effects of mitochondrial dysfunction and excessive production of oxidative stress impairs the neurons targeted by 6-OHDA from exerting their normal physiological functions and consequently triggers their death.

### **1.3.3 6-OHDA Lesion of the MFB**

As previously mentioned, lesioning of the rat nigrostriatal dopaminergic system with 6-OHDA is the most commonly used animal model of PD (Torres & Dunnett, 2012). In experimental models of PD, 6-OHDA is preferentially injected into the striatum, the substantia nigra or the ascending medial forebrain bundle (MFB). The neurotoxic consequences of 6-OHDA at these different sites all vary slightly from one another in terms of behavioural effects and neuroanatomic depletion of dopamine.

The MFB is a collection of ascending and descending fibers that connect the medial and basal forebrain structures with the midbrain and hypothalamus (Shiosaka et al., 1980). Amongst the numerous fibers, the MFB consists of axons of dopaminergic neurons of the nigrostriatal pathway (A9 cells) projecting from the SNpc to the caudate putamen (CPu), and of the mesolimbic pathway (A10 cells) projecting from the ventral tegmental area to the nucleus accumbens (Deumens, Blokland, & Prickaerts, 2002). Direct injection of 6-OHDA into the MFB unilaterally causes a near complete destruction of A9 and A10 cell groups (Perese, Ulman, Viola, Ewing, & Bankiewicz, 1989). Bilateral MFB lesions results

in animals suffering from severe aphagia and adipsia, whereas unilaterally lesioned rodents are capable of normal eating and drinking (Zigmond & Stricker, 1973). Thus, the unilateral 6-OHDA model was preferred and used in this research project.

Unilateral injection of 6-OHDA into the MFB produces a well-established syndrome involving: (1) near total depletion of dopamine in the CPu ipsilateral to the lesion, (2) denervation supersensitivity of dopamine receptors in the CPu ipsilateral to the lesion, and (3) a characteristic rotational behaviour in response to amphetamine and apomorphine (Perese et al., 1989; Deumens et al., 2002). These hemiparkinsonian rats demonstrate various changes in motor behaviour, particularly in an asymmetric manner. After unilateral lesioning of the MFB, rats initially display a preferential turning behaviour toward the side of the lesion (Deumens et al., 2002). When drugs that act on the dopaminergic system are administered, such as amphetamine and apomorphine, hemiparkinsonian rats display further active rotational behaviour (Ungerstedt, 1968). This drug-induced rotational phenotype is due to an imbalance in dopamine activity between the lesioned and non-lesioned striata. With this imbalance in dopamine, animals tend to rotate away from the side of greater activity (Ungerstedt, 1971). When hemiparkinsonian rats are challenged with amphetamine, they display ipsilateral rotations towards the lesioned side. As a dopamine releasing agent, amphetamine stimulates the release of dopamine and blocks its reuptake. This results in greater dopamine activity on the side of the intact nigrostriatal projection, and thus animals rotate toward the lesioned side. On the other hand, when hemiparkinsonian rats are challenged with apomorphine, they display contralateral rotations away from the lesioned side. This is due to the phenomenon known as supersensitivity, in which there is an upregulation of D1 and D2 postsynaptic receptors in the denervated striatum. With this supersensitivity of dopamine receptors, there is greater dopamine activity on the side of the lesioned nigrostriatal projection, and thus animals rotate away from the lesioned side (Ungerstedt, 1971; Deumens et al., 2002). Only rats who demonstrate extensive lesions (>90% reduction in dopaminergic fiber density in the CPu) will demonstrate contralateral rotational behaviour following administration of apomorphine (Hudson et al., 1993). However, rats with moderate lesioning (75-90% reduction in dopaminergic fiber density in the CPu) will demonstrate ipsilateral rotational behaviour following administration of amphetamine but no significant circling behaviour

in the presence of apomorphine. Thus, apomorphine is better than amphetamine to predict the extent of CPu lesioning following 6-OHDA injection into the MFB (Hudson et al., 1993; Deumens et al., 2002). Although it varies from study to study, there is a general consensus that a minimum of 6 or 7 net contralateral rotations per minute is the standard for a successful complete 6-OHDA lesion, which corresponds to approximately 95-99.8% depletion of dopamine content in the CPu and 85% depletion in the SNpc (Perese et al., 1989; Hudson et al., 1993; Deumens et al., 2002, Yuan, Sarre, Ebinger, & Michotte, 2005; Torres & Dunnett, 2012).

In addition to this characteristic rotational phenotype, many other changes in behaviour have been demonstrated in this hemiparkinsonian model. 6-OHDA lesioned animals at the MFB display clear motor coordination deficits, as measured by the rotarod (Monville, Torres, & Dunnett, 2006; Carvalho et al., 2013). Following 6-OHDA lesioning of the MFB, animals spent a significantly much shorter time balancing on the rotating rod and were more prone to falls, as compared to control animals. Moreover, assessment of exploratory and locomotor activity by the open field test, in which rats are allowed to freely roam, demonstrated that 6-OHDA lesioned rats display significantly lower motor activity than control animals (Carvalho et al., 2013). Following 6-OHDA lesioning, both the total distance traversed and the number of ambulatory episodes significantly reduced by a factor of four, as compared to controls. Furthermore, 6-OHDA lesioned rats spent significantly more time hanging to a wire during the grip strength test (Ma et al., 2014). This reflects an increase in muscular tension and indicates that 6-OHDA lesioned rats develop greater limb rigidity. In addition, 6-OHDA lesioned animals develop anhedonic behaviour, a main feature of depressive-like behaviour. This was demonstrated by a significant reduction in preference for sucrose in the sucrose preference test (Carvalho et al., 2013). However, 6-OHDA lesioned animals do not demonstrate significant differences in terms of time spent on the open arms versus closed arms of an elevated plus maze, which is used to assess anxiety-like behaviour (Carvalho et al., 2013). Finally, the effect of 6-OHDA lesions on cognitive performance remains controversial. A study by Ma et al. (2014) reported that 6-OHDA lesioned rats demonstrate a significant increase in latency in locating the platform during spatial learning trials of the Morris water maze task. On the other hand, a behavioural characterization study by Carvalho et al. (2013) described that both reference and working

memory performance were not affected by unilateral lesioning of the MFB as measured by Morris water maze test (Carvalho et al., 2013). In brief, 6-OHDA lesioned rodents demonstrate clear motor deficits, which are demonstrated by an array of spontaneous and forced motor tests. However, the effects of MFB lesioning on cognition appear to be less clear. Also, it is important to note that specific changes in gait are also observed in unilateral 6-OHDA lesioned rats. These features will be discussed in further detail in Chapter 1.4.3.

In conclusion, the 6-OHDA rat model of PD arguably best mimics the human disease at advanced stages in terms of neurochemical and behavioural features. Although it has a few drawbacks, including being limited to unilateral injections, it remains well suited to test preclinical PD therapeutics and changes in specific motor parameters. Thus, unilateral lesioning of the MFB with 6-OHDA was the chosen hemiparkinsonian animal model used to conduct this research project.

## 1.4 Gait Dysfunction in Parkinson's Disease

### 1.4.1 Overview

The act of walking with an automatic and rhythmic gait is a seemingly simple task. However, in fact, it involves a complex integration of cortical, subcortical, brainstem and spinal cord neural networks to process external sensory information and generate this automatic and rhythmic pattern of movement (Nutt, Marsden, & Thompson, 1993). In PD, this rhythmic sequence is lost and gait disturbances present as short, shuffling steps with freezing episodes, which frequently result in falls that are severely debilitating (Williams et al., 2006; Lewis & Marker, 2009).

Classically, gait is defined as the pattern of leg movements used to complete a stride. A stride is the period spanning from the placement of one foot to the ground to when that same foot is placed on the ground again. Each stride comprises of a phase of stance, during which the foot is in contact with the ground and a phase of swing, during which the foot is not in contact with the ground. Affected gait in PD characteristically includes reduced

walking velocity (slowness), shorter step length, shorter stride length, increased double support time and reduced arm swing (Sofuwa et al., 2005). However, in current literature, the appropriate selection of gait parameters remains inconsistent and the conclusions that can be drawn from each gait parameter to understand the neurocircuitry dysfunction involved in gait and PD is unclear. Many studies have attempted to further elucidate the changes in specific gait parameters seen in PD and study their potential improvements following treatment, such as levodopa and DBS (Blin, Ferrandez, Pailhous, & Serratrice, 1991; Verghese, Holtzer, Lipton, & Wang, 2009; Hollman, McDade, & Petersen, 2011).

A study by Lord, Galna, & Rochester (2013) examined different features of gait, including pace, rhythm and variability, in order to associate specific gait parameters to each feature and understand their changes in pathological conditions. Pace refers to the speed of walking and is primarily linked to the gait parameters of step velocity and step length (Lord et al., 2013). These kinematic parameters tend to be L-DOPA sensitive and improve following treatment (Blin et al., 1991). On the other hand, rhythm is related to the temporal parameters of gait and animal models have demonstrated the involvement of central pattern generators within the cervical and lumbar regions of the spinal cord (Marder & Calabress, 1996). Temporal parameters of gait, such as duration of stride and swing, tend to be resistant to L-DOPA treatment (Blin et al., 1991, Lord et al., 2013). Variability refers to the step-to-step fluctuations and appears to also be L-DOPA resistant (Blin et al., 1991). Furthermore, current literature presents conflicting conclusions on the response of gait to STN-DBS. Some studies report an improvement in certain aspects of gait with long term STN-DBS treatment (Krack et al., 2003; Cantiniaux et al., 2010; Zibetti et al., 2011), whereas contradictory studies report no benefit or even worsening of gait (Kelly et al., 2006; Kelly et al., 2010).

Overall, gait dysfunction in PD directly affects mobility, which can severely impair a patient's quality of life. Thus, there is an ongoing need to dissect the specific parameters of gait and potential effects of intervention to understand the true complexity of gait.

### **1.4.2 Gait Assessment Tools for Animal Models**

Currently, there are many behavioural tests available to investigate different aspects of gait in rodent models, and each are associated with its own strengths and weaknesses. The cylinder test, used to measure forelimb use, akinesia and asymmetry, is limited by the fact that it is manually scored and restricted to only forelimbs (Tillerson et al., 2001; Iancu, Mohapel, Brundin, & Paul, 2005). Other tests that evaluate forced locomotion, such as the rotarod and treadmill, allow for investigation of more dynamic gait parameters, but do not dissect specific changes in walking patterns (Iancu et al., 2005, Monville et al., 2006). Lastly, footprint tracking, in which an animal walks down a paper after their paws are dipped in ink, only measures static gait parameters (De Medinaceli, Freed, & Wyatt, 1982).

In more recent years, the introduction of the CatWalk gait analysis system has provided for an automated and simultaneous quantification of many static and dynamic aspects of gait during voluntary walking (Hamers, Lankhorst, van Laar, Veldhuis, & Gispen, 2001). The CatWalk apparatus consists of a long-enclosed walkway designed to allow animals to traverse freely at their natural speed from one side to the other. The walkway comprises of a glass plate floor illuminated by a green light. As the paws of the animal contacts the glass floor, the green light is scattered against a red backdrop. This scattering of light is captured by a high speed video camera mounted below the glass. Based on the captured data (position, pressure and surface area) of each footprint, the CatWalk software is able to measure many parameters of gait. A sample of raw CatWalk data to illustrate the light scattering technique of this apparatus is provided in Appendix 2.

Several studies have demonstrated that Catwalk is a reliable tool in assessing gait for rodent models of many neurodegenerative disorders including PD (Vlamings et al., 2007; Chuang et al., 2010; Vandeputte et al., 2010). Specifically, this device has been validated for measuring abnormalities in gait and locomotion in the 6-OHDA rodent model of PD (Westin, Janssen, Sager, & Temel, 2012; Zhou et al., 2015). A list of gait parameters detected by the CatWalk apparatus and their definitions are described in Table 1.



**Table 1 – Definition of Gait Parameters**

<b>Parameter</b>	<b>Definition</b>
<b>Average Speed (cm/s)</b>	Distance traversed on the walkway divided by time
<b>Body Speed Variation (%)</b>	Difference between body speed and average speed divided by average speed
<b>Cadence (steps/s)</b>	Number of steps taken per second
<b>Duty Cycle (%)</b>	Stand as a percentage of step cycle
<b>Initial Dual Stance (s)</b>	Duration of the first step in a step cycle of a paw that the contralateral paw also contacts the walkway
<b>Max Contact Area (cm<sup>2</sup>)</b>	Maximum area of a paw that contacts the walkway
<b>Mean Intensity</b>	Mean pressure of a paw that contacts the walkway
<b>Single Stance (s)</b>	Duration of contact for a single paw when the contralateral paw is in swing
<b>Stand (s)</b>	Duration of contact of a paw with the walkway
<b>Step Cycle (s)</b>	Duration of two consecutive contacts of the same paw
<b>Stride Length (cm)</b>	Distance between two consecutive placements of the same paw
<b>Swing (s)</b>	Duration of no contact of a paw with the walkway
<b>Swing Speed (cm/s)</b>	Speed of a paw during swing
<b>Terminal Dual Stance (s)</b>	Duration of the second step in a step cycle of a paw that the contralateral paw also contacts the walkway

### **1.4.3 Gait Changes in the 6-OHDA Model of Parkinson's Disease**

A study by Zhou et al. (2015) investigated the differences in gait deficits of different unilateral 6-OHDA rat models of PD. Specifically, this study analyzed the changes in static and dynamic gait parameters after administration of 6-OHDA into the MFB, CPu or SNpc. The authors observed only mild gait impairment in the CPu lesioned animals, but significant impairments in the MFB and SNpc groups. The MFB lesioned animals demonstrated greater impairment than the SNpc lesioned rats and thus, the authors suggested that 6-OHDA lesioning of the MFB is the most appropriate rodent model to study gait dysfunction. Specifically, experiments by Chuang et al. (2010) and Zhou et al. (2015) demonstrated that approximately 4 weeks following 6-OHDA lesioning of the MFB, animals displayed a decrease in max contact area, mean intensity, stride length and swing speed and an increase in stand, swing, step cycle, duty cycle and terminal dual stance. In addition, significant differences in contralateral compared to ipsilateral limbs

were observed for static gait parameters, specifically max contact area and mean intensity. However, these asymmetric differences were not detected for dynamic gait parameters.

Moreover, additional studies have associated the gait changes observed in rodent PD models to certain clinical phenotypes of PD patients (Chuang et al., 2010; Westin et al., 2012; Zhou et al., 2015). Hypokinesia and an increase in muscle rigidity is reflected by the reduction in stride length and swing speed in PD rats (Zhou et al., 2015). This is similar to the clinical signs that are often seen in PD patients who take smaller steps while walking. Furthermore, an increase in stand and swing duration, along with a decrease in swing speed, contribute to an overall reduction in average speed of hemi-PD rodents (Lee, Hsieh, Liang, Yeh, & Chen, 2012; Zhou et al., 2015). These changes are reflective of the decrease in pace seen in PD patients.

In sum, unilateral injection of 6-OHDA into the MFB produces evident and stable gait deficits that are well-characterized and validated by the CatWalk apparatus. Therefore, the CatWalk test was used to analyze changes in static and dynamic gait parameters of 6-OHDA lesioned rodents in this research project.

## 1.5 Botulinum Neurotoxins

### 1.5.1 Overview and Mechanism

Botulinum neurotoxins (BoNTs) are a family of metalloproteases synthesized by different strains of the anaerobic bacteria, *Clostridium botulinum* (Ermengem, 1897; Hatheway, 1989). This family comprises of seven antigenically distinct serotypes (BoNT-A to BoNT-G), which target specific machinery at synaptic terminals to block the release of neurotransmitters (Burgen, Dickens, & Zatman, 1949; Lacy & Stevens, 1999). These neurotoxins exert their paralytic action by a multistep mechanism: 1) binding, 2) internalization, 3) membrane translocation and 4) proteolytic cleavage (Simpson, 1981; Montecucco, Papini, & Schiavo, 1994).

BoNTs are secreted as an inactive precursor consisting of a single 150 kDa polypeptide chain, which is subsequently cleaved to yield the active neurotoxin. The active form

contains a 100 kDa heavy (H) chain and a 50 kDa light (L) chain linked together by a single disulphide bond (Sakaguchi, 1982; Montecucco & Schiavo, 1995). The carboxy-terminal of the heavy chain (H<sub>C</sub>) mediates the uptake of the toxin into axon terminals by specific receptor binding and the amino-terminal (H<sub>N</sub>) facilitates membrane translocation (Lacy & Stevens, 1999; Rossetto & Montecucco, 2008). Specifically, the H<sub>C</sub> of BoNT-A binds to isoforms A-C of the synaptic vesicle protein 2 (SV2) receptor and to the GT1B polysialoganglioside (Dong et al., 2006; Kozaki et al., 1998). After binding to the SV2 receptor, BoNT-A utilizes synaptic vesicle recycling to mediate its endocytosis into presynaptic terminals (Simpson, 2004). Following internalization, the reduction in pH leads to a conformational change in which H<sub>N</sub> acts as a transmembrane chaperone for the L chain to translocate pass the vesicle membrane into the cytosol (Koriatzova & Montal, 2003). Through a reduction of the disulphide bond, the L chain is released into the cytosol, where it displays its enzymatic effects by cleaving specific components of the synaptic vesicle docking-fusion apparatus known as the soluble *N*-ethylmaleimide-sensitive factor attachment protein receptor (SNARE) complex (Schiavo, Matteoli, & Montecucco, 2000). Synaptic SNARE proteins are essential for neuroexocytosis and their cleavage by BoNTs results in the inhibition of neurotransmitter release. BoNT-A acts as zinc-dependent endopeptidase that targets synaptosomal-associated protein 25 (SNAP-25) of the SNARE complex (Blasi et al., 1993). Specifically, BoNT-A cleaves SNAP-25 by hydrolyzing the Gln<sup>197</sup>-Arg<sup>198</sup> peptide bond (Schiavo et al., 1993). The cleaved SNAP-25 is now unable to mediate fusion of vesicles carrying neurotransmitters to the presynaptic membrane and thus, neuroexocytosis is impaired.

### **1.5.2 BoNT-A Effects in Non-Cholinergic Systems**

The effect of BoNT-A has been best studied in its ability to block the release of the neurotransmitter acetylcholine (Simpson, 1981). However, BoNT-A is not limited to inhibiting acetylcholine release, and has been demonstrated to also inhibit the release of other neurotransmitters from synaptosomes, including glutamate, glycine, noradrenaline, and dopamine (Sanchez-Prieto et al., 1987; Bigalke, Heller, Bizzini, & Habermann, 1981; Ashton & Dolly, 1988; McMahon et al., 1992). A study by Sanchez-Prieto (1987) demonstrated that BoNT-A significantly inhibits Ca<sup>2+</sup> dependent glutamate exocytosis

from cerebral cortical synaptosomes. In this *in vitro* experiment, the authors found that inhibition of glutamate exocytosis by BoNT-A develops over 2 hours. Furthermore, a similar study by Bigalke et al. (1981) demonstrated that BoNT-A significantly inhibits evoked release of noradrenaline and glycine from particulate preparations of rat brain and spinal cord tissue. The extent of noradrenaline and glycine inhibition was very similar to that of cholinergic blockage, with approximately 80% inhibition at 10 ug/mL of BoNT-A. In contrast, inhibition of GABA by BoNT-A was drastically lower and required a significantly higher dose (by approximately five-fold) to achieve comparable levels of inhibition to that of acetylcholine. Moreover, a study by Ashton and Dolly (1988) also demonstrated that BoNT-A was significantly weaker in its maximum ability to impede GABA release compared to acetylcholine release (40% compared to 90% neurotransmitter inhibition). These studies were further supported by work conducted by McMahon et al. (1992), which compared the inhibitory effect of tetanus toxins to BoNTs on a variety of neurotransmitters and neuropeptides. The authors concluded that BoNT-A was able to significantly inhibit release of glutamate from synaptosomes, whereas only tetanus toxin additionally inhibited the release of GABA, aspartate, and met-enkephalin. All of this experimental data offers support to suggest that GABAergic terminals are considerably less sensitive to BoNT-A than glutamatergic terminals.

The molecular basis for this differential sensitivity of BoNT-A on specific terminals remains unclear (Verderio et al., 2006; Verderio et al., 2007). A series of experiments conducted by Verderio et al. postulate that the relative resistance of GABAergic synapses to BoNT-A may be due to a differential expression of SNAP-25. In both cultured neurons and brain slices, hippocampal GABAergic terminals lacked the classical SNAP-25 of the SNARE complex (Verderio et al., 2004). This absence of SNAP-25 was thought to underlie its resistance to BoNT-A because exogenous expression of SNAP-25 in GABAergic neurons induced sensitivity to BoNT-A (Verderio et al., 2007). Although this work was conducted in hippocampal neurons, a comprehensive neuroanatomical distribution of SNAP-25 was mapped in an entire rodent brain by Oyler et al. in 1989. They reported relatively lower levels of SNAP-25 present in the BG compared to other brain regions. Furthermore, differences in intrinsic calcium dynamics between glutamatergic and GABAergic synapses also contribute to the preferential inhibitory action of BoNT-A

(Grumelli, Corradini, Matteoli, & Verderio, 2010). The reduced effectiveness of BoNT-A in GABAergic synapses is attributable to the higher evoked calcium responsiveness of these inhibitory neurons (Grumelli et al., 2010; Akaike et al., 2010). Finally, a chief difference between glutamatergic and GABAergic terminals that most likely underlies the differential sensitivity of BoNT-A is their expression of the SV2 receptor, which is necessary for the internalization of BoNT-A (Simpson, 2004). Quantitative analysis of SV2B in glutamatergic versus GABAergic axon terminals demonstrated 80% colocalization of SV2B with a glutamatergic marker, whereas only 15% colocalization of SV2B with a GABAergic marker (Bragina et al., 2012). The reduced levels of the SV2 receptor in GABA terminals significantly contributes to BoNT-A resistance in these inhibitory neurons.

Regardless of the molecular mechanism underlying the preferential inhibitory action of BoNT-A on cholinergic and glutamatergic rather than GABAergic terminals, this differential sensitivity can be exploited to treat pathologies that result because of imbalances in excitatory and inhibitory neurotransmission. This includes the changes in BG circuitry seen in PD, as previously described in Chapter 1.2.2.

### **1.5.3 Use of BoNT-A for Parkinson's Disease**

With its ability to suppress cholinergic activity at the neuromuscular junction, BoNT-A has been commonly used clinically as a peripheral treatment for tremor in PD (Kim, Yiannikas, Mahant, Vucic, & Fung, 2014; Samotus, Rahimi, Lee, & Jog, 2016; Zakin & Simpson, 2017). As a clinical therapeutic, the peak effect of BoNT-A typically occurs at 4 weeks post-injection and repeated injections given every 3-4 months (Kim et al., 2014).

Moreover, emerging research on rodents suggests a role for the direct administration of BoNT-A in the central nervous system (Hawlotschka et al., 2013; Mazzocchio & Caleo, 2015). Several studies have shown that direct injection of BoNT-A in the spinal cord and brain can serve as a modulator for pain and PD, respectively (Chaddock et al., 2004; Wree et al., 2010). Studies by Wree et al. (2010) demonstrated that ipsilateral injections of 1-2 ng of BoNT-A at the striatum could block cholinergic overactivation of GABAergic

medium spiny neurons in the 6-OHDA rat model of PD. By locally interrupting release of acetylcholine, apomorphine-induced rotational behaviour in hemiparkinsonian rats was abolished up to 6 months. A minimum dose of 100 pg of BoNT-A revealed beneficial but insignificant effects, whereas a maximum dose of 5 ng lead to occasional lethality. The behavioural effects of BoNT-A in 6-OHDA lesioned rats were further studied by Antipova et al. (2013). After 3 months of treatment with 2 ng of BoNT-A in the striatum, hemiparkinsonian rats showed an equalization of forelimb use (measured by the cylinder test) compared to untreated rats. However, no motor improvements were detected by the rotarod test or open field test following intrastriatal BoNT-A treatment.

The results of these studies, along with several other experiments involving direct administration of BoNT in the brain, demonstrate that central injection of BoNT in rodents is not cytotoxic and offers an immense potential as a novel therapeutic to neurodegenerative diseases, such as PD.

## 1.6 Rationale

### 1.6.1 Overview

With over 7 million people affected by PD globally, there is an ongoing need to research the mechanisms underlying its pathogenesis and to identify novel management and therapeutic interventions (Chapter 1.1.1). PD is characterized by the degeneration of dopaminergic neurons in the SNpc (Chapter 1.1.2), but the exact molecular mechanisms underlying this neuronal death remain unclear (Chapter 1.1.3). This neurodegenerative disorder is associated with both motor and non-motor symptoms (Chapters 1.1.4 and 1.4.1), which are currently managed by a combination of medications and/or surgical options (Chapter 1.1.5). Current interventions offer symptomatic relief but have not been able to slow the rate of progression of PD, nor have been confirmed as displaying neuroprotective, neurorescuing or neurorestorative effects. There is still an unmet need for exploring novel interventions that offer innovative neuromodulatory effects with an already understood mechanism.

In PD, the death of dopaminergic neurons in the SNpc leads to changes in BG circuitry (Chapter 1.2.2.). Current concepts of BG circuitry propose that loss of striatal dopamine in PD results in an imbalance of the direct and indirect pathways, which contribute to greater inhibitory outflow to the thalamocortical motor centers. Amongst this intricate network, the STN, the only glutamatergic BG nuclei, plays an important role in the facilitation or inhibition of movement. It is well accepted that in PD, the STN is considered overactive due to its increase in glutamatergic outflow to the output nucleus, the GPi (rodent equivalent: EPN). Thus, the STN has become a key target site for implementing interventions to treat and manage symptoms of PD. Novel pharmacological or surgical therapies that are able to reduce STN neuronal overactivity or impair glutamate transmission at its target structures, such as the GPi/EPN may be highly promising in the treatment of PD.

BoNT-A is a commonly used toxin in medicine, cosmetics and research due to its ability to block the release of acetylcholine from axon terminals. The ability of BoNT-A to cleave SNAP-25 of the SNARE complex to prevent neuroexocytosis has been extensively studied and is already well-established (Chapter 1.5.1). There is strong research to support the fact that BoNT-A has the ability to impair release of other neurotransmitters besides acetylcholine (Chapter 1.5.2). This includes a preference for glutamatergic terminals and a reduced effect of GABAergic terminals. In the past decade, there has been more and more research to investigate the possibility of direct BoNT-A injections in the brain (Chapter 1.5.3). Central injections of BoNT-A have been demonstrated to be safe in rodents and promising for a variety of diseases, including PD.

Central administration of BoNT-A offers immense potential as a novel therapeutic for PD, as it provides many of the unmet needs and criteria discussed throughout this chapter. Direct injection of BoNT-A at the GPi/EPN could preferentially target the incoming overactive projections of glutamate from the STN to the EPN without interfering with afferent GABAergic projections. As with most preclinical studies, this work could be studied in an animal model of PD (Chapter 1.3.1). Out of the available models of PD, unilateral lesioning of the MFB with 6-OHDA in rats was chosen as the hemiparkinsonian model best suited to conduct this research project (Chapter 1.3.3). Both motor and gait

dysfunction in this PD model has already been well characterized by numerous behavioural studies (Chapters 1.3.3 and 1.4.3) and thus, the subsequent changes following BoNT-A administration in this model can be readily detected and studied.

### **1.6.2 Hypothesis**

It was hypothesized that administration of BoNT-A at the EPN would have modulated glutamate release from the STN, which would have consequently led to changes in BG circuitry to improve motor impairments of a hemiparkinsonian animal.

### **1.6.3 Objectives**

Overall, this project aimed to assess the molecular and behavioural effects of BoNT-A injections at the EPN of the unilateral 6-OHDA rat model of PD. The objectives of this study were as follows:

- 1) To determine changes in locomotion and gait by the CatWalk apparatus following intra-EPN administration of BoNT-A
- 2) To evaluate changes in drug induced rotations by the apomorphine rotation test following intra-EPN administration of BoNT-A
- 3) To establish an optimal dose of BoNT-A for intra-EPN
- 4) To measure the temporal pattern of efficacy of intra-EPN BoNT-A
- 5) To determine neuroanatomical and molecular changes of the EPN by immunohistochemistry following direct administration of BoNT-A

### **1.6.4 Predictions**

The predictions were as follows:

- 1) Direct administration of BoNT-A at the EPN would have improved gait and motor performance of 6-OHDA lesioned animals
- 2) Injection of BoNT-A at the EPN would have reduced apomorphine-induced pathological rotations of 6-OHDA lesioned rodents



- 3) A dose in the 'ng' range would have been necessary to mediate the BoNT-A induced behavioural improvements
- 4) The effects of BoNT-A would have been transient, with restoration of both structural and behavioural alterations
- 5) The changes in behaviour would have been caused by a differential effect of BoNT-A on glutamatergic projections from the STN and GABAergic terminals from the striatum to the EPN

## Chapter 2

### 2 Materials and Methods

This chapter outlines the materials and methods used to conduct this study. Figure 2 provides a summary of the timeline of the experimental protocol. All experimental work was performed under the guidelines of the Animal Care Committee at Western University and followed the approved Animal Use Protocol #2015-087 (Appendix 1).

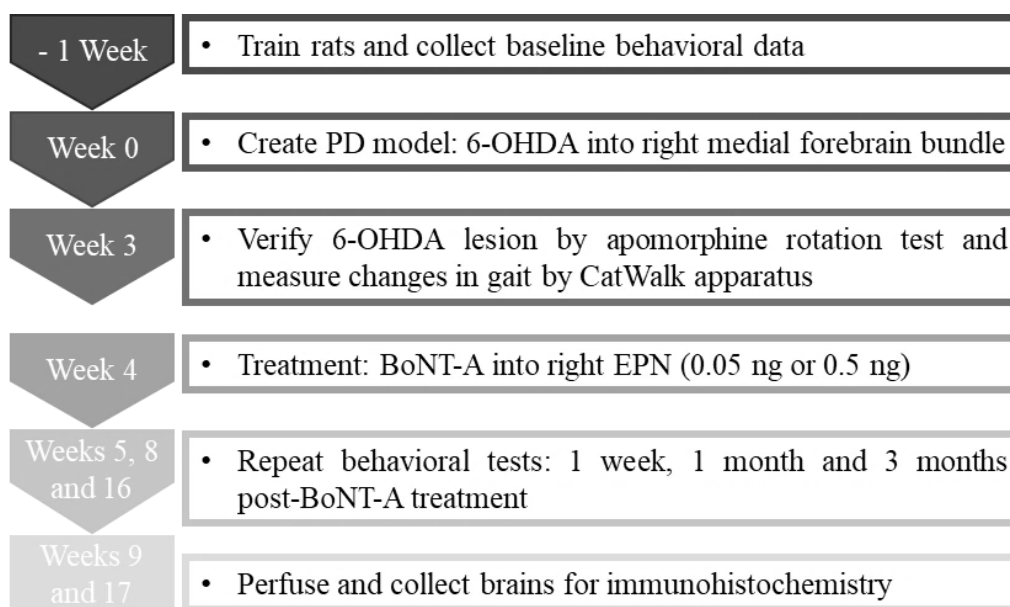


**Figure 2 – Experimental timeline**

#### 2.1 Experimental Animals

Adult male Sprague-Dawley rats (Charles River Canada), weighing 250-300 grams at the time of the first surgery, were used in this study. All experimental work was conducted in accordance with the guidelines of the Animal Care Committee at Western University. This study was approved by the committee (AUP 2015-087) and all regulatory materials regarding the use of BoNT-A in animals was also approved. Animals were housed in standard cages in a temperature-controlled room ( $22\pm 1^{\circ}\text{C}$ ) under 12 hr light/12 hr dark conditions with controlled access to food and water. Food restriction was used to regulate

the weight of the animals throughout the prolonged study. Animals were fed 15-20 grams of food daily to limit weight gain to approximately 20 grams per week.

The breakdown of experimental animals is represented in Figure 3. Animals were divided into four experimental groups: (1) sham lesioned animals receiving vehicle (n=12), (2) sham lesioned animals receiving BoNT-A (0.5 ng) (n=12), (3) 6-OHDA lesioned animals receiving vehicle (n=12), and (4) 6-OHDA lesioned animals receiving BoNT-A (n=24). All groups were further subdivided into a set of animals to be sacrificed at 1 month post-BoNT-A treatment (n=4) for immunostaining and a set of animals to be sacrificed at 3 months post-BoNT-A treatment (n=8) following completion of behavioural studies. Group 4 animals were further subdivided into those that were injected with a low dose (0.05 ng) of BoNT-A (n=8) and those that were injected with a high dose (0.5 ng) of BoNT-A (n=16). An additional set of group 4 animals injected with a high dose were sacrificed at 1 week post-BoNT-A treatment (n=4).

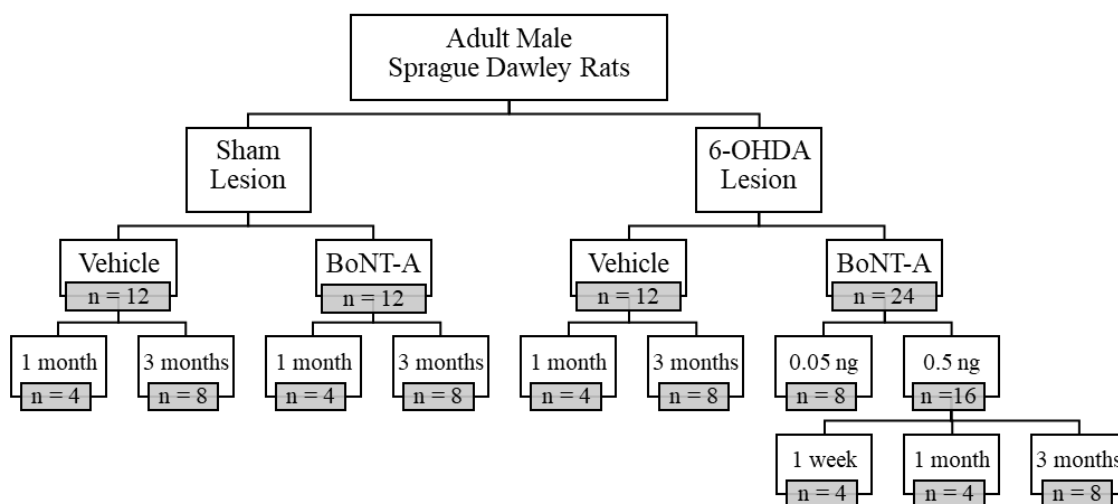


**Figure 3 – Experimental animal groups**

## 2.2 6-OHDA Lesioning of the MFB

Hemiparkinsonism was induced by unilateral injection of 6-OHDA into the right MFB. All animals were administered desipramine hydrochloride (25 mg/kg, IP.; Sigma) 30-60 minutes before 6-OHDA infusion to protect noradrenergic terminals. Animals were anaesthetized with a mixture of ketamine (80 mg/kg, IP) and xylazine (5 mg/kg, IP) and placed on a stereotaxic apparatus (Kopf Instruments). Sedation was monitored using a gentle toe pinch withdrawal reflex and thermoregulation was provided by heat lamp and monitored by a rectal thermometer. The head of the animal was shaved by an electric razor and the surgical site was cleaned with surgical soap, isopropyl alcohol and a chlorohexidine solution before incision. A midline skin incision (2 cm) was made and all soft tissue from the surface of the skull was removed to expose the skull. All stereotaxic coordinates were calculated from Bregma according the rat brain atlas of Paxinos and Watson (2009). A burr hole of approximately 1 mm was drilled to introduce a 31G injection cannula (PlasticsOne) at the right MFB (AP -1.8, L 2, DV 8.3) (Appendix 3). The cannula was attached to a Hamilton syringe by polyethylene tubing for the delivery of 6-OHDA. A total volume of 4  $\mu$ L of a 6-OHDA solution (8  $\mu$ g/rat: 4  $\mu$ L of 100 mg/50 mL 6-OHDA dissolved in 0.9% saline containing 0.1% ascorbic acid; Sigma) was injected over 4 minutes and the cannula was left in place for an additional 5 minutes before being slowly withdrawn. Sham lesioned control animals received an equivalent volume of 0.9% saline containing 0.1% ascorbic acid.

## 2.3 BoNT-A Injection at the EPN

Four weeks after 6-OHDA surgery, successfully lesioned rats and controls were subjected to BoNT-A injection. Stereotaxic surgery was performed under ketamine/xylazine anesthesia and surgical preparation was completed consistent with the 6-OHDA surgery. Administration of BoNT-A (List, Campbell, USA) at the right EPN (AP -2.5, L 3.0, DV 7.7) was delivered through a 31G injection cannula attached to a Hamilton syringe by polyethylene tubing (Appendix 3). A total volume of 0.5  $\mu$ L of a BoNT-A solution was injected over 5 minutes and the cannula was left in place for an additional 5 minutes before

being slowly withdrawn. Animals received either a high dose at 0.5 ng of BoNT-A (0.5  $\mu$ L of 1 ng/ $\mu$ L BoNT-A dissolved in phosphate buffered saline (PBS) containing 0.1% bovine serum albumin (BSA)) or a low dose at 0.05 ng of BoNT-A (0.5  $\mu$ L of 100 pg/ $\mu$ L BoNT-A dissolved in PBS containing 0.1% BSA). Control animal received an equivalent volume of PBS with 0.1% BSA.

## 2.4 Behavioural Tests

Behavioural studies were performed before and after BoNT-A injection to evaluate the potential changes in motor activity and gait following treatment.

### 2.4.1 Apomorphine-Induced Rotation Test

Three weeks after 6-OHDA surgery and 1 week prior to BoNT-A injection, the 6-OHDA lesion quality was tested by apomorphine-induced rotations. Since the right MFB was unilaterally lesioned, it was expected that injection of apomorphine lead to contralateral rotations away from the lesioned side (see Chapter 1.3.3 for details).

Following injection of apomorphine (0.25 mg/kg, SC.; Sigma), rats were placed individually in empty colony cages with a video camera recording their behaviour for 30 minutes. Subsequently, rotations were counted over 15 minutes of video footage to determine the average rotation per minute for each rat. Only rats showing more than seven contralateral rotations per minute were used in subsequent experiments as parkinsonian animals. This drug-induced rotation test was repeated at 1 week, 1 month and 3 months after administration of BoNT-A treatment.

### 2.4.2 CatWalk Studies

The CatWalk XT (Noldus, Wageningen, Netherlands) apparatus was used to observe and assess gait of voluntarily moving rats (see Chapter 1.4.2 for details). All animals were trained to cross the walkway in a consistent manner prior to any experimentation. Training was performed by placing a sucrose pellet at the end of the walkway in the home cage of

the animal. Animals were then placed on the open end of the platform and allowed to freely traverse the walkway towards their home cage. A gait trial was considered successful if the animal completes the walk across the whole platform within 8 seconds and without any turns. In each session, a minimum of three compliant trials for each rat was recorded and non-compliant trials were excluded from the study.

Training and baseline testing was performed for all rats one week prior to 6-OHDA lesion. Three weeks after 6-OHDA surgery and one week prior to BoNT-A injection, animals were retested on the CatWalk to assess deviations in gait and locomotion. Following BoNT-A treatment, CatWalk testing was repeated at 1 week, 1 month and 3 months for all animal groups.

## 2.5 Perfusion and Tissue Collection

After completion of behavioural studies, animals were sacrificed with an overdose of sodium pentobarbital (250 mg/kg; IP). Once all reflexes were gone, a transcardial perfusion was performed. An abdominal incision was made to enter the body cavity. This opening was extended through the diaphragm, pass the rib cages and into the thoracic cavity to expose the heart. A needle attached to a pump was inserted through the left ventricle into the aorta and an opening was made in the right atrium. 400 mL of 0.9% saline was pumped through the animal to remove the blood, followed by 400 mL of 4% of paraformaldehyde solution to fix the tissue. After the perfusion, brains were removed from the skull and postfixed in the perfusion solution for 24-48 hours. Brains were then transferred and placed in 25-30% sucrose for at least 48 hours for cryoprotection.

## 2.6 Immunohistochemistry

### 2.6.1 Immunofluorescence Staining

Following cryoprotection, brains were cut into blocks containing the region of interest. Blocks were mounted with optimal cutting temperature compound and coronal brain

sections of 40  $\mu\text{m}$  thickness were prepared by a freezing microtome. Every tenth section was collected for immunohistochemical staining. Sections were washed three times with phosphate buffer (PB) and then, blocked in PB containing 0.1% Triton X-100, 15% BSA and animal serum (corresponding to the secondary antibody) for 1 hour at room temperature on a rotator. Primary antibodies were diluted in distilled  $\text{H}_2\text{O}$  containing 15% BSA and animal serum, and incubations were performed overnight at room temperature on a rotator. Refer to Table 2 for a list of primary antibodies used in this study. Following primary antibody incubation, sections were washed three times with PB and either stained with an Alexa Fluor conjugated secondary antibody (Invitrogen by Thermo Fisher Scientific) or with a biotinylated secondary antibody (Vector Laboratories) for 1 hour at room temperature on a rotator. Alexa Fluor 594- conjugated donkey anti-mouse secondary antibody, biotinylated goat anti-mouse secondary antibody and/or biotinylated goat anti-guinea pig antibody were diluted at 1:200 in PB containing 15% BSA and animal serum. After three washes in PB, sections previously incubated with a biotinylated secondary antibody were amplified using the avidin-biotin complex method (Vectastain Elite ABC-HRP Kit, Vector Laboratories) for 1 hour at room temperature on a rotator. Sections were washed three times with PB and further amplified by the tyramide signal amplification method (TSA Biotin System, PerkinElmer) for 10 minutes at room temperature. After three washes in PB, fluorescein avidin DCS (Vector Laboratories) was diluted at 1:250 in PB and sections were incubated for 1.5 hours at room temperature on a rotator. Sections were washed a final three times before being mounted on 1 mm thick Superfrost plus slides (VWR International) and sealed with No. 1 cover glasses (VWR International) with Vectashield antifade mounting medium (Vector Laboratories).

### **2.6.2 TH Staining**

For verification of unilateral 6-OHDA lesioning, staining for tyrosine hydroxylase (TH) at the striatum and substantia nigra was performed. All the same steps as immunofluorescence staining were performed, up to and including amplification with the avidin-biotin complex method. Following three washes, TH was detected by the 3,3'-diaminobenzidine method for 5 minutes (Sigma-Aldrich). Sections were washed a final three times before being mounted on 1 mm thick Superfrost plus slides (VWR International). Sections were then

dehydrated and cleared by transferring slides in increasing concentration of ethanol (75% to 95% to 100% (1) to 100% (2)) for 2 minutes each, followed by two consecutive washes in 100% xylene for 5 minutes. Finally, coverslips were added and sealed with SHUR/Mount xylene-based liquid mounting medium (Triangle Biomedical Sciences Inc).

Table 2 – List of Primary Antibodies for Immunostaining

Antibody	Manufacturer	Catalog #	Clonality	Origin	Dilution
<b>anti-GAD67</b>	EMD Millipore	MAB5406	Monoclonal	Mouse	1:500
<b>anti-GFAP</b>	Sigma Aldrich	G3893	Monoclonal	Mouse	1:250
<b>anti-synaptophysin</b>	Sigma Aldrich	S5768	Monoclonal	Mouse	1:2000
<b>anti-TH</b>	Sigma Aldrich	T1299	Monoclonal	Mouse	1:250
<b>anti-vGluT2</b>	EMD Millipore	AB2251-I	Polyclonal	Guinea Pig	1:1000

### 2.6.3 Microscopy

For immunofluorescence, images were acquired on a Leica TCS SP8 confocal microscope through a HC PL APO 20x/0.7 CS, HC PL APO 40x/1.30 oil CS2 or HC PL APO 63x/1.40 oil CS2 objectives using an excitation wavelength of 488 nm or 594 nm by a 20 mW AOTF diode laser. For each antibody, a minimum of 3 coronal sections per animal were analyzed in order to analyze a minimum range of 1200  $\mu\text{m}$  in depth. For each section of the EPN, an area of 580x580  $\mu\text{m}$  was analyzed at 20x, 290x290  $\mu\text{m}$  at 40x and 193x193  $\mu\text{m}$  at 60x. Images were taken at a z-stack of 33 sections with section interval of 0.6  $\mu\text{m}$  (20x), 0.3  $\mu\text{m}$  (40x) or 0.3 (63x). Acquisition parameters were kept consistent for sections stained with the same antibody. Each series of z-stack images were processed with a maximum intensity projection tool on ImageJ to create a final image with pixels containing the maximum value of the whole stack. The mean intensity of each whole stack was then measured by ImageJ.

For TH staining, images were acquired on a Leica TCS SP8 confocal microscope through a HC PL Fluotar 5x/0.15 dry objective. A minimum of 3 coronal sections per animal were analyzed in order to analyze a minimum range of 1200  $\mu\text{m}$  in depth. Images of complete coronal sections were stitched by LAS X life science software and processed by ImageJ.



## 2.7 Statistical Analysis

All data is expressed as mean  $\pm$  standard error of mean. Statistical analysis was performed using GraphPad Prism 7. All groups were tested with a D'Agostino and Pearson normality test. For analysis of CatWalk data, a comparison of the animals before and after BoNT-A injection was performed with a repeated measures one-way ANOVA followed by a Tukey's post hoc test. For immunofluorescence staining, a comparison of animal groups was performed with a Kruskal-Wallis test followed by a Dunn's post hoc test. Specifically, for GFAP staining, a comparison between untreated and treated rats was analyzed by an unpaired Student's t-test. A critical value for significance of  $p < 0.05$  was used throughout the study.

## Chapter 3

### 3 Results

#### 3.1 Results of the Apomorphine Rotation Test

As expected, subcutaneous injection of apomorphine in sham lesioned rats did not induce any significant rotational behaviour (Timepoint 0 in Figure 4 A and B). Apomorphine in 6-OHDA lesioned animals caused contralateral rotations away from the lesion, with an average of 8.305 rotations per minute in all successfully 6-OHDA lesioned animals (Timepoint 0 in Figure 4 C-E).

Rotational behaviour was tested again at 1 week, 1 month and 3 months following BoNT-A injection into the ipsilateral EPN. Control vehicle (PBS) injections into the EPN did not cause any apomorphine-induced rotations in sham lesioned rats (Figure 4 A), nor did it abolish the pathological contralateral rotations in 6-OHDA lesioned animals (Figure 4 C). Specifically, 6-OHDA animals treated with vehicle injections continued to rotate on apomorphine at an average of 8.358 rotations per minute at 1 week, 8.400 at 1 month, and 8.758 at 3 months. This was insignificantly different from the 8.242 rotations prior to treatment. Injection of 0.5 ng of BoNT-A in sham lesioned animals had no effect on rotational behaviour (i.e. it did not halt nor induce any pathological rotations) (Figure 4 B).

Administration of 0.5 ng of BoNT-A in 6-OHDA lesioned animals significantly abolished the apomorphine-induced rotations completely at 1 week and 1 month post-treatment ( $F(1,10) = 152.7$ ,  $p < 0.0001$ ) (Figure 4 D). Comparison of apomorphine-induced rotations of 6-OHDA lesioned rats prior to and following 0.5 ng BoNT-A administration to the EPN was significant at 1 week ( $p = 0.0001$ ) and 1 month ( $p = 0.0001$ ), but was insignificant at 3 months ( $p = 0.0603$ ). Hemi-PD rats only demonstrated 1.125 rotations per minute at 1 week and 1.080 at 1 month post-treatment. However, the number of rotations per minute returned up to 7.317 after 3 months following BoNT-A injection, which was not significantly different from the group average of 8.433 rotations per minute prior to any treatment.

Dose-response studies have indicated that injections of the lower doses (0.05 ng) of BoNT-A in 6-OHDA lesioned animals mildly reduced the average number of rotations at 1 week ( $F(2,19) = 4.734$ ,  $p = 0.0140$ ), but failed to abolish rotations at 1 month or 3 months (Figure 4 E). The initial reduction at 1 week was weakly significant ( $p = 0.0344$ ) and became insignificant at 1 month ( $p = 0.3199$ ) or 3 months ( $p = 0.417$ ).

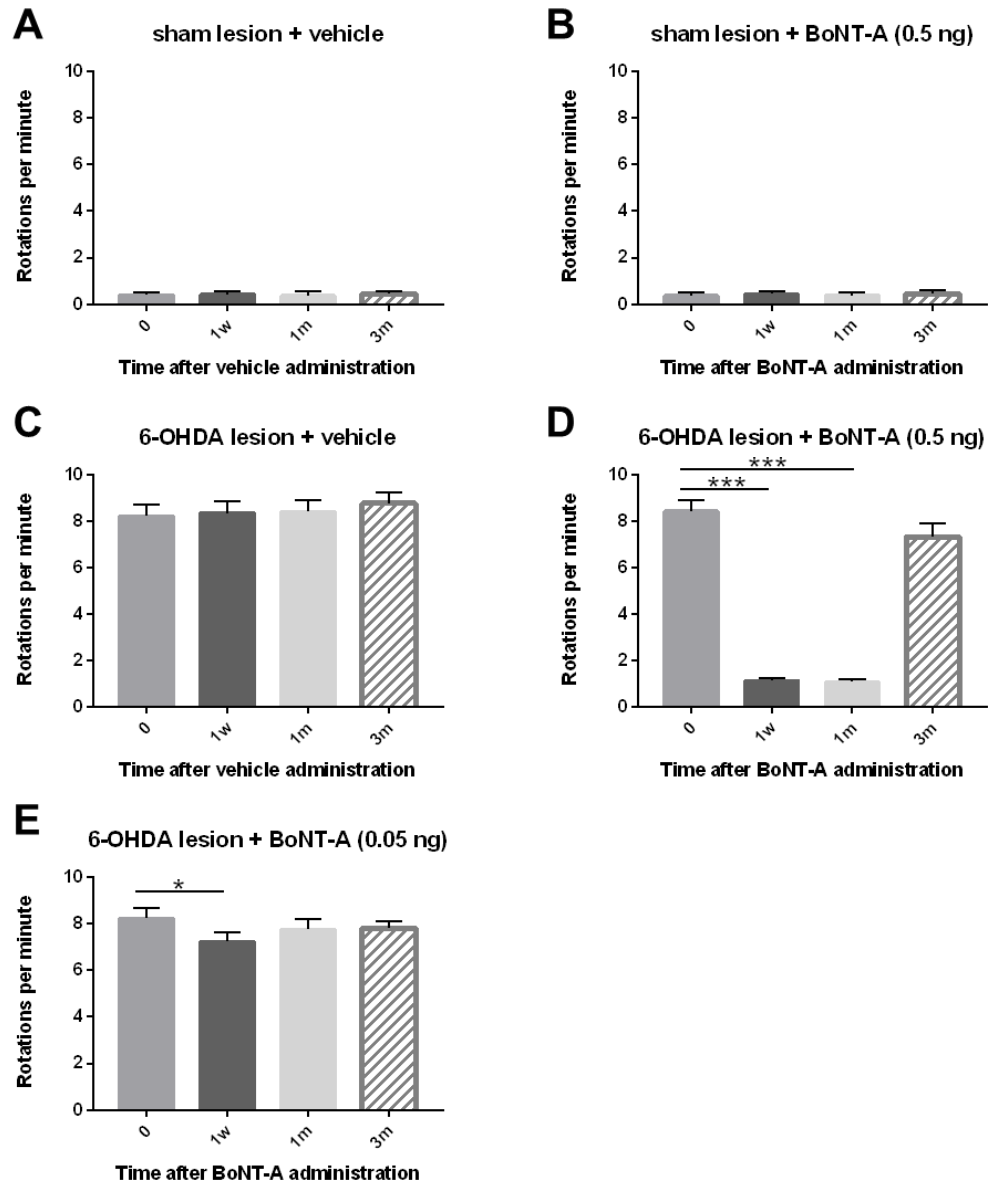


**Figure 4 – Apomorphine-induced rotation of hemi-PD rats treated with BoNT-A**

Changes in apomorphine (0.25 mg/kg) induced rotation after administration of BoNT-A at the EPN (n=8 per group). Control lesioned rats showed no rotations after vehicle (A) or BoNT-A injection (B). Vehicle injection had no effect on pathological rotations in 6-OHDA lesioned rats (C). 0.5 ng of BoNT abrogated rotations in 6-OHDA rats at 1 week and 1 month, but rotations re-emerged at 3 months (D). 0.05 ng of BoNT reduced rotations at 1 week but failed to reduce pathological rotations at 1 month and 3 months (E). All results are presented as mean  $\pm$  sem. Asterisks indicate significant changes compared to initial values (0) according to repeated measures one-way ANOVA and post hoc Tukey test. \* $p < 0.05$  \*\*\* $p < 0.001$

## 3.2 Results of the CatWalk Apparatus

### 3.2.1 Changes in Average Speed

The average speed of animals was determined by using the CatWalk apparatus prior to and following 6-OHDA lesioning of the right MFB. As expected, sham lesioning of the MFB did not significantly change the average speed of animals compared to their naïve state (naïve vs timepoint 0 in Figure 5 A and B). On the other hand, 6-OHDA lesioning of the MFB significantly reduced the average speed of animals from 57.1 cm/s for naïve animals to 34.4 cm/s following lesioning (naïve vs timepoint 0 in Figure 5 C [ $F(2,14) = 34.87$ ,  $p = 0.0046$ ]) and from 51.48 cm/s for naïve animals to 36.39 cm/s following lesioning (naïve vs timepoint 0 in Figure 5 D [ $F(2,17) = 44.96$ ,  $p = 0.0017$ ]).

Average speed was tested again at 1 week, 1 month and 3 months following BoNT-A injection into the ipsilateral EPN. Control vehicle (PBS) injections at the EPN did not alter the average speed of sham lesioned rats (Figure 5 A), nor did it improve the impaired speed of 6-OHDA lesioned animals (Figure 5 C). More specifically, 6-OHDA animals treated with vehicle injections continued to walk at an average speed of 26.49 cm/s at 1 week, 30.5 cm/s at 1 month, and 31.11 cm/s at 3 months. This was not significantly different from the average speed of 34.4 cm/s prior to BoNT-A treatment. Furthermore, injection of 0.5 ng of BoNT-A did not significantly reduce or increase the average speed of sham lesioned animals (Figure 5 B).

Importantly, administration of 0.5 ng of BoNT-A significantly improved the average speed of 6-OHDA lesioned animals at 1 week and 1 month post-treatment ( $F(2,17) = 44.96$ ,  $p < 0.0001$ ) but the change was not significant at 3 months (Figure 5 D). 6-OHDA lesioned rats increased their average speed to 63.37 cm/s at 1 week ( $p < 0.0001$ ) and to 63.74 cm/s at 1 month ( $p = 0.0003$ ) post BoNT-A injection. However, their average speed reduced back to 35.24 cm/s at 3 months, which was similar to their average of 36.69 cm/s prior to BoNT-A administration.

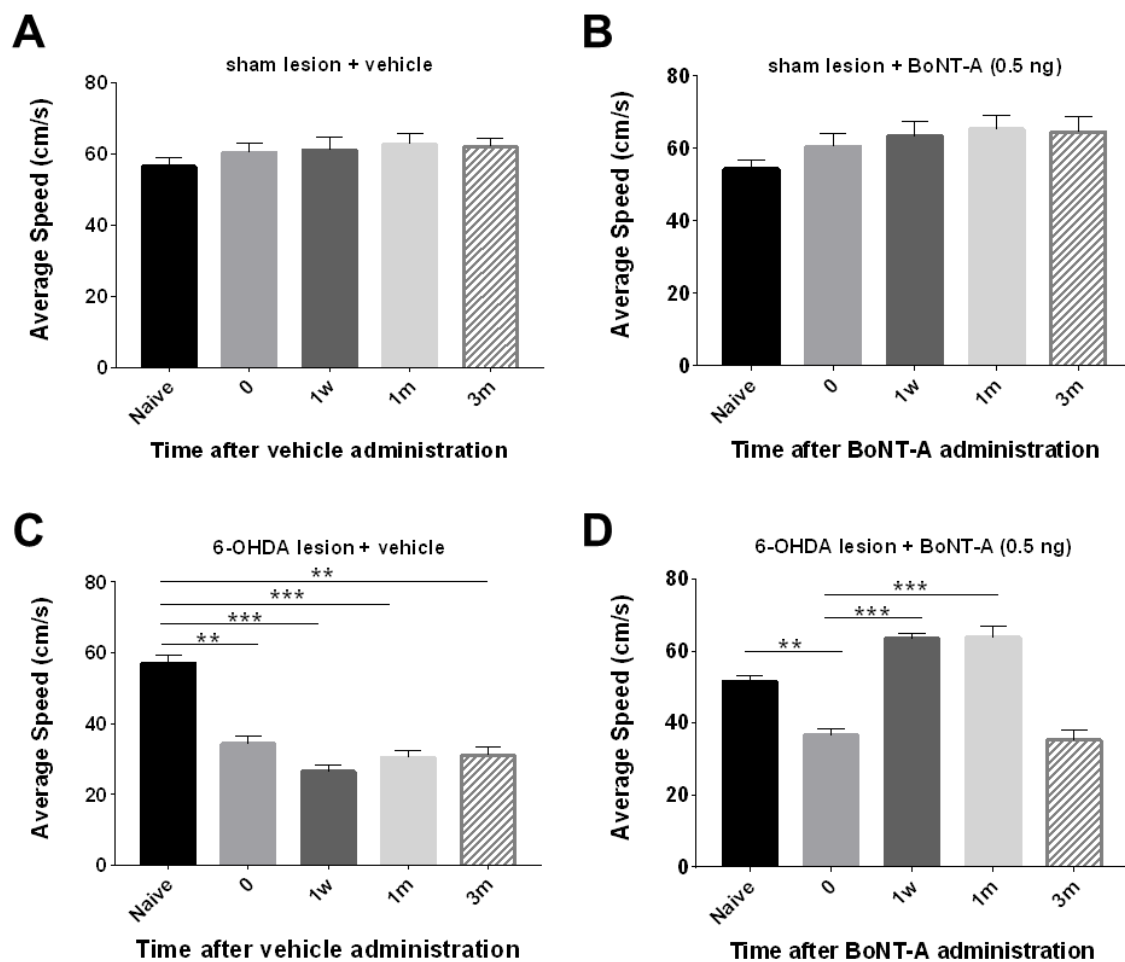


**Figure 5 – Average speed of hemi-PD rats treated with BoNT-A**

Changes in average speed after injection of 0.5 ng of BoNT-A at the EPN (n=8 per group). Experimental timepoints are reflected on the x-axis: naïve rats tested prior to any surgeries, 6-OHDA (or sham lesioned) animals tested at week 0, and BoNT-A (or sham vehicle) animals tested at 1 week, 1 month or 3 months following treatment. Control lesioned rats showed no changes in speed after vehicle (A) or BoNT-A injection (B). Vehicle injection did not improve the slowness of 6-OHDA lesioned rats (C). 0.5 ng of BoNT improved the slowness of 6-OHDA lesioned rats at 1 week and 1 month, but no effect was seen at 3 months (D). All results are presented as mean  $\pm$  sem. Asterisks indicate significant changes compared to pre-lesioned animals (C) or lesioned animals (D) according to repeated measures one-way ANOVA and post hoc Tukey test. \*\*p<0.01 \*\*\*p<0.001

### 3.2.2 Changes in Body Speed Variation

The CatWalk apparatus was also used to detect changes in body speed variation (a measure of consistency of walking speed). Unsurprisingly, sham lesions did not significantly alter the body speed variation of rodents compared to their naïve state (naïve vs timepoint 0 in Figure 6 A and B). However, the body speed variation of animals increased significantly following 6-OHDA lesioning, from 12.73% for naïve animals to 34.16% (naïve vs timepoint 0 in Figure 6 C [ $F(2,17) = 5.076$ ,  $p = 0.0116$ ]) and from 11.21% for naïve animals to 33.19% (naïve vs timepoint 0 in Figure 6 D [ $F(2,14) = 25.99$ ,  $p < 0.0001$ ]).

After BoNT-A injection into the ipsilateral EPN, body speed variation was re-measured. Control vehicle (PBS) injections at the EPN did not change the body speed variation of sham lesioned rats (Figure 6 A), nor did it reduce the higher variation of 6-OHDA lesioned animals (Figure 6 C). 6-OHDA animals treated with PBS injections maintained a body speed variation of 33.76% at 1 week, 30.77% at 1 month, and 29.44% at 3 months, which was insignificant from the 34.16% variation prior to BoNT-A treatment. Likewise, injection of 0.5 ng of BoNT-A in sham lesioned animals had no effect on the body speed variation of sham lesioned animals (Figure 6 B).

Notably, 0.5 ng of BoNT-A injected at the EPN significantly reduced the pathological body speed variation of 6-OHDA lesioned animals at 1 week and 1 month post-treatment ( $F(2,14) = 25.99$ ,  $p < 0.0001$ ), but the effect was insignificant at 3 months (Figure 6 D). After BoNT-A administration, the body speed variation of 6-OHDA lesioned rats decreased to 12.32% at 1 week ( $p = 0.0057$ ) and 9.869% at 1 month ( $p = 0.0024$ ). However, their body speed variation returned back to 31.52% at 3 months, which was insignificant from their body speed variation of 33.19% prior to BoNT-A treatment.

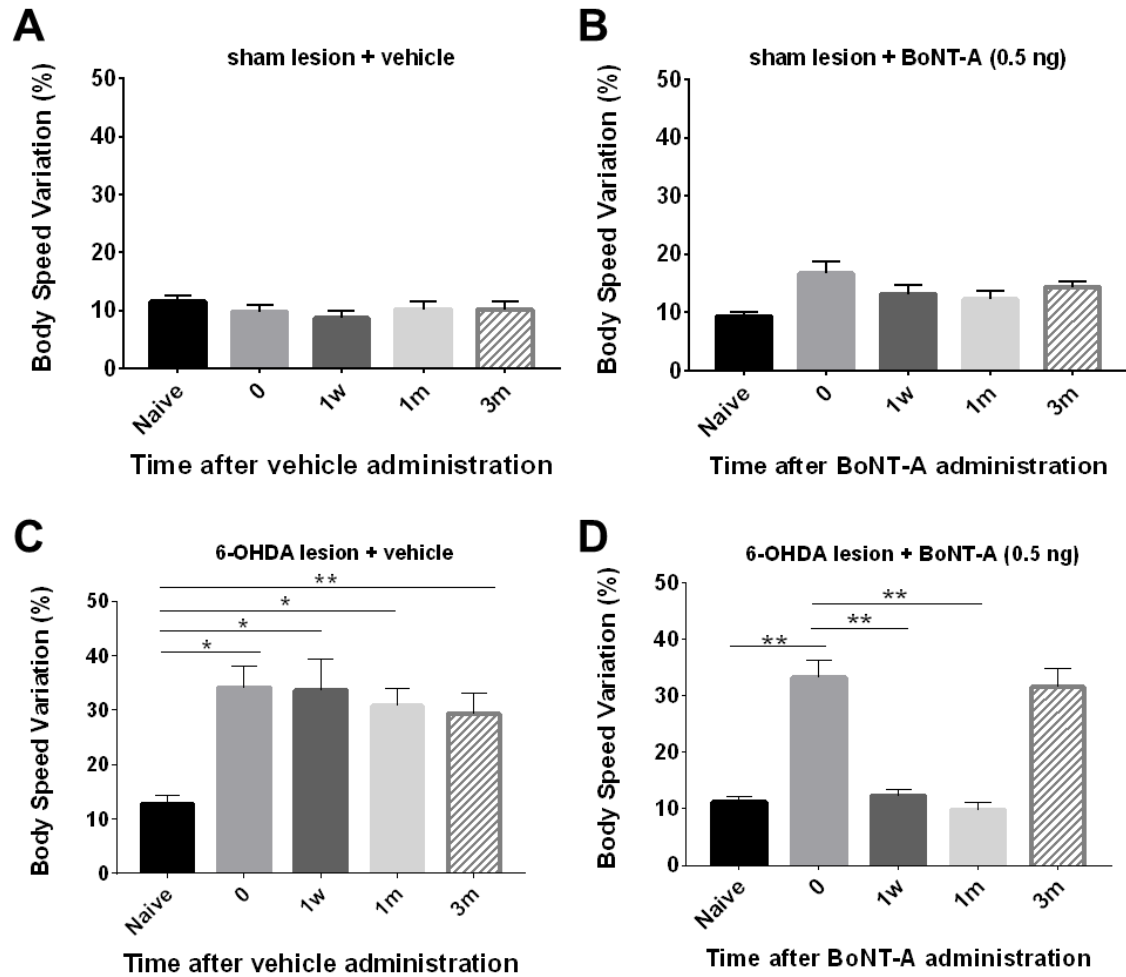


**Figure 6 – Body speed variation of hemi-PD rats treated with BoNT-A**

Changes in body speed variation after infusion of 0.5 ng of BoNT-A at the EPN (n=8 per group). Experimental timepoints are reflected on the x-axis: naïve rats tested prior to any surgeries, 6-OHDA (or sham lesioned) animals tested at week 0, and BoNT-A (or sham vehicle) animals tested at 1week, 1 month or 3 months following treatment. Control lesioned rats showed no changes in body speed variation after vehicle (A) or BoNT-A injection (B). Vehicle injection did not reduce the increased body speed variation of 6-OHDA lesioned rats (C). 0.5 ng of BoNT reduced the body speed variation of 6-OHDA lesioned rats at 1 week and 1 month, but no effect was seen at 3 months (D). All results are presented as mean  $\pm$  sem. Asterisks indicate significant changes compared to pre-lesioned animals (C) or lesioned animals (D) according to repeated measures one-way ANOVA and post hoc Tukey test. \*p<0.05 \*\*p<0.01



### 3.2.3 Changes in Cadence

The cadence (number of steps taken per second) was measured by the CatWalk apparatus before and after 6-OHDA lesioning of the MFB. As expected, sham lesioning of the MFB did not significantly change the cadence compared to their naïve state (naïve vs timepoint 0 in Figure 7 A and B). On the other hand, 6-OHDA lesioning of the MFB significantly reduced the cadence of animals from 11.33 steps per second for naïve animals to 7.156 steps per second following lesioning (naïve vs timepoint 0 in Figure 7 C [ $F(3,25) = 36.75$ ,  $p = 0.0004$ ]) and from 11.11 steps per second for naïve animals to 7.368 steps per second following lesioning (naïve vs timepoint 0 in Figure 7 D [ $F(2,18) = 26.42$ ,  $p = 0.0005$ ]).

Cadence was tested again at 1 week, 1 month and 3 months following BoNT-A injection into the ipsilateral EPN. Control vehicle (PBS) injections at the EPN did not alter the cadence of sham lesioned rats (Figure 7 A), nor did it increase the dysregulated cadence of 6-OHDA lesioned animals (Figure 7 C). More specifically, 6-OHDA animals continued to walk with a cadence of 5.569 steps per second at 1 week, 6.55 steps per second at 1 month, and 6.124 steps per second at 3 months after PBS injections. This was insignificant from the cadence of 7.156 prior to BoNT-A treatment. Furthermore, injection of 0.5 ng of BoNT-A did not significantly reduce or increase the cadence of sham lesioned animals (Figure 7 B).

Importantly, administration of 0.5 ng of BoNT-A significantly improved the cadence of 6-OHDA lesioned animals at 1 week and 1 month post-treatment ( $F(2,18) = 26.42$ ,  $p < 0.0001$ ), but was insignificant at 3 months (Figure 7 D). 6-OHDA lesioned rats increased their cadence to 11.14 steps per second at 1 week ( $p < 0.0001$ ) and 11.94 steps per second at 1 month ( $p = 0.0024$ ) post BoNT-A injection. These values are similar to their cadence of 11.11 steps per second in their naïve state. However, their cadence lowered to 7.099 steps per second at 3 months, which was similar to their average of 7.368 steps per second prior to BoNT-A administration.

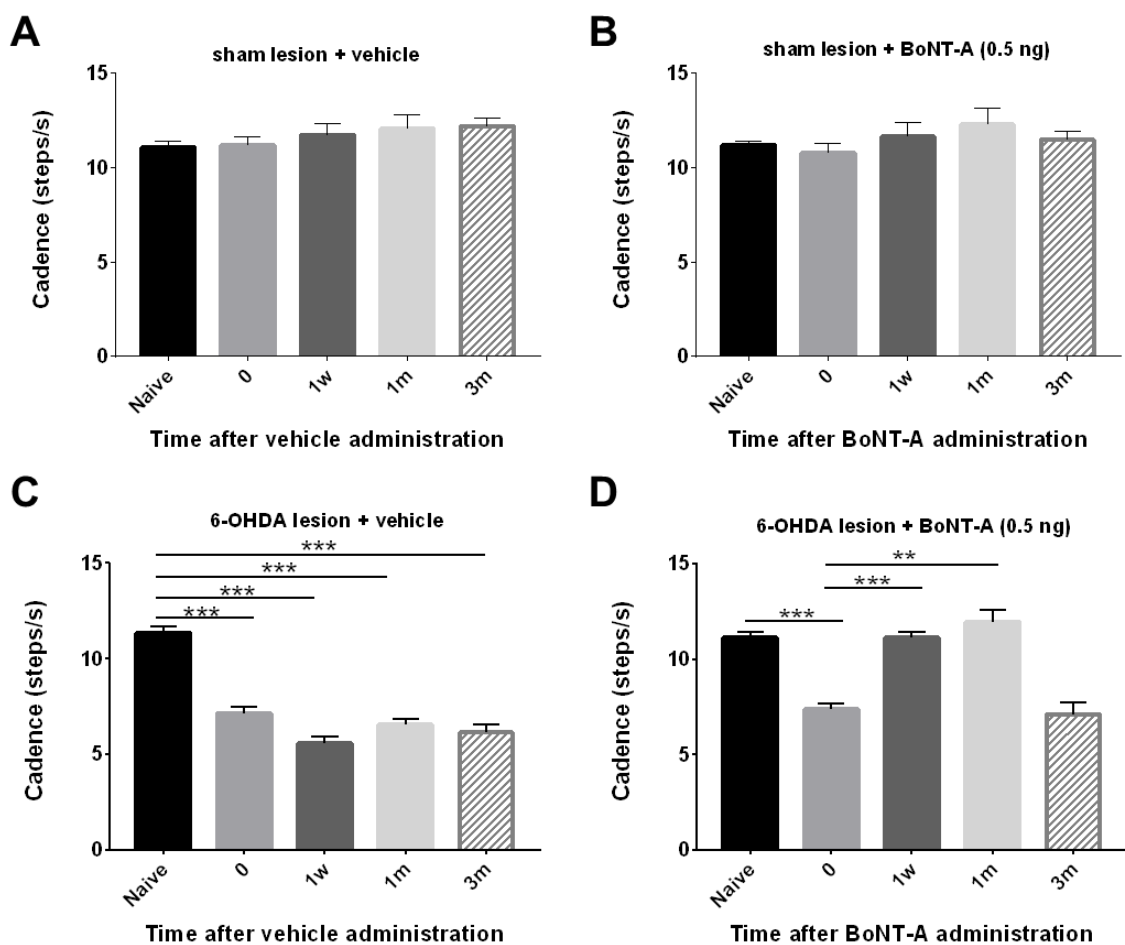


**Figure 7 – Cadence of hemi-PD rats treated with BoNT-A**

Changes in cadence after administration of 0.5 ng of BoNT-A at the EPN (n=8 per group). Experimental timepoints are reflected on the x-axis: naïve rats tested prior to any surgeries, 6-OHDA (or sham lesioned) animals tested at week 0, and BoNT-A (or sham vehicle) animals tested at 1 week, 1 month or 3 months following treatment. Control lesioned rats showed no changes in cadence after vehicle (A) or BoNT-A injection (B). Vehicle injection did not improve the reduction in cadence of 6-OHDA lesioned rats (C). 0.5 ng of BoNT increased the cadence of 6-OHDA lesioned rats at 1 week and 1 month, but no effect was seen at 3 months (D). All results are presented as mean  $\pm$  sem. Asterisks indicate significant changes compared to pre-lesioned animals (C) or lesioned animals (D) according to repeated measures one-way ANOVA and post hoc Tukey test. \*\*p<0.01 \*\*\*p<0.001

### 3.2.4 Changes in Stand

The CatWalk apparatus was used to measure the stand (duration of contact during a step cycle) for each paw (RF: right front, RH: right hind, LF: left front, and LH: left hind). Sham lesioning of the MFB did not significantly alter the stand of animals in any of their paws (naïve vs timepoint 0 in Figure 8 A and B). Furthermore, in these sham lesioned animals, no changes in stand were detected in any of the paws across all timepoints following vehicle injection (Figure 8 A) or 0.5 ng of BoNT-A (Figure 8 B) at the EPN.

Consistent with previous studies, animals demonstrated a significant increase in stand following 6-OHDA lesioning of the MFB (naïve vs timepoint 0 in Figure 8 C and D). In fact, the duration of stand approximately doubled from an average of 0.2084 seconds to 0.3901 seconds across all paws of 6-OHDA lesioned animals,.

After vehicle injection at the EPN, stand across all paws of lesioned animals remained elevated for the following 3 months (Figure 8 C). On the contrary, following administration of 0.5 ng of BoNT-A at the EPN, stand significantly reduced across all paws of lesioned animals (Figure 8 D). At 1 week following BoNT-A infusion, stand significantly reduced to 0.1947 seconds for the RF ( $F(1,9) = 13.64$ ,  $p = 0.0021$ ), 0.2049 seconds for the RH ( $F(1,8) = 15.38$ ,  $p = 0.0002$ ), 0.1927 seconds for the LF ( $F(1,11) = 16.64$ ,  $p = 0.0009$ ) and 0.2041 seconds for the LH ( $F(1,8) = 15$ ,  $p < 0.0001$ ). At 1 month following BoNT-A injection, stand remained significantly reduced at 0.2066 seconds for the RF ( $F(1,9) = 13.64$ ,  $p = 0.0003$ ), 0.2146 seconds for the RH ( $F(1,8) = 15.38$ ,  $p < 0.0001$ ), 0.1956 seconds for the LF ( $F(1,11) = 16.64$ ,  $p = 0.0013$ ) and 0.2203 seconds for the LH ( $F(1,8) = 15$ ,  $p < 0.0001$ ). However, at 3 months following BoNT-A, stand time returned to a longer duration at 0.4146 seconds for the RF, 0.4374 seconds for the RH, 0.3547 seconds for the LF and 0.4659 seconds for the LH.

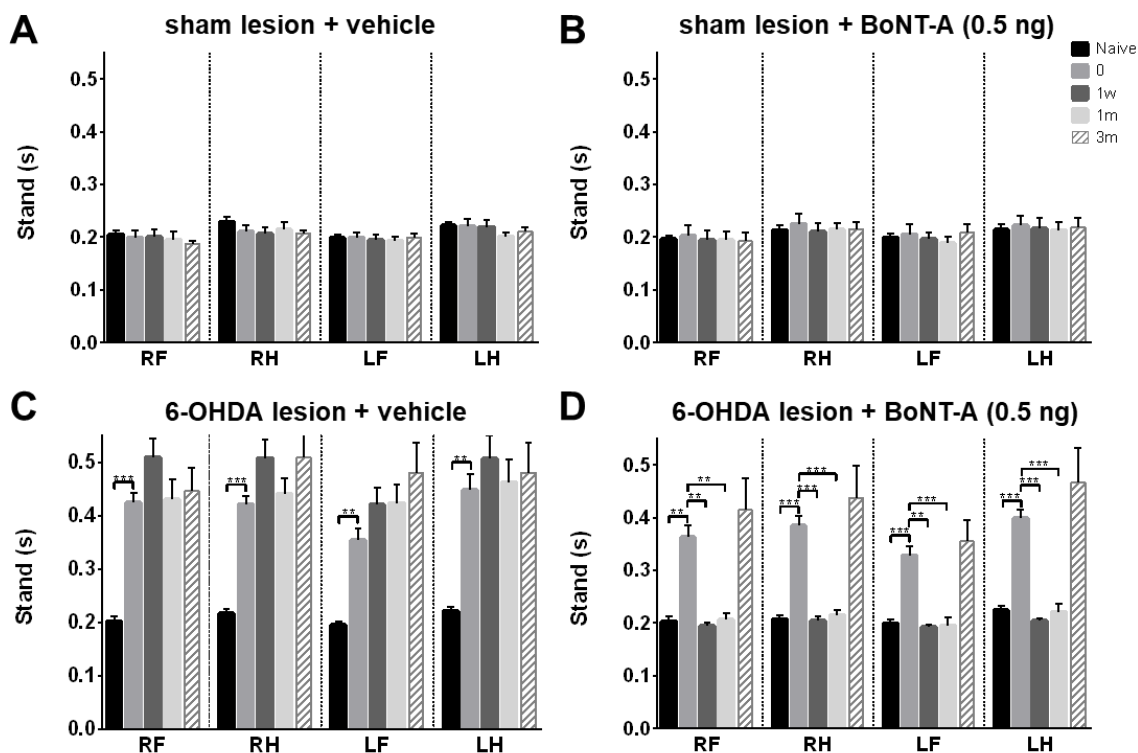


**Figure 8 – Stand of hemi-PD rats treated with BoNT-A**

Changes in stand after injection of 0.5 ng of BoNT-A at the EPN (n=8 per group). Paws were measured individually (RF: right front, RH: right hind, LF: left front, and LH: left hind) and organized on the x-axis. Experimental timepoints are reflected according to the legend: naïve rats tested prior to any surgeries, 6-OHDA (or sham lesioned) animals tested at week 0, and BoNT-A (or sham vehicle) animals tested at 1 week, 1 month or 3 months following treatment. Sham lesioned rats showed no changes in stand after vehicle (A) or BoNT-A injection (B). Vehicle injection did not reduce the increased stand of 6-OHDA lesioned rats (C). 0.5 ng of BoNT decreased the stand of 6-OHDA lesioned rats at 1 week and 1 month, but no effect was seen at 3 months (D). All results are presented as mean  $\pm$  sem. Asterisks indicate significant changes compared to pre-lesioned animals (C) or lesioned animals (D) according to repeated measures one-way ANOVA and post hoc Tukey test. \*\*p<0.01 \*\*\*p<0.001

### 3.2.5 Changes in Swing

Swing, the duration of no contact during a step cycle, was also measured for each paw by the CatWalk apparatus. Sham lesioning of the MFB had no effect on the swing of any of the paws (naïve vs timepoint 0 in Figure 9 A and B). Additionally, in these sham lesioned animals, vehicle injection (Figure 9 A) or 0.5 ng of BoNT-A at the EPN (Figure 9 B) did not significantly alter swing in any of the paws across any timepoint.

On the contrary, animals displayed a significant increase in swing following 6-OHDA lesioning of the MFB (naïve vs timepoint 0 in Figure 9 C and D). The time of swing across all paws increased from an average of 0.1471 seconds in naïve animals to 0.2001 seconds in successfully 6-OHDA lesioned animals.

Following vehicle injection at the EPN of 6-OHDA lesioned animals, swing across all paws remained longer for the following 3 months (Figure 9 C). On the contrary, infusion of 0.5 ng of BoNT-A at the EPN lead to a significant reduction of swing across all paws of lesioned animals (Figure 9 D). At 1 week following BoNT-A injection, swing significantly decreased to 0.1543 seconds for the RF ( $F(1,10) = 9.226$ ,  $p = 0.001$ ), 0.1412 seconds for the RH ( $F(2,14) = 14.5$ ,  $p = 0.0133$ ), 0.1588 seconds for the LF ( $F(1,13) = 6.704$ ,  $p = 0.0258$ ) and 0.1365 seconds for the LH ( $F(1,11) = 20.59$ ,  $p = 0.0046$ ). At 1 month following BoNT-A infusion, swing remained significantly reduced at 0.1542 seconds for the RF ( $F(1,10) = 9.226$ ,  $p = 0.0025$ ), 0.1339 seconds for the RH ( $F(2,14) = 14.5$ ,  $p = 0.0052$ ), 0.1511 seconds for the LF ( $F(1,13) = 6.704$ ,  $p = 0.0154$ ) and 0.1308 seconds for the LH ( $F(1,11) = 20.59$ ,  $p = 0.0042$ ). However, at 3 months following BoNT-A administration, the longer swing duration of lesioned animals re-emerged: 0.1965 seconds for the RF, 0.1834 seconds for the RH, 0.2093 seconds for the LF and 0.1759 seconds for the LH.

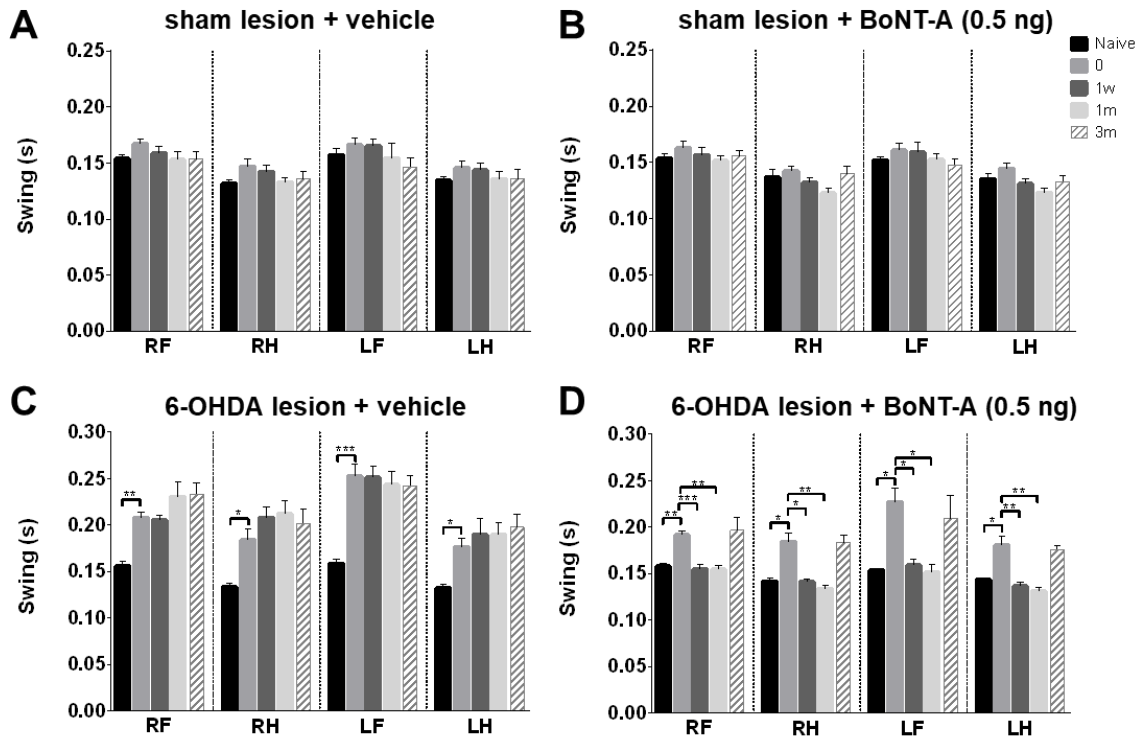


**Figure 9 – Swing of hemi-PD rats treated with BoNT-A**

Changes in swing after infusion of 0.5 ng of BoNT-A at the EPN (n=8 per group). Paws were measured individually (RF: right front, RH: right hind, LF: left front, and LH: left hind) and organized on the x-axis. Experimental timepoints are reflected according to the legend: naïve rats tested prior to any surgeries, 6-OHDA (or sham lesioned) animals tested at week 0, and BoNT-A (or sham vehicle) animals tested at 1 week, 1 month or 3 months following treatment. Sham lesioned rats showed no changes in swing after vehicle (A) or BoNT-A injection (B). Vehicle injection did not reduce the increased swing of 6-OHDA lesioned rats (C). 0.5 ng of BoNT decreased the swing of 6-OHDA lesioned rats at 1 week and 1 month, but no effect was seen at 3 months (D). All results are presented as mean  $\pm$  sem. Asterisks indicate significant changes compared to pre-lesioned animals (C) or lesioned animals (D) according to repeated measures one-way ANOVA and post hoc Tukey test. \* $p < 0.05$  \*\* $p < 0.01$  \*\*\* $p < 0.001$

### 3.2.6 Changes in Step Cycle

Step cycle (also referred to as stride), which is the duration between two consecutive contacts of the same paw, was measured by the CatWalk apparatus. Step cycle was not significantly affected by sham lesioning of the MFB (naïve vs timepoint 0 in Figure 10 A and B). Moreover, vehicle injection (Figure 10 A) or 0.5 ng of BoNT-A at the EPN (Figure 10 B) in these sham lesioned control animals had no significant effect in step cycle in any of the paws across all experimental timepoints.

Consistent with the changes seen in stand and swing, 6-OHDA lesioning of the MFB resulted in a significant increase in step cycle (naïve vs timepoint 0 in Figure 10 C and D). The step cycle across all paws increased from an average of 0.3539 seconds in naïve animals to 0.5868 seconds in 6-OHDA lesioned animals.

In 6-OHDA lesioned animals, vehicle injection at the EPN had no effect on the elevated step cycle in all paws (Figure 10 C). Injection of 0.5 ng of BoNT-A at the EPN significantly reduced the step cycle across all paws of 6-OHDA lesioned animals (Figure 10 D). At 1 week following BoNT-A infusion, step cycle significantly decreased to 0.3494 seconds for the RF ( $F(1,8) = 9.739$ ,  $p = 0.0025$ ), 0.3448 seconds for the RH ( $F(1,8) = 14.28$ ,  $p = 0.0009$ ), 0.3540 seconds for the LF ( $F(1,11) = 12.65$ ,  $p = 0.0023$ ) and 0.3421 seconds for the LH ( $F(1,9) = 15.07$ ,  $p = 0.0002$ ). At 1 month following BoNT-A injection, step cycle remained significantly reduced at 0.3623 seconds for the RF ( $F(1,8) = 9.739$ ,  $p = 0.0008$ ), 0.3471 seconds for the RH ( $F(1,8) = 14.28$ ,  $p = 0.0003$ ), 0.3450 seconds for the LF ( $F(1,11) = 12.65$ ,  $p = 0.0028$ ) and 0.3507 seconds for the LH ( $F(1,9) = 15.07$ ,  $p = 0.0002$ ). However, at 3 months following BoNT-A administration, the longer step cycle of lesioned animals re-emerged: 0.648 seconds for the RF, 0.6314 seconds for the RH, 0.5811 seconds for the LF and 0.6431 seconds for the LH.

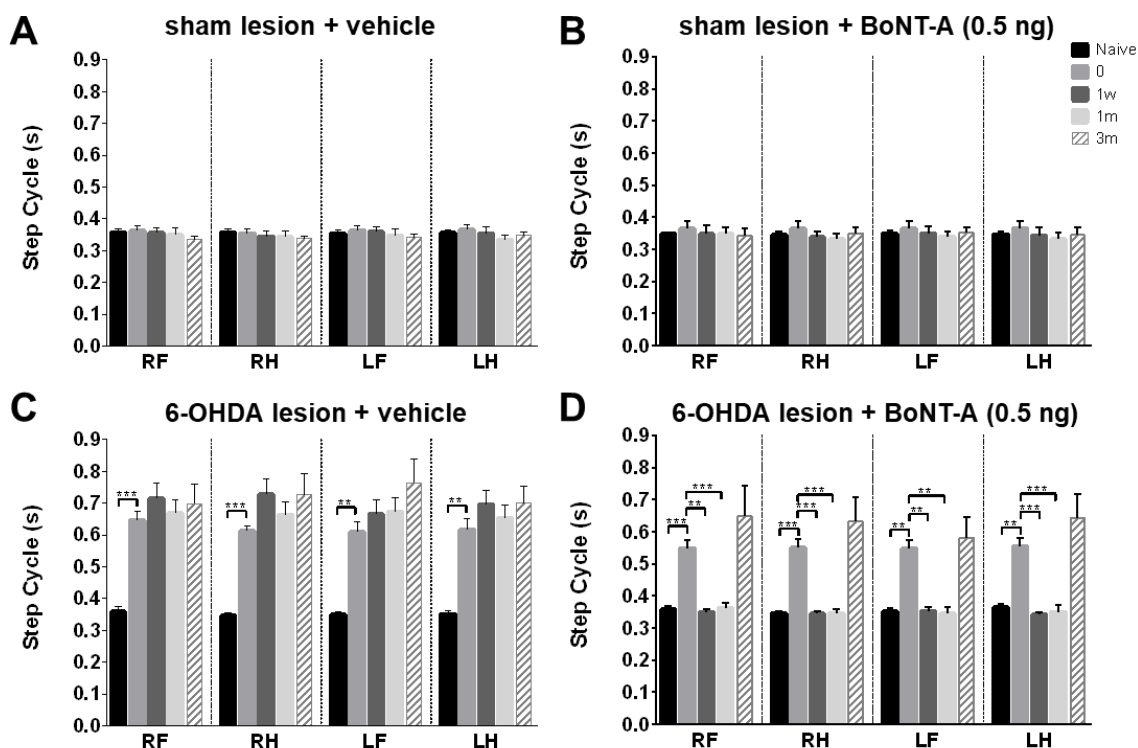


**Figure 10 – Step cycle of hemi-PD rats treated with BoNT-A**

Changes in step cycle after injection of 0.5 ng of BoNT-A at the EPN (n=8 per group). Paws were measured individually (RF: right front, RH: right hind, LF: left front, and LH: left hind) and organized on the x-axis. Experimental timepoints are reflected according to the legend: naïve rats tested prior to any surgeries, 6-OHDA (or sham lesioned) animals tested at week 0, and BoNT-A (or sham vehicle) animals tested at 1 week, 1 month or 3 months following treatment. Sham lesioned rats showed no changes in step cycle after vehicle (A) or BoNT-A injection (B). Vehicle injection did not reduce the increased step cycle of 6-OHDA lesioned rats (C). 0.5 ng of BoNT decreased the step cycle of 6-OHDA lesioned rats at 1 week and 1 month, but no effect was seen at 3 months (D). All results are presented as mean  $\pm$  sem. Asterisks indicate significant changes compared to pre-lesioned animals (C) or lesioned animals (D) according to repeated measures one-way ANOVA and post hoc Tukey test. \*\*p<0.01 \*\*\*p<0.001



### 3.2.7 Changes in Duty Cycle

The CatWalk apparatus was also used to detect changes in duty cycle, which is stand represented as a percentage of step cycle. No significant changes in duty cycle were detected following sham lesioning of the MFB (naïve vs timepoint 0 in Figure 11 A and B). Similarly, vehicle injection (Figure 11 A) or 0.5 ng of BoNT-A at the EPN (Figure 11 B) in these sham lesioned control animals did not affect duty cycle of the paws.

Along with the changes seen in stand and step cycle, 6-OHDA lesioning of the MFB lead to a significant increase in duty cycle (naïve vs timepoint 0 in Figure 11 C and D). Duty cycle across all paws increased from an average of 56.68 in naïve animals to 64.08% in 6-OHDA lesioned animals.

In these lesioned animals, vehicle injection at the EPN did not affect the increased duty cycle in any paw (Figure 11 C). On the contrary, infusion of 0.5 ng of BoNT-A at the EPN significantly decreased the duty across all paws of 6-OHDA lesioned animals (Figure 11 D). After 1 week of BoNT-A injection, duty cycle significantly returned to 55.04% for the RF ( $F(2,19) = 8.601, p = 0.0045$ ), 56.38% for the RH ( $F(1,12) = 8.028, p = 0.0041$ ), 54.61% for the LF ( $F(1,12) = 7.771, p = 0.0075$ ) and 58.95% for the LH ( $F(2,14) = 7.947, p = 0.0006$ ). After 1 month, the reduced duty cycle persisted significantly at 55.99% for the RF ( $F(2,19) = 8.601, p = 0.0336$ ), 59.57% for the RH ( $F(1,12) = 8.028, p = 0.0007$ ), 54.76% for the LF ( $F(1,12) = 7.771, p = 0.0312$ ) and 59.66% for the LH ( $F(2,14) = 7.947, p = 0.0091$ ). However, after 3 months following BoNT-A injection, the duty cycle of parkinsonian animals increased to 64.52% for the RF, 65.33% for the RH, 60.91% for the LF and 67.49% for the LH.

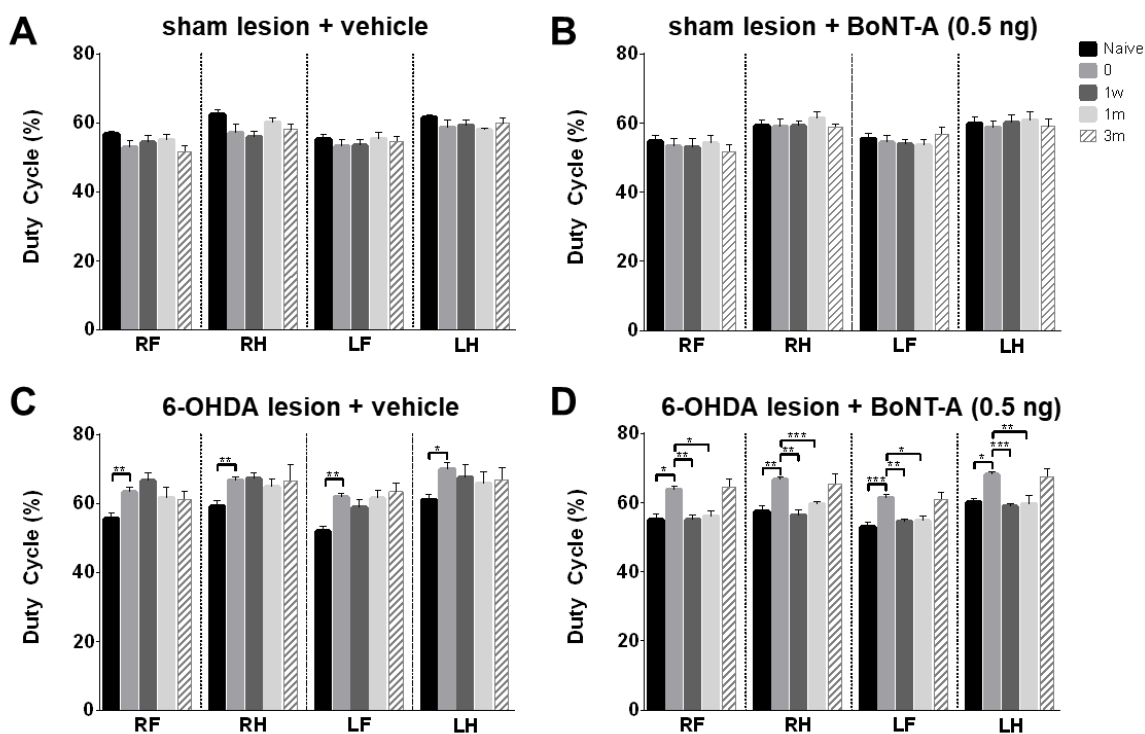


**Figure 11 – Duty cycle of hemi-PD rats treated with BoNT-A**

Changes in duty cycle after administration of 0.5 ng of BoNT-A at the EPN (n=8 per group). Paws were measured individually (RF: right front, RH: right hind, LF: left front, and LH: left hind) and organized on the x-axis. Experimental timepoints are reflected according to the legend: naïve rats tested prior to any surgeries, 6-OHDA (or sham lesioned) animals tested at week 0, and BoNT-A (or sham vehicle) animals tested at 1 week, 1 month or 3 months following treatment. Sham lesioned rats showed no changes in duty cycle after vehicle (A) or BoNT-A injection (B). Vehicle injection did not reduce the increased duty cycle of 6-OHDA lesioned rats (C). 0.5 ng of BoNT decreased the duty cycle of 6-OHDA lesioned rats at 1 week and 1 month, but no effect was seen at 3 months (D). All results are presented as mean  $\pm$  sem. Asterisks indicate significant changes compared to pre-lesioned animals (C) or lesioned animals (D) according to repeated measures one-way ANOVA and post hoc Tukey test. \* $p < 0.05$  \*\* $p < 0.01$  \*\*\* $p < 0.001$

### **3.2.8 Changes in Single Stance**

Single stance, the duration of contact for a single paw when the contralateral paw is in swing, was also measured by the CatWalk apparatus. Sham lesioning of the MFB did not significantly affect single stance (naïve vs timepoint 0 in Figure 12 A and B). Likewise, single stance was unaffected by vehicle injection (Figure 12 A) or 0.5 ng of BoNT-A at the EPN (Figure 12 B) in these sham lesioned control animals.

Consistent with other CatWalk studies involving parkinsonian rodents, 6-OHDA lesioning of the MFB resulted in a significant increase in single stance (naïve vs timepoint 0 in Figure 12 C and D). Single stance across all paws increased from an average of 0.1422 seconds in naïve animals to 0.1955 seconds in 6-OHDA lesioned animals.

In these 6-OHDA lesioned animals, vehicle injection at the EPN had no effect on the increased single stance in any paw (Figure 12 C). However, injection of 0.5 ng of BoNT-A at the EPN significantly decreased the single stance across all paws of 6-OHDA lesioned animals (Figure 12 D). Following 1 week of BoNT-A injection, single stance significantly decreased to 0.1535 seconds for the RF ( $F(1,12) = 12.19, p = 0.0065$ ), 0.1335 seconds for the RH ( $F(2,14) = 12.92, p = 0.0063$ ), 0.1484 seconds for the LF ( $F(2,18) = 10.21, p = 0.0005$ ) and 0.1363 seconds for the LH ( $F(2,15) = 13.54, p = 0.0201$ ). After 1 month, the reduced single stance remained significantly lower at 0.1533 seconds for the RF ( $F(1,12) = 12.19, p = 0.0004$ ), 0.1254 seconds for the RH ( $F(2,14) = 12.92, p = 0.0052$ ), 0.1488 seconds for the LF ( $F(2,18) = 10.21, p = 0.0020$ ) and 0.1296 seconds for the LH ( $F(2,15) = 13.54, p = 0.0050$ ). However, 3 months following BoNT-A injection, the single stance of lesioned animals returned to 0.2126 seconds for the RF, 0.1680 seconds for the RH, 0.1729 seconds for the LF and 0.1815 seconds for the LH.

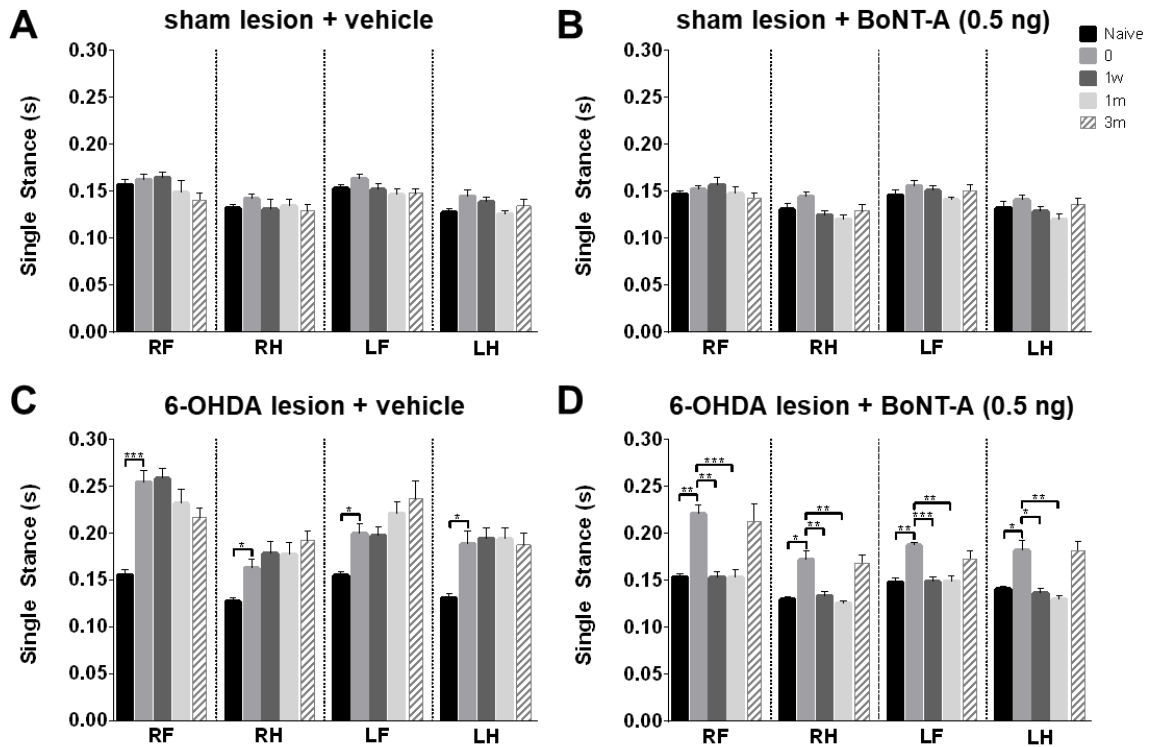


**Figure 12 – Single stance of hemi-PD rats treated with BoNT-A**

Changes in single stance after infusion of 0.5 ng of BoNT-A at the EPN (n=8 per group). Paws were measured individually (RF: right front, RH: right hind, LF: left front, and LH: left hind) and organized on the x-axis. Experimental timepoints are reflected according to the legend: naïve rats tested prior to any surgeries, 6-OHDA (or sham lesioned) animals tested at week 0, and BoNT-A (or sham vehicle) animals tested at 1 week, 1 month or 3 months following treatment. Sham lesioned rats showed no changes in single stance after vehicle (A) or BoNT-A injection (B). Vehicle injection did not reduce the increased single stance of 6-OHDA lesioned rats (C). 0.5 ng of BoNT decreased the single stance of 6-OHDA lesioned rats at 1 week and 1 month, but no effect was seen at 3 months (D). All results are presented as mean  $\pm$  sem. Asterisks indicate significant changes compared to pre-lesioned animals (C) or lesioned animals (D) according to repeated measures one-way ANOVA and post hoc Tukey test. \*p<0.05 \*\*p<0.01 \*\*\*p<0.001

### **3.2.9 Changes in Initial Dual Stance**

The CatWalk apparatus was also used to detect initial dual stance, the duration of the first step in a step cycle of a paw that the contralateral paw also contacts the walkway. Sham lesioning of the MFB had no significant effect on initial dual stance (naïve vs timepoint 0 in Figure 13 A and B). Furthermore, in these sham lesioned control animals, initial dual stance was neither affected by vehicle injection (Figure 13 A) or 0.5 ng of BoNT-A at the EPN (Figure 13 B).

Following 6-OHDA lesioning of the MFB, a significant increase in initial dual stance was observed across all paws (naïve vs timepoint 0 in Figure 13 C and D). Initial dual stance across all paws increased from an average of 0.0358 seconds in naïve animals to 0.1072 seconds in 6-OHDA lesioned animals.

Subsequently, vehicle injection at the EPN of 6-OHDA lesioned animals had no effect on the increased initial dual stance in any paw (Figure 13 C). However, administration of 0.5 ng of BoNT-A at the EPN significantly decreased the initial dual stance across all paws of 6-OHDA lesioned animals (Figure 13 D). At 1 week following BoNT-A injection, initial dual stance significantly decreased to 0.0309 seconds for the RF ( $F(1,9) = 8.499$ ,  $p = 0.0337$ ), 0.0380 seconds for the RH ( $F(1,9) = 7.302$ ,  $p = 0.0268$ ), 0.0185 seconds for the LF ( $F(1,7) = 1.952$ ,  $p = 0.0035$ ) and 0.0355 seconds for the LH ( $F(1,8) = 5.502$ ,  $p = 0.0058$ ). At 1 month, the shorter initial dual stance remained significantly lower at 0.0487 seconds for the RH ( $F(1,9) = 7.302$ ,  $p = 0.0494$ ), 0.0236 seconds for the LF ( $F(1,7) = 1.952$ ,  $p = 0.0103$ ) and 0.0485 seconds for the LH ( $F(1,8) = 5.502$ ,  $p = 0.0179$ ), however was insignificant at 0.0414 seconds for the RF. At 3 months following BoNT-A injection, the initial dual stance of lesioned animals returned to 0.1139 seconds for the RF, 0.1585 seconds for the RH, 0.1342 seconds for the LF and 0.1229 seconds for the LH.

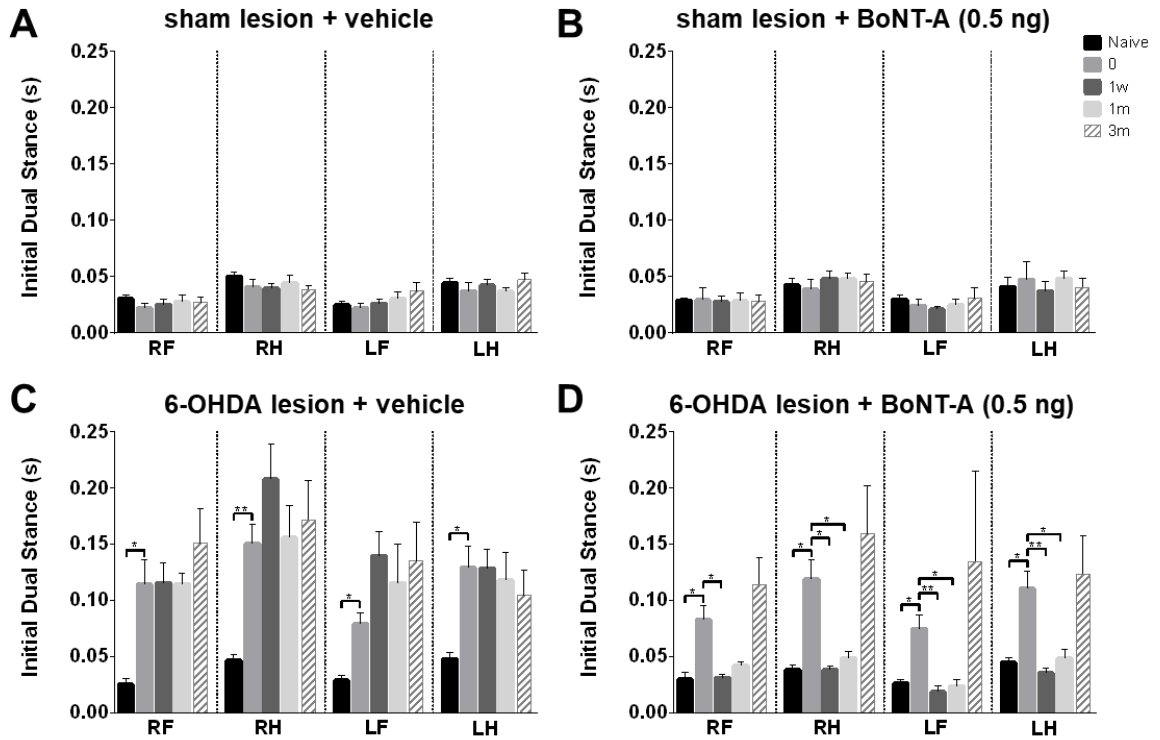


**Figure 13 – Initial dual stance of hemi-PD rats treated with BoNT-A**

Changes in initial dual stance after administration of 0.5 ng of BoNT-A at the EPN (n=8 per group). Paws were measured individually (RF: right front, RH: right hind, LF: left front, and LH: left hind) and organized on the x-axis. Experimental timepoints are reflected according to the legend: naïve rats tested prior to any surgeries, 6-OHDA (or sham lesioned) animals tested at week 0, and BoNT-A (or sham vehicle) animals tested at 1 week, 1 month or 3 months following treatment. Sham lesioned rats showed no changes in initial dual stance after vehicle (A) or BoNT-A injection (B). Vehicle injection did not reduce the increased initial dual stance of 6-OHDA lesioned rats (C). 0.5 ng of BoNT decreased the initial dual stance of 6-OHDA lesioned rats at 1 week and 1 month, but no effect was seen at 3 months (D). All results are presented as mean  $\pm$  sem. Asterisks indicate significant changes compared to pre-lesioned animals (C) or lesioned animals (D) according to repeated measures one-way ANOVA and post hoc Tukey test. \*p<0.05 \*\*p<0.01 \*\*\*p<0.001

### **3.2.10 Changes in Terminal Dual Stance**

Terminal dual stance, the duration of the second step in a step cycle of a paw that the contralateral paw also contacts the walkway, was also measured by the CatWalk apparatus. No significant changes in terminal dual stance were detected following sham lesioning of the MFB (naïve vs timepoint 0 in Figure 14 A and B). Similarly, vehicle injection (Figure 14 A) or 0.5 ng of BoNT-A at the EPN (Figure 14 B) in these sham lesioned control animals did not affect the terminal dual stance of the paws.

Following 6-OHDA lesioning of the MFB, a significant increase in terminal dual stance was detected only in the left paws (naïve vs timepoint 0 in Figure 14 C and D). Terminal dual stance of the LF increased from 0.0256 seconds in naïve animals to 0.1164 seconds in 6-OHDA lesioned animals, and from 0.0440 seconds to 0.1356 seconds for the LH. Although an increase in terminal dual stance was observed in the right paws, it was not significant.

In 6-OHDA lesioned animals, vehicle injection at the EPN had no effect on the increased terminal dual stance of the left paws (Figure 14 C). However, injection of 0.5 ng of BoNT-A at the EPN significantly decreased the terminal dual stance in the left paws of 6-OHDA lesioned animals (Figure 14 D). At 1 week post-BoNT-A injection, terminal dual stance significantly decreased to 0.0288 seconds for the LF ( $F(1,10) = 11.31, p = 0.0057$ ) and to 0.0381 seconds for the LH ( $F(1,7) = 8.025, p = 0.0011$ ). At 1 month post-BoNT-A, terminal dual stance remained significantly decreased at 0.0345 seconds for the LF ( $F(1,10) = 11.31, p = 0.0181$ ) and 0.0493 seconds for the LH ( $F(1,7) = 8.025, p = 0.0049$ ). However, at 3 months post-BoNT-A injection, the terminal dual stance of lesioned animals increased to 0.1022 seconds for the LF and 0.1704 seconds for the LH.

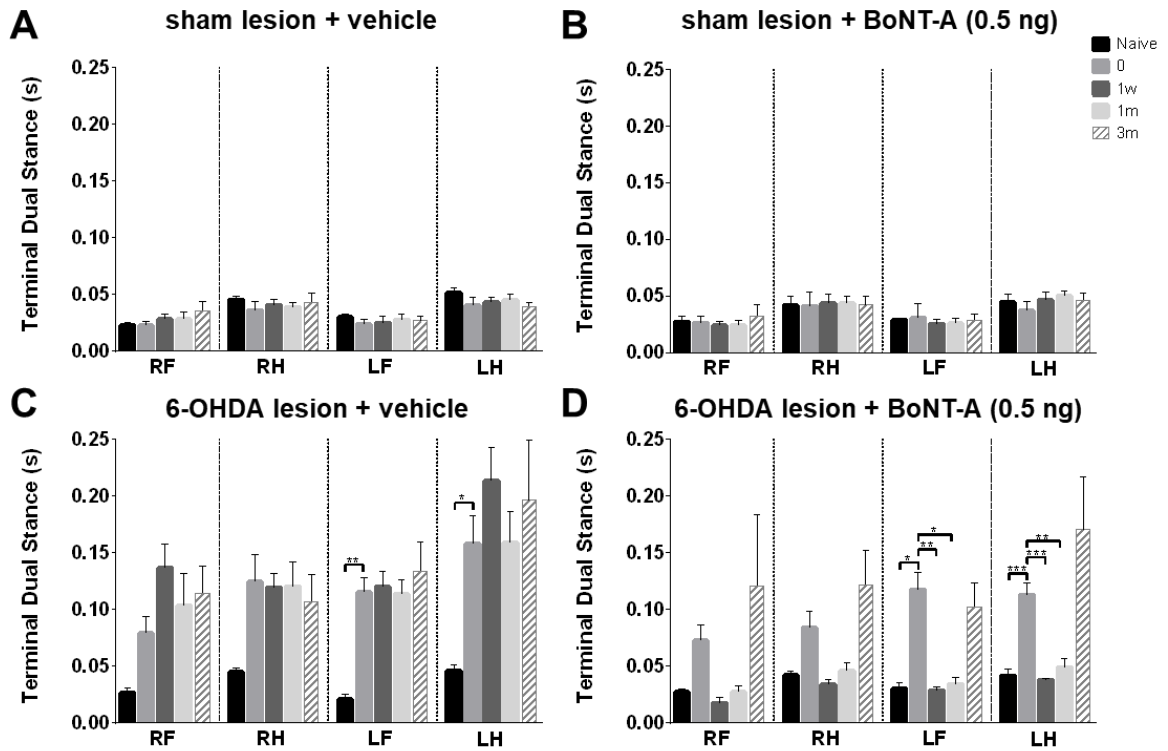


**Figure 14 – Terminal dual stance of hemi-PD rats treated with BoNT-A**

Changes in terminal dual stance after injection of 0.5 ng of BoNT-A at the EPN (n=8 per group). Paws were measured individually (RF: right front, RH: right hind, LF: left front, and LH: left hind) and organized on the x-axis. Experimental timepoints are reflected according to the legend: naïve rats tested prior to any surgeries, 6-OHDA (or sham lesioned) animals tested at week 0, and BoNT-A (or sham vehicle) animals tested at 1 week, 1 month or 3 months following treatment. Sham lesioned rats showed no changes in terminal dual stance after vehicle (A) or BoNT-A injection (B). Vehicle injection did not reduce the increased terminal dual stance in the left paws of 6-OHDA lesioned rats (C). 0.5 ng of BoNT decreased the terminal dual stance in the left paws of 6-OHDA lesioned rats at 1 week and 1 month, but no effect was seen at 3 months (D). All results are presented as mean  $\pm$  sem. Asterisks indicate significant changes compared to pre-lesioned animals (C) or lesioned animals (D) according to repeated measures one-way ANOVA and post hoc Tukey test. \*p<0.05 \*\*p<0.01 \*\*\*p<0.001



### **3.2.11 Changes in Swing Speed**

The CatWalk apparatus was also used to detect the swing speed across all paws. Sham lesioning of the MFB did not significantly affect the swing speed of animals in any of their paws (naïve vs timepoint 0 in Figure 15 A and B). Additionally, in these control animals, vehicle injection (Figure 15 A) or 0.5 ng of BoNT-A at the EPN (Figure 15 B) did not significantly alter swing speed in any of the paws across all experimental timepoints.

Swing speed significantly decreased following 6-OHDA lesioning of the MFB (naïve vs timepoint 0 in Figure 15 C and D). The average swing speed across all paws reduced from 148.8 cm/seconds in naïve animals to 114.8 cm/seconds in 6-OHDA lesioned animals.

In these 6-OHDA lesioned animals, vehicle injection at the EPN had no significant effects on swing speed in any paw (Figure 15 C). Infusion of 0.5 ng of BoNT-A at the EPN significantly increased the swing speed across all paws of 6-OHDA lesioned animals (Figure 15 D). At 1 week after BoNT-A administration, swing speed significantly increased to 159.0 cm/seconds for the RF ( $F(2,18) = 18.47, p = 0.0001$ ), 169.2 cm/seconds for the RH ( $F(2,16) = 20.89, p = 0.0003$ ), 153.4 cm/seconds for the LF ( $F(2,17) = 10.29, p = 0.0037$ ) and 174.6 cm/seconds for the LH ( $F(2,18) = 30.24, p = 0.0008$ ). At 1 month after BoNT-A injection, swing speed remained significantly elevated at 163.0 cm/seconds for the RF ( $F(2,18) = 18.47, p = 0.0022$ ), 181.3 cm/seconds for the RH ( $F(2,16) = 20.89, p = 0.0023$ ), 161.9 cm/seconds for the LF ( $F(2,17) = 10.29, p = 0.0010$ ) and 186.6 cm/seconds for the LH ( $F(2,18) = 30.24, p = 0.0008$ ). However, at 3 months after BoNT-A infusion, lesioned animals returned to a slower swing speed, 118.7 cm/seconds for the RF, 121.5 cm/seconds for the RH, 125.9 cm/seconds for the LF and 128.3 cm/seconds for the LH.

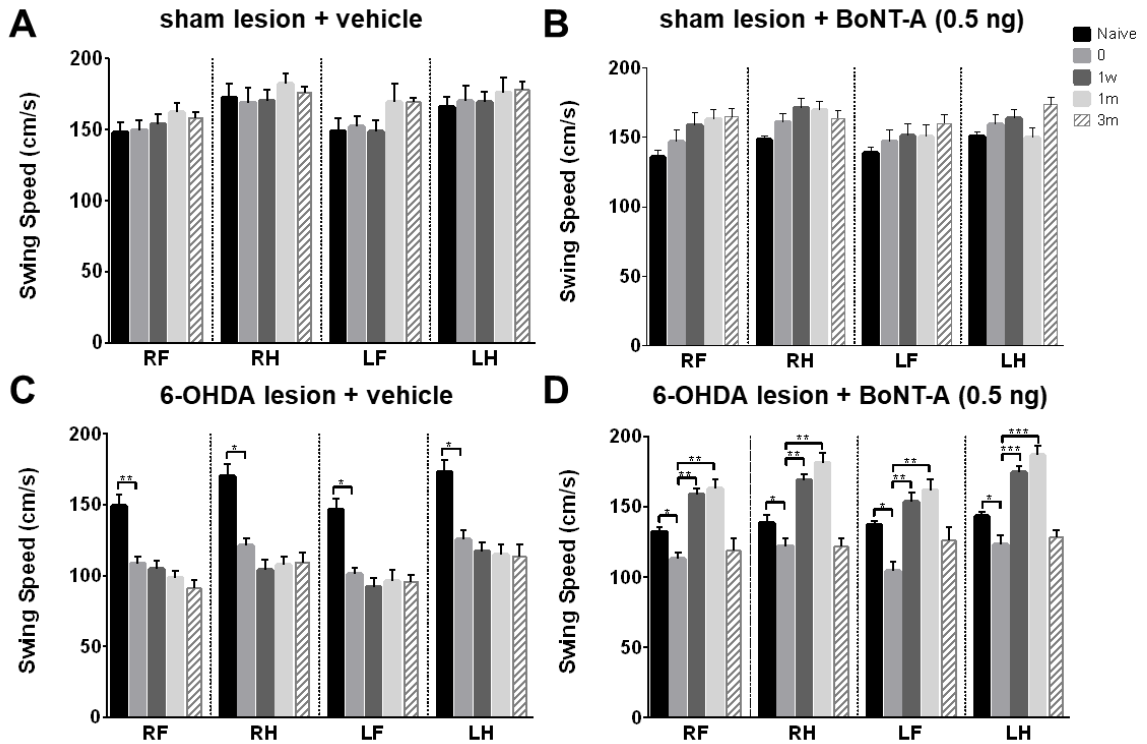


**Figure 15 – Swing speed of hemi-PD rats treated with BoNT-A**

Changes in swing speed after infusion of 0.5 ng of BoNT-A at the EPN (n=8 per group). Paws were measured individually (RF: right front, RH: right hind, LF: left front, and LH: left hind) and organized on the x-axis. Experimental timepoints are reflected according to the legend: naïve rats tested prior to any surgeries, 6-OHDA (or sham lesioned) animals tested at week 0, and BoNT-A (or sham vehicle) animals tested at 1 week, 1 month or 3 months following treatment. Sham lesioned rats showed no changes in swing speed after vehicle (A) or BoNT-A injection (B). Vehicle injection did not improve the reduced swing speed of 6-OHDA lesioned rats (C). 0.5 ng of BoNT increased the swing speed of 6-OHDA lesioned rats at 1 week and 1 month, but no effect was seen at 3 months (D). All results are presented as mean  $\pm$  sem. Asterisks indicate significant changes compared to pre-lesioned animals (C) or lesioned animals (D) according to repeated measures one-way ANOVA and post hoc Tukey test. \*p<0.05 \*\*p<0.01 \*\*\*p<0.001

### **3.2.12 Changes in Stride Length**

The stride length, the distance between two consecutive placements of the same paw, was also measured by the CatWalk apparatus. Stride length was not significantly affected by sham lesioning of the MFB (naïve vs timepoint 0 in Figure 16 A and B). Furthermore, following vehicle injection (Figure 16 A) or 0.5 ng of BoNT-A (Figure 16 B) at the EPN, no changes in stride length were detected in any of the paws of sham lesioned animals.

6-OHDA lesioning of the MFB resulted in a slight reduction in stride length but no significance was detected (naïve vs timepoint 0 in Figure 16 C and D). The average stride length across all paws decreased insignificantly from 22.03 cm in naïve animals to 20.70 cm in 6-OHDA lesioned animals.

Subsequently, vehicle injection at the EPN of 6-OHDA lesioned animals did not alter stride length (Figure 16 C). However, injection of 0.5 ng of BoNT-A at the EPN significantly increased the stride length 6-OHDA lesioned animals (Figure 16 D). This change was present at different time points for specific paws (Figure 16 D). At 1 week following BoNT-A administration, stride length significantly increased to 23.89 cm for the RF ( $F(2,17) = 7.945$ ,  $p = 0.0071$ ), 23.50 cm for the RH ( $F(2,19) = 11.35$ ,  $p = 0.0003$ ), but no significant changes were detected in either left paws. At 1 month after BoNT-A injection, stride length significantly increased across all paws, to 24.60 cm for the RF ( $F(2,17) = 7.945$ ,  $p = 0.0009$ ), 23.97 cm for the RH ( $F(2,19) = 11.35$ ,  $p = 0.0085$ ), 23.73 cm for the LF ( $F(2,19) = 6.179$ ,  $p = 0.0259$ ) and 23.99 cm for the LH ( $F(2,18) = 5.42$ ,  $p = 0.0261$ ). However, at 3 months after BoNT-A infusion, stride length decreased in lesioned animals to 21.51 cm for the RF, 21.53 cm for the RH, 20.50 cm for the LF and 22.04 cm for the LH.

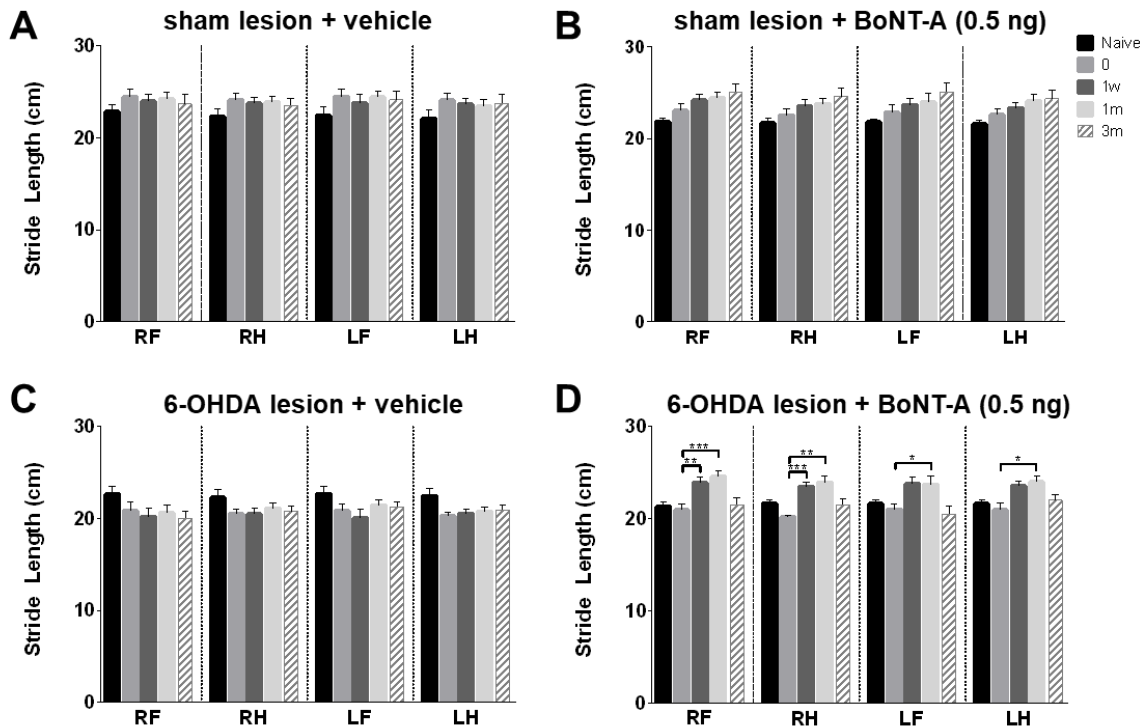


**Figure 16 – Stride length of hemi-PD rats treated with BoNT-A**

Changes in stride length after administration of 0.5 ng of BoNT-A at the EPN (n=8 per group). Paws were measured individually (RF: right front, RH: right hind, LF: left front, and LH: left hind) and organized on the x-axis. Experimental timepoints are reflected according to the legend: naïve rats tested prior to any surgeries, 6-OHDA (or sham lesioned) animals tested at week 0, and BoNT-A (or sham vehicle) animals tested at 1 week, 1 month or 3 months following treatment. Sham lesioned rats showed no changes in stride length after vehicle (A) or BoNT-A injection (B). 6-OHDA lesioning of the MFB did not significantly alter stride length (C and D). Vehicle injection had no effect on stride length of 6-OHDA lesioned rats (C). 0.5 ng of BoNT increased the stride length of 6-OHDA lesioned rats in the right paws at 1 week and in all paws at 1 month (D). All results are presented as mean  $\pm$  sem. Asterisks indicate significant changes compared to pre-lesioned animals (C) or lesioned animals (D) according to repeated measures one-way ANOVA and post hoc Tukey test. \* $p < 0.05$  \*\* $p < 0.01$  \*\*\* $p < 0.001$

### **3.2.13 Changes in Max Contact Area**

The max contact area of each paw was also measured by the CatWalk apparatus. As expected, max contact area was unaffected by sham lesioning of the MFB (naïve vs timepoint 0 in Figure 17 A and B). Subsequently, in these control animals, vehicle injection (Figure 17 A) or 0.5 ng of BoNT-A at the EPN (Figure 17 B) did not significantly affect the max contact area of any of the paws across all experimental timepoints.

Consistent with findings from other CatWalk studies involving parkinsonian rodents, 6-OHDA lesioning of the MFB resulted in an asymmetric reduction of max contact area in only the left paws (naïve vs timepoint 0 in Figure 17 C and D). The max contact area of the LF decreased from 2.592 cm<sup>2</sup> in naïve animals to 1.620 cm<sup>2</sup> in 6-OHDA lesioned animals, and from 2.084 cm<sup>2</sup> to 1.315 cm<sup>2</sup> in the LH. No significant reduction in max contact area was detected in the right paws of 6-OHDA lesioned animals.

Subsequently, in 6-OHDA lesioned animals, vehicle injection at the EPN had no significant effects on max contact area (Figure 17 C). Administration of 0.5 ng of BoNT-A at the EPN also had no significant effect on max contact area in either affected (left) or unaffected (right) paws of 6-OHDA lesioned animals (Figure 17 D). No changes were detected at any of the tested experimental timepoints.

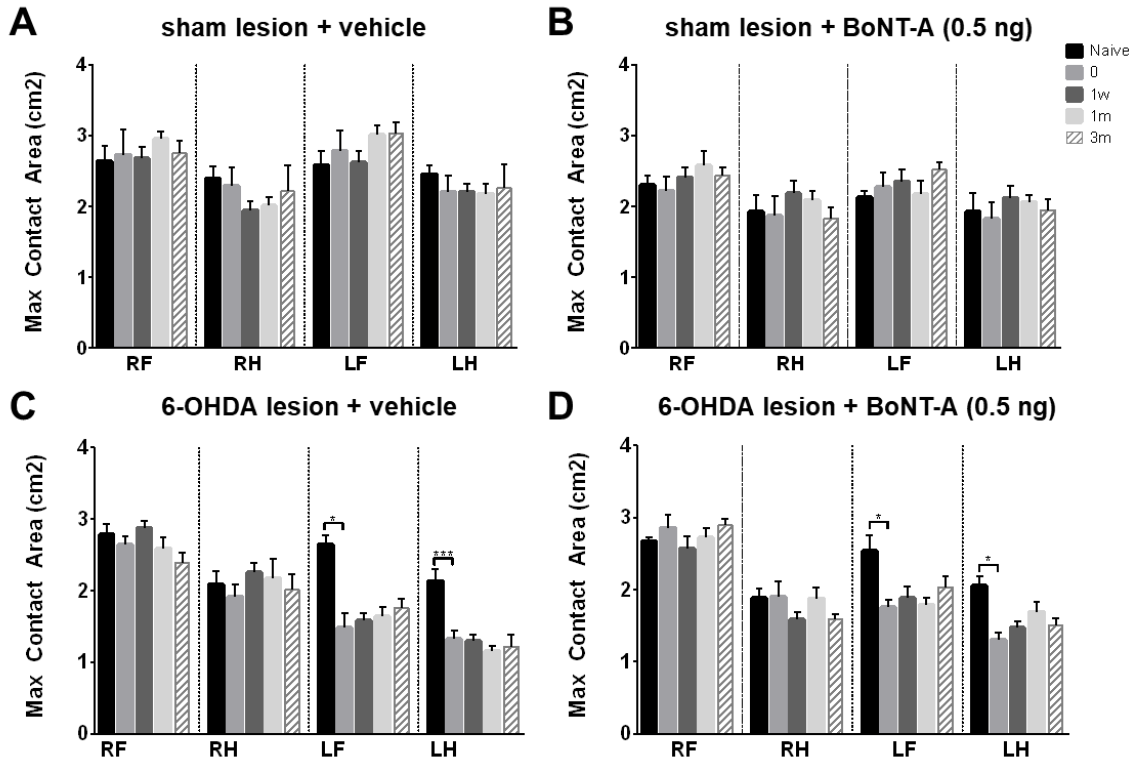


**Figure 17 – Max contact area of hemi-PD rats treated with BoNT-A**

Changes in max contact area after infusion of 0.5 ng of BoNT-A at the EPN (n=8 per group). Paws were measured individually (RF: right front, RH: right hind, LF: left front, and LH: left hind) and organized on the x-axis. Experimental timepoints are reflected according to the legend: naïve rats tested prior to any surgeries, 6-OHDA (or sham lesioned) animals tested at week 0, and BoNT-A (or sham vehicle) animals tested at 1 week, 1 month or 3 months following treatment. Sham lesioned rats showed no changes in max contact area after vehicle (A) or BoNT-A injection (B). 6-OHDA lesioning of the MFB significantly reduced max contact area of left paws (C and D). 6-OHDA lesioned rats showed no improvements in max contact area after vehicle (C) or BoNT-A injection (D). All results are presented as mean  $\pm$  sem. Asterisks indicate significant changes compared to pre-lesioned animals (C) or lesioned animals (D) according to repeated measures one-way ANOVA and post hoc Tukey test. \*p<0.05 \*\*\*p<0.001

### **3.2.14 Changes in Mean Intensity**

Lastly, the CatWalk apparatus was used to detect the mean intensity of all paws. Sham lesioning of the MFB did not significantly affect the mean intensity of animals in any of their paws (naïve vs timepoint 0 in Figure 18 A and B). In these control animals, vehicle injection (Figure 18 A) or 0.5 ng of BoNT-A at the EPN (Figure 18 B) did not significantly affect the mean intensity of any of the paws across all experimental timepoints.

Similar to the results of max contact area, 6-OHDA lesioning of the MFB resulted in an asymmetric reduction of mean intensity in only left paws (naïve vs timepoint 0 in Figure 18 C and D). The mean intensity of the LF decreased from 83.18 in naïve animals to 59.35 in 6-OHDA lesioned animals, and from 79.84 to 57.15 in the LH. No significant changes in mean intensity was detected in the right paws of 6-OHDA lesioned animals.

In these hemiparkinsonian animals, vehicle injection at the EPN had no significant effects on mean intensity (Figure 18 C). Infusion of 0.5 ng of BoNT-A at the EPN also had no significant effect on mean intensity in either affected (left) or unaffected (right) paws of 6-OHDA lesioned animals (Figure 17 D). No significant changes were observed at any of the tested experimental timepoints.

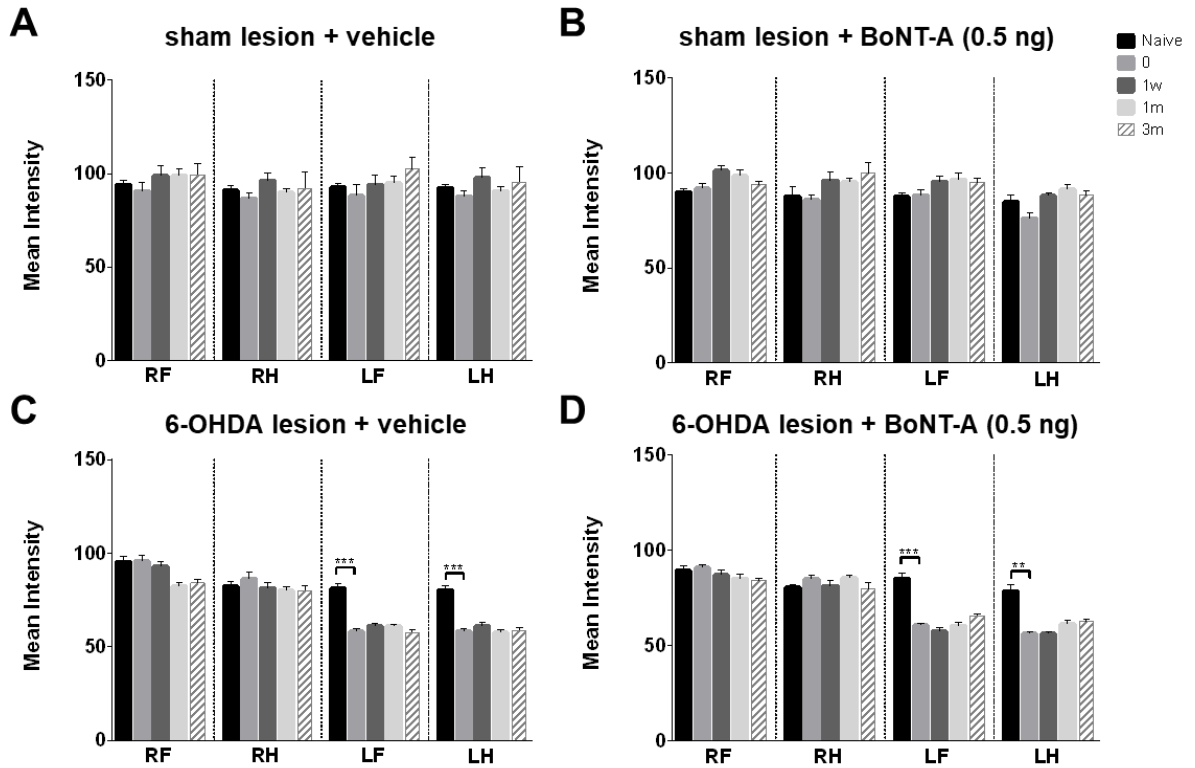


**Figure 18 – Mean intensity of hemi-PD rats treated with BoNT-A**

Changes in mean intensity after injection of 0.5 ng of BoNT-A at the EPN (n=8 per group). Paws were measured individually (RF: right front, RH: right hind, LF: left front, and LH: left hind) and organized on the x-axis. Experimental timepoints are reflected according to the legend: naïve rats tested prior to any surgeries, 6-OHDA (or sham lesioned) animals tested at week 0, and BoNT-A (or sham vehicle) animals tested at 1 week, 1 month or 3 months following treatment. Sham lesioned rats showed no changes in mean intensity after vehicle (A) or BoNT-A injection (B). 6-OHDA lesioning of the MFB significantly reduced mean intensity of left paws (C and D). 6-OHDA lesioned rats showed no improvements in mean intensity after vehicle (C) or BoNT-A injection (D). All results are presented as mean  $\pm$  sem. Asterisks indicate significant changes compared to pre-lesioned animals (C) or lesioned animals (D) according to repeated measures one-way ANOVA and post hoc Tukey test. \*\*p<0.01 \*\*\*p<0.001



### 3.2.15 Changes in Walking Pattern

Overall, all the aforementioned quantitative gait parameters can be reflected in the walking pattern of experimental animals (Figure 19). Naïve untreated animals traversed the walkway with short consistent steps (Figure 19 A). Following 6-OHDA lesioning, animals walked at an irregular pace with fewer steps per second, cumulating in a longer time to traverse the walkway (Figure 19 B). The walking pattern of lesioned animals returned to normal (consistent repetitive short steps) after administration of BoNT-A at 1 week and 1 month (Figure 19 C and D). An irregular walking pattern consisting of long uneven steps re-emerged at 3 months following BoNT-A treatment (Figure 19 E).

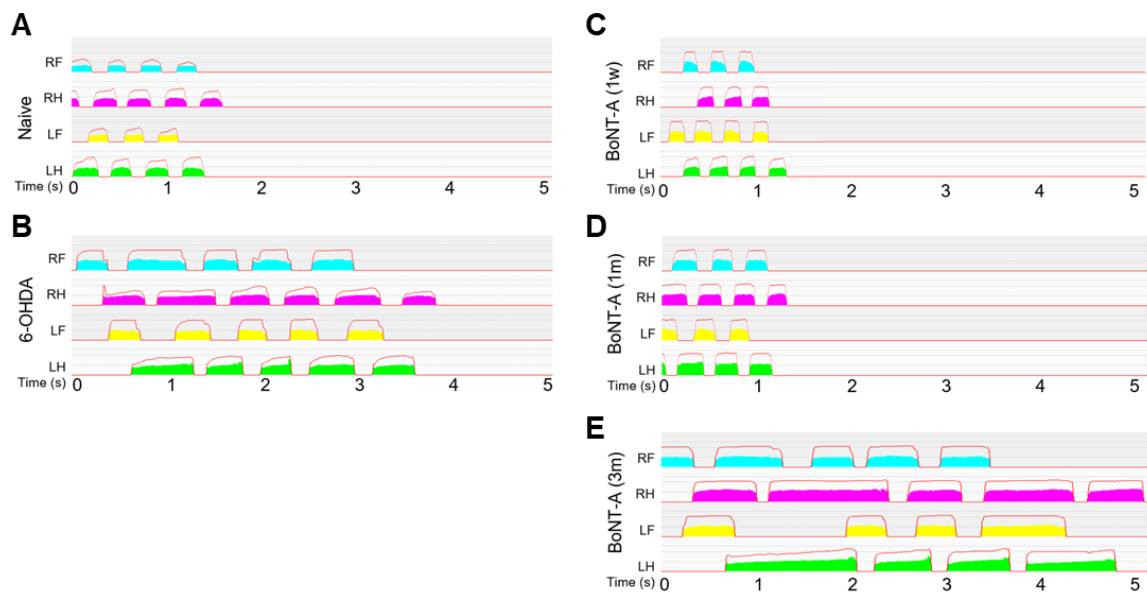


**Figure 19 – Walking pattern of hemi-PD rats treated with BoNT-A**

Walking pattern and individual paws (RF: right front, RH: right hind, LF: left front, and LH: left hind) were measured at given experimental timepoints on the y-axis. Normal walking pattern of naïve untreated animals (A). 6-OHDA lesioned animals crossed the walkway at a slower irregular pace (B). Following BoNT-A infusion, walking pattern of animals appeared normal at 1 week (C) and 1 month (D), but abnormalities re-emerged at 3 months (E).

### 3.2.16 Summary of CatWalk Results

The gait changes induced by 6-OHDA lesioning and subsequent 1-month post BoNT-A injection at the EPN is summarized in Table 3.

**Table 3 – Summary of CatWalk Results**

<b>Parameter</b>	<b>Effect of 6-OHDA Lesioning</b>	<b>Effect of BoNT-A Treatment at 1 month</b>
<b>Average Speed (cm/s)</b>	↓	↑
<b>Body Speed Variation (%)</b>	↑	↓
<b>Cadence (steps/s)</b>	↓	↑
<b>Duty Cycle (%)</b>	↑	↓
<b>Initial Dual Stance (s)</b>	↑	↓
<b>Max Contact Area (cm<sup>2</sup>)</b>	↓ (left only)	n.s.
<b>Mean Intensity</b>	↓ (left only)	n.s.
<b>Single Stance (s)</b>	↑	↓
<b>Stand (s)</b>	↑	↓
<b>Step Cycle (s)</b>	↑	↓
<b>Stride Length (cm)</b>	n.s.	↑
<b>Swing Speed (cm/s)</b>	↓	↑
<b>Terminal Dual Stance (s)</b>	↑ (left only)	↓ (left only)

### 3.3 Results of Immunohistochemical Staining

#### 3.3.1 Verification of 6-OHDA Lesion

Unilateral 6-OHDA lesioning of the MFB was verified post-mortem in all animals by significant reduction of TH-positive terminals in the striatum (Figure 20 A) and TH-positive cell bodies in the SNpc (Figure 20 B) on the injected right side.

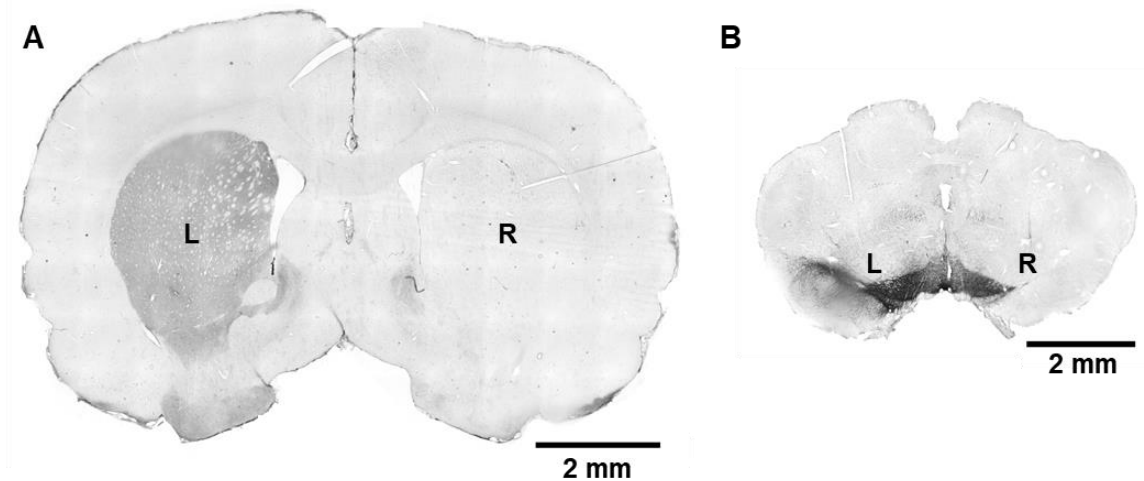


**Figure 20 – 6-OHDA lesioning of the MFB**

6-OHDA lesioning of the right MFB results in reduction in TH immunoreactivity in the ipsilateral striatum (A) and the substantia nigra (B). Presence of TH was detected in the left (L) side), whereas reduction of TH was seen in the right (R) side. Scale bars 2 mm

### **3.3.2 BoNT-A Selectively Targets Glutamatergic Terminals**

Immunofluorescent labelling of synaptophysin was used to identify the density of all types of synaptic terminals, vesicular glutamate transporter 2 (vGluT2) was used to identify glutamatergic terminals, while glutamate decarboxylase 67 kDa (GAD67) was used for GABAergic terminals.

6-OHDA lesioning of the MFB had no significant effect on the immunoreactivity of synaptophysin (Figure 21 A versus C), vGluT2 (Figure 21 F versus H) or GAD67 (Figure 21 K versus M) at the EPN. Likewise, injection of 0.5 ng of BoNT-A at the EPN had no significant effect on any markers in control animals (Figure 21 B, G and L). However, administration of 0.5 ng of BoNT-A at the EPN significantly reduced the synaptophysin immunoreactivity at the EPN of 6-OHDA lesioned animals (Figure 21 D). The mean intensity of synaptophysin labelling decreased from 21.62 to 4.077 following BoNT-A administration at 1 month in 6-OHDA lesioned animals ( $H = 19.52$ ,  $p = 0.0009$ ) (Figure 21 E). A corresponding decrease of vGluT2 was detected at the EPN following BoNT-A administration in lesioned animals (Figure 21 I). The mean intensity of vGluT2 reduced from 8.906 to 2.112 at 1 month post-infusion of 0.5 ng of BoNT-A in lesioned animals ( $H = 22.48$ ,  $p = 0.0007$ ) (Figure 21 J). However, no significant changes in GAD67 staining were observed after BoNT-A treatment in lesioned animals (Figure 21 N and O).

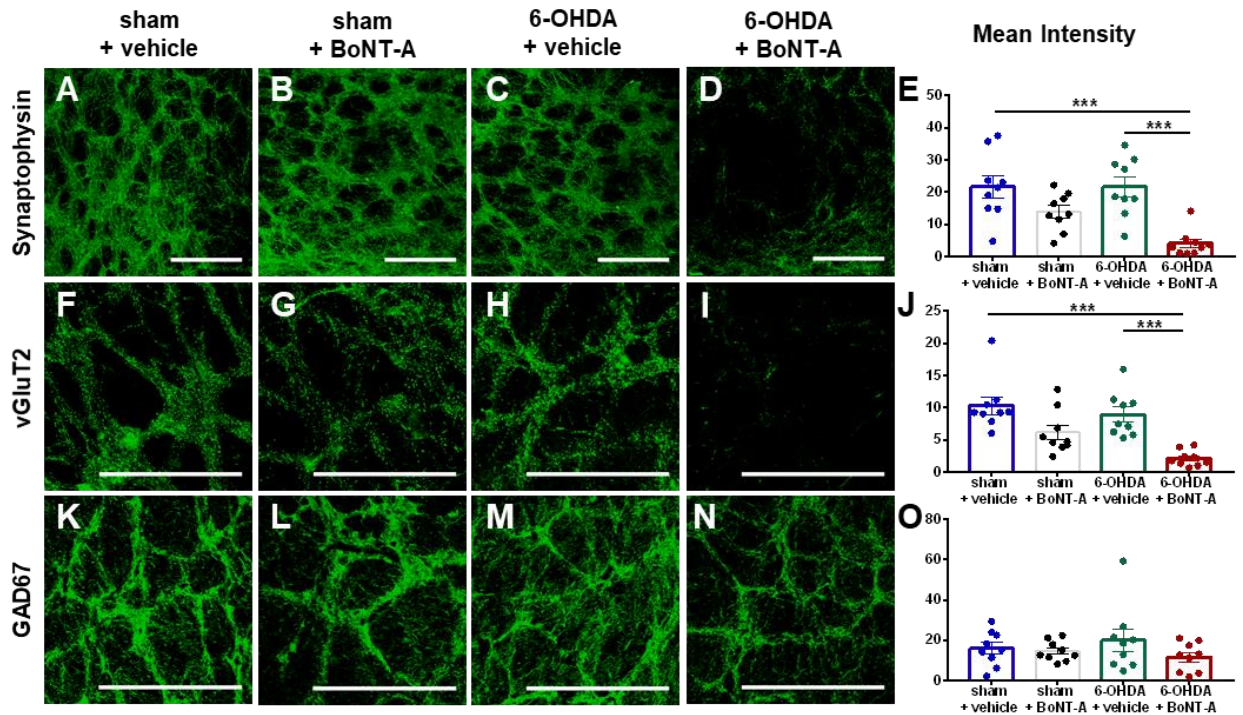


**Figure 21 – Immunostaining of synaptic markers at the EPN**

Immunolabelling at the EPN of synaptophysin (A-D), vGluT2 (F-I) and GAD67 (K-N) of control animals treated with vehicle (first column), control animals treated with BoNT-A (second column), lesioned animals treated with vehicle (third column) and lesioned animals treated with BoNT-A at 1 month (fourth column). Reduction in synaptophysin and vGluT2 were detected at the EPN at 1 month following BoNT-A administration in 6-OHDA lesioned animals. No change in GAD67 immunostaining was detected after BoNT-A injection. Mean intensity (last column) was measured for each image, where each dot represents a processed section (n=9). All results are presented as mean  $\pm$  sem. Asterisks indicate significant changes between groups according to Kruskal-Wallis test and post hoc Dunn test. \*\*\* $p < 0.001$  Scale bar: 200  $\mu$ m

### **3.3.3 Effects of BoNT-A Injection are Non-Permanent**

Administration of 0.5 ng of BoNT-A at the EPN of lesioned animals significantly reduced the synaptophysin immunoreactivity at the EPN as early as 1 week post-injection (Figure 22 A). This reduction in synaptophysin labelling persisted at 1 month post-injection (Figure 22 B). However, at 3 months post-injection, synaptophysin levels increased (Figure 22 C). The mean intensity of synaptophysin labelling was 5.75 at 1 week ( $H = 16.95$ ,  $p = 0.0077$ ), 4.08 at 1 month ( $H = 16.95$ ,  $p = 0.0002$ ), compared to 17.61 at 3 months (Figure 22 D).

Correspondingly, infusion of BoNT-A at the EPN of lesioned animals significantly decreased the immunoreactivity of vGluT2 at the EPN at 1 week post-injection (Figure 22 E). At 1 month post-administration, the level of vGluT2 labelling continued to decrease (Figure 22 F). However, at 3 months post-injection, vGluT2 immunoreactivity increased (Figure 22 G). The mean intensity of vGluT2 labelling was 4.77 at 1 week ( $H = 17.36$ ,  $p = 0.0320$ ), 2.112 at 1 month ( $H = 17.36$ ,  $p = 0.0001$ ), compared to 10.54 at 3 months (Figure 22 H).

On the contrary, injection of BoNT-A at the EPN had no significant effects on GAD67 immunolabelling at any of the tested experimental timepoints (Figure 22 I, J and K). The mean intensity of GAD67 labelling remained consistently insignificant at 11.73 at 1 week, 11.66 at 1 month and 15.04 at 3 months (Figure 22 L).

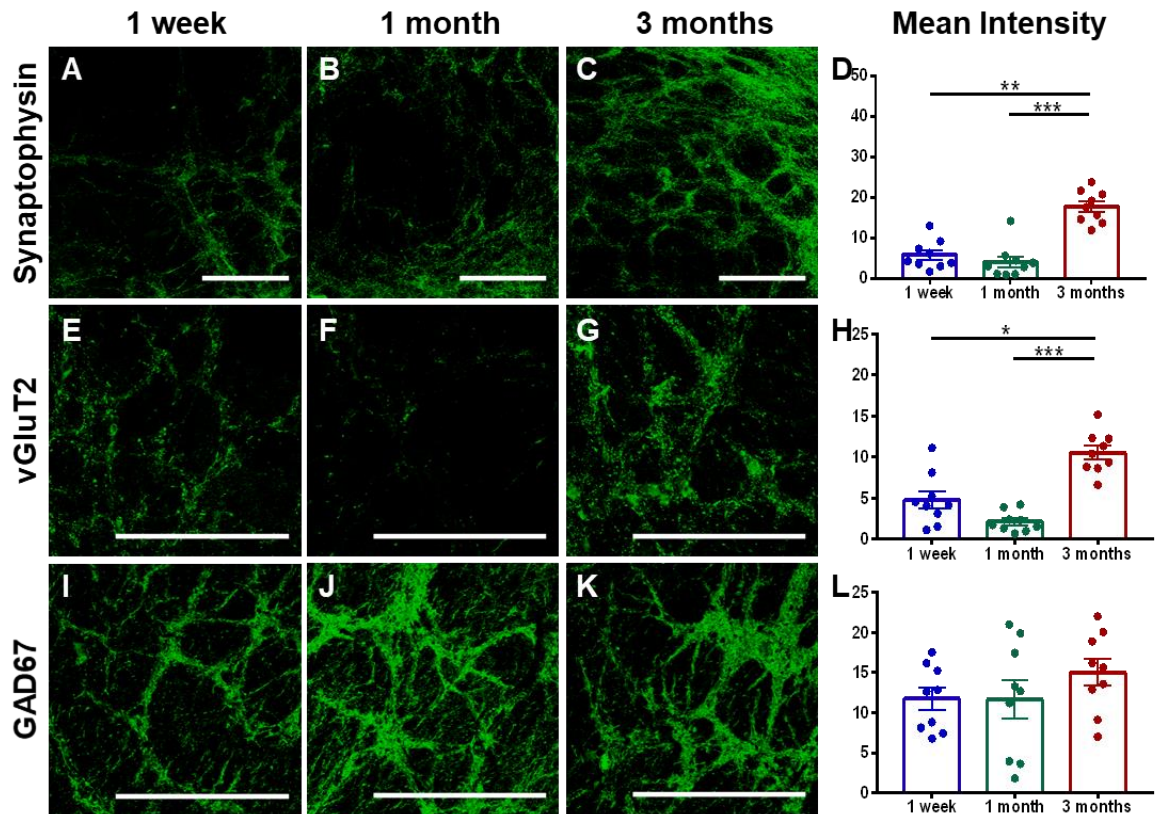


**Figure 22 – Effect of BoNT-A on synaptic markers at various timepoints**

Immunolabelling at the EPN of synaptophysin (A-C), vGluT2 (E-G) and GAD67 (I-K) of 6-OHDA lesioned animals injected with BoNT-A at 1 week (first column), 1 month (second column) and 3 months (third column). Reduction in synaptophysin and vGluT2 were detected at the EPN at 1 week and 1 month following BoNT-A administration in 6-OHDA lesioned animals. No change in GAD67 immunostaining was detected after BoNT-A injection. Mean intensity (last column) was measured for each image, where each dot represents a processed section (n=9). All results are presented as mean  $\pm$  sem. Asterisks indicate significant changes between groups according to Kruskal-Wallis test and post hoc Dunn test. \*p<0.05 \*\*p<0.01 \*\*\*p<0.001 Scale bar: 200  $\mu$ m

### **3.3.4 BoNT-A Infusion Elicits a Small Immune Response**

Immunofluorescent labelling of glial fibrillary acidic protein (GFAP) was used as an astrocyte marker to detect inflammation. Vehicle injection at the EPN of 6-OHDA lesioned animals resulted in detectable levels of GFAP at the EPN (Figure 23 A and B). Moreover, infusion of 0.5 ng of BoNT-A at the EPN of lesioned animals lead to a pronounced upregulation of GFAP expression, proliferation and overlap (Figure 23 C and D). Specifically, the mean intensity of GFAP immunoreactivity significantly increased from 10.58 in vehicle treated animals to 14.25 in BoNT-A infused animals ( $p = 0.0025$ ) (Figure 23 E).



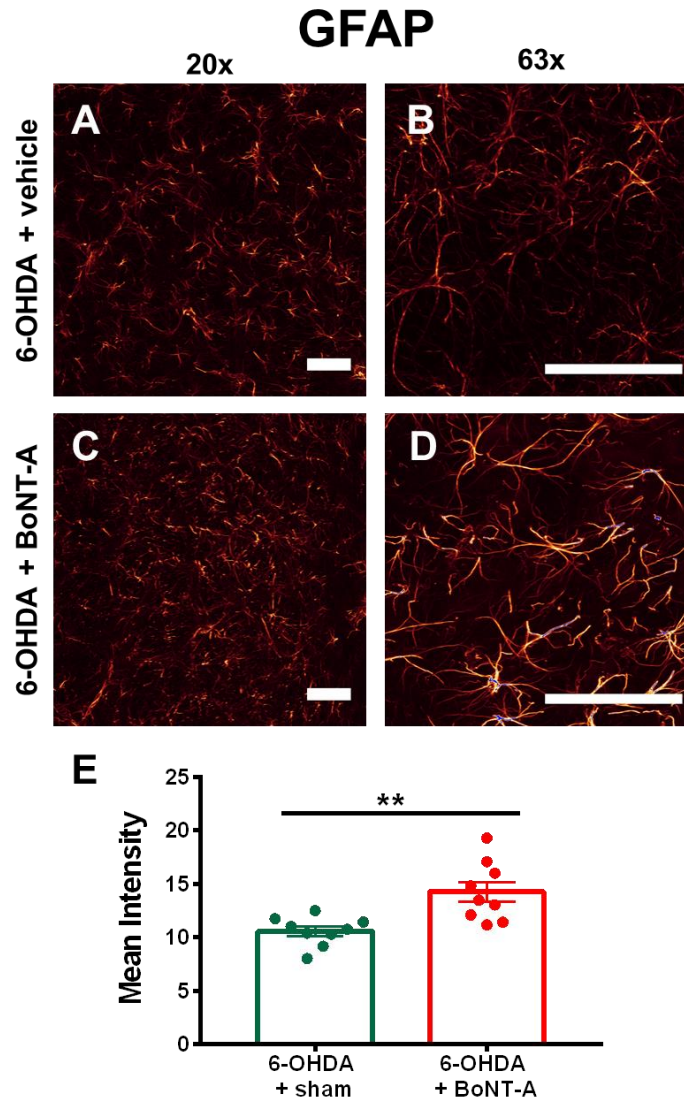


**Figure 23 – GFAP expression in lesioned animals treated with BoNT-A or vehicle**

Immunolabelling of GFAP at the EPN of 6-OHDA lesioned animals injected with vehicle (A/B) or BoNT-A (C/D). Detectable levels of GFAP were present following vehicle injection at the EPN. Upregulation of GFAP expression was observed at 1 month following 0.5 ng of BoNT-A infusion in 6-OHDA lesioned animals. First column displays lower magnification (20x) and second column displays higher magnification (63x). Mean intensity (E) was measured for each lower magnification image, where each dot represents a processed section (n=9). All results are presented as mean  $\pm$  sem. Asterisks indicate significant changes between groups according to an unpaired Student's t-test. \*\*p<0.01 Scale bar: 50  $\mu$ m

## Chapter 4

### 4 Discussion

#### 4.1 Safety of Central BoNT-A Injection

In recent years, numerous studies have reported on the safety and viability of direct injections of BoNT in the central nervous system of various rodent models of neurological diseases, including PD and epilepsy (Hawlitshka et al., 2013; Mazzocchio & Caleo, 2015; Chaddock et al., 2004; Wree et al., 2010). Due to its well-established mechanism of action to deplete acetylcholine exocytosis, intrastriatal injections of BoNT-A have been administered to improve motor deficits in PD rodent models (Wree et al., 2010; Antipova et al., 2013; Mehlan et al., 2016). Consistent with the findings of these previous studies involving the striatum, our results demonstrate that central administration of BoNT-A at the EPN is also safe. No mortality of any experimental animals was seen following infusions of either 0.05 ng or 0.5 ng of BoNT-A into the EPN. However, contrary to Antipova et al. (2013) in which no changes in GFAP immunostaining at the striatum was seen between untreated controls and BoNT-A treated animals, an increase in GFAP activity was detected following BoNT-A injection at the EPN. This upregulation of GFAP expression suggests that BoNT-A does induce inflammation leading to gliosis in the EPN.

In addition to the viability and safety of central BoNT-A injections, our results demonstrate that both behavioural and molecular effects induced by BoNT-A are transient. At 3 months post-BoNT-A infusion, the mobility of 6-OHDA lesioned rodents, as assessed by the CatWalk apparatus, returned to levels consistent with pre-injection (i.e. return of parkinsonian motor impairments). The re-emergence of pathological apomorphine-induced rotations at 3 months also demonstrate that BoNT-A effects are only transient and does not induce permanent changes within the BG. Moreover, based on our immunohistochemical findings, the reduction of synaptophysin and vGluT2 at the EPN was transient, as the density of these synaptic markers increased following 3 months post-injection. This reversal of both behavioural and molecular effects at approximately 3 months follows a similar timeline of treatment waning and physiological recovery involving injections in peripheral targets in a clinical setting (Kim et al., 2014; Samotus et al., 2016; Zakin &

Simpson, 2017). As a clinical therapeutic for tremor, the time of peak BoNT-A effect is typically observed at 4 weeks post-injection, with repeat injections occurring every 3-4 months. Thus, the central effects of BoNT-A observed in our study reflects a very similar timeline to its well-established peripheral use.

Overall, our study demonstrated a safe and transient effect of BoNT-A in the central nervous system to alleviate motor impairments in a rodent PD model.

## 4.2 Selectivity of Central BoNT-A Injection

In addition to its ability to inhibit acetylcholine release, there is clear evidence that BoNT-A also affects other excitatory neurotransmitter exocytosis including glutamate (Sanchez-Prieto et al., 1987; Bigalke et al., 1981; Ashton & Dolly, 1988; McMahon et al., 1992). Although these studies have reported on the ability of BoNT-A to suppress glutamate release, this work has been predominantly studied in vitro with the use of synaptosomes or cultured neurons. Moreover, injection of another BoNT subtype, BoNT-E has been used in vivo to suppress glutamate hyperactivity in the central nervous system of a mouse model of epilepsy (Antonucci et al., 2008). However, at present, no study has yet to directly investigate the use of BoNT-A in the brain to inhibit glutamate neuroexocytosis in an animal model. Our study directly investigated the effect of intracerebral botulinum neurotoxin A to selectively block glutamate neurotransmission in an animal model and its physiological application to produce a sufficient and quantifiable behavioural outcome.

The selectivity of BoNT-A on specific neuronal types was observed by immunofluorescence labelling of select biomarkers. Our results support the findings of in vitro studies that demonstrated a preference of BoNT-A on excitatory versus inhibitory synapses. This clear bias was demonstrated by the significant reduction in glutamatergic synaptic density marked by vGluT2 and lack of significant effect on GABAergic synapses identified by GAD67 at the EPN of BoNT-A treated lesioned animals. In the study by Sanchez-Prieto et al. (1987), this preference of BoNT-A on glutamatergic terminals developed approximately 2 hours following administration in cultured cortical

synaptosomes. In this study, this preferential action of BoNT-A appeared at the earliest tested experimental timepoint (1 week) and dissipated by the last experimental timepoint (3 months). From our results, the effect of BoNT-A on vGluT-2 labelled neurons was more effective at 1 month compared to 1 week, indicating a gradual and continuous effect.

A study by Cai et al. (2017) explored the colocalization of BoNT-A with different biomarkers of motor neurons, neighbouring neurons, nerve fibers or glial cells at the spinal cord following intramuscular injections of BoNT-A. In contrast to the findings observed in our study, the authors did not report any effect of BoNT-A on glutamatergic neurons due to a lack of colocalization of cleaved SNAP-25 with glutamatergic neurons. However, these discrepancies may be attributed to differences in experimental technique and objectives. The study by Cai et al. was looking for a secondary effect on glutamatergic neurons at the spinal cord after retrograde transport from a peripheral muscle injection of BoNT-A. In contrast, our research project investigated a direct effect of BoNT-A on glutamatergic terminals at the site of central injection at the EPN. Furthermore, the study by Cai et al. utilized an antibody for cleaved SNAP-25 (the established target of BoNT-A) in order to visualize co-localization between cleaved SNAP-25 and various neuronal biomarkers, including vGluT2 for glutamatergic neurons. The authors failed to see co-localization of cleaved SNAP-25 with any biomarkers for glutamatergic, GABAergic or catecholaminergic synaptic contacts. Surprisingly, the authors also did not report any co-localization of cleaved SNAP-25 with even cholinergic neurons using 2D confocal techniques, but was able to observe co-localization with 3D reconstruction. Thus, based on the methods and objectives of this study, it is not unexpected that BoNT-A had no effect on glutamatergic terminals. It is important to note that in our study, no co-localization analysis was performed with vGluT2 and cleaved SNAP-25 as the commercial available antibody for cleaved SNAP-25 failed to demonstrate specificity (data not shown). This limitation is expanded in more detail in Chapter 4.6.2.

Thus, our study is the first to report a significant histological effect by BoNT-A on glutamatergic terminals at the site of injection of an in vivo model.

### 4.3 Changes in Basal Ganglia Circuitry Following BoNT-A: Rotational Behaviour

In experimental models of PD for preclinical research, it is well-established that unilateral injection of 6-OHDA into the MFB results in near total depletion of dopamine in the ipsilateral striatum. Within the denervated striatum, supersensitivity occurs in the remaining neurons, in which there is an upregulation of D1 and D2 postsynaptic receptors (Perese et al., 1989). Thus, when unilaterally lesioned animals are challenged with apomorphine, there is greater dopamine activity on the lesioned nigrostriatal projections (Ungerstedt, 1971; Deumens et al., 2002). In the ipsilateral BG network, the supersensitive excitatory D1 activity contributes to increased inhibition from the striatum to the GPi through the direct pathway and thus, less inhibition on thalamocortical centres. The supersensitive inhibitory D2 receptors results in less inhibition from the striatum to the GPe through the indirect pathway and thus, more inhibition on the STN. Thus, the suppressed excitatory activity of the STN onto the GPi results in less inhibitory activity of the GPi to thalamocortical centres. The net alterations in BG circuitry all contribute to increased cortical activity ipsilateral to the lesion and thus, contralateral rotations away from the lesioned side.

From our results, selective inhibition of glutamatergic input from the STN to EPN by BoNT-A significantly abolishes this apomorphine-induced rotational behaviour. Since the only intervention administered was the injection of BoNT-A within the EPN, the reduction of pathological rotations can be related to the established effect of BoNT-A, which is the suppression of incoming signals to the EPN. However, based on the aforementioned changes in BG circuitry in relationship to the supersensitive dopamine receptors and consequent contralateral apomorphine-induced rotations, it would be expected that suppression of STN excitatory activity to the GPi would fail to suppress the pathological rotational behaviour of 6-OHDA lesioned animals and could even worsen apomorphine-induced rotations, which is opposite to the outcome observed in our study. Thus, the observed abolishment of pathological rotations in BoNT-A injected animals may be due to secondary effects of BoNT-A, such as retrograde transport of BoNT-A from STN terminals to incoming cortical afferents, ultimately resulting in suppression of motor cortical activity.

Similarly, BoNT-A could be mediating effects that alter the firing pattern of glutamatergic STN terminals, which could result in re-organization of BG activity that consequently leads to reduction of pathological rotations. This proposed electrophysiological change will be further discussed as a future direction in Chapter 4.6.3.

#### 4.4 Changes in Basal Ganglia Circuitry Following BoNT-A: Locomotion

It is well-established that loss of dopamine in PD results in changes of BG circuitry including an increase of STN activity on the GPi (Figure 24 A). This re-arrangement of the BG network leads to a reduction of thalamocortical activity and is therefore, linked to parkinsonian motor symptoms including gait impairments (Takakusaki, 2017). Thus, this study hypothesized that suppression of STN overactivity could lead to a re-balancing of BG circuitry to consequently improve motor impairments. From the data acquired by the CatWalk apparatus, hemiparkinsonian animals displayed an overall improvement in gait at 1 week and 1 month following BoNT-A injection. Overall, 6-OHDA lesioned animals traversed the walkway with a more consistent and rapid pace. The specific changes seen for each gait parameter and their functional neuroanatomy significance for gait control are discussed in Chapter 4.5.5. However, here we address the general changes in BG circuitry following BoNT-A injection that could lead to overall improvements in locomotion.

Unlike any previous CatWalk studies involving parkinsonian animals that observed improvements in gait following a specific intervention, this is the first study in which the connectivity between the STN-EPN was directly targeted and investigated. A study by Chuang et al. (2010), in which the CatWalk system was used, demonstrated that engrafting dopaminergic neurons derived from embryonic stem cells into the ipsilateral striatum of lesioned animals significantly improved their walking pattern and swing speed. Similarly, a study by Westin et al. (2012) reported that a single dose of levodopa mixed with Benserazide (a peripheral dopamine decarboxylase inhibitor) significantly improved numerous gait parameters (including stride length, swing speed, stand and step cycle) in a bilateral 6-OHDA model. However, our study focused on an intervention within the STN-

EPN, and not at the striatum. There is clear evidence that modulation at these sites are already promising with surgical interventions in PD patients, such as lesioning and DBS, to alleviate motor impairments (Benabid et al., 1987; Deep-Brain Stimulation for Parkinson's Disease Study Group, 2001).

By utilizing the ability of BoNT-A to block glutamate release from the STN, there is decreased excitatory outflow to the output nucleus of the BG, the GPi/EPN (Figure 24 B). This reduced activation of the EPN results in less inhibition to the ventral anterior and ventral lateral thalamic nuclei, which in turn stimulate the motor cortex to facilitate movement. In this paradigm, the loss of dopamine is not replenished or directly modulated, nor is the direct pathway affected by BoNT-A. The recovery of impaired mobility observed in the study offers support that despite a significant dopaminergic lesion, gait function can be significantly restored. Thus, blockade of STN activity by BoNT-A leads to sufficient reorganization of the BG network needed to generate a consistent rhythmic pattern of walking.

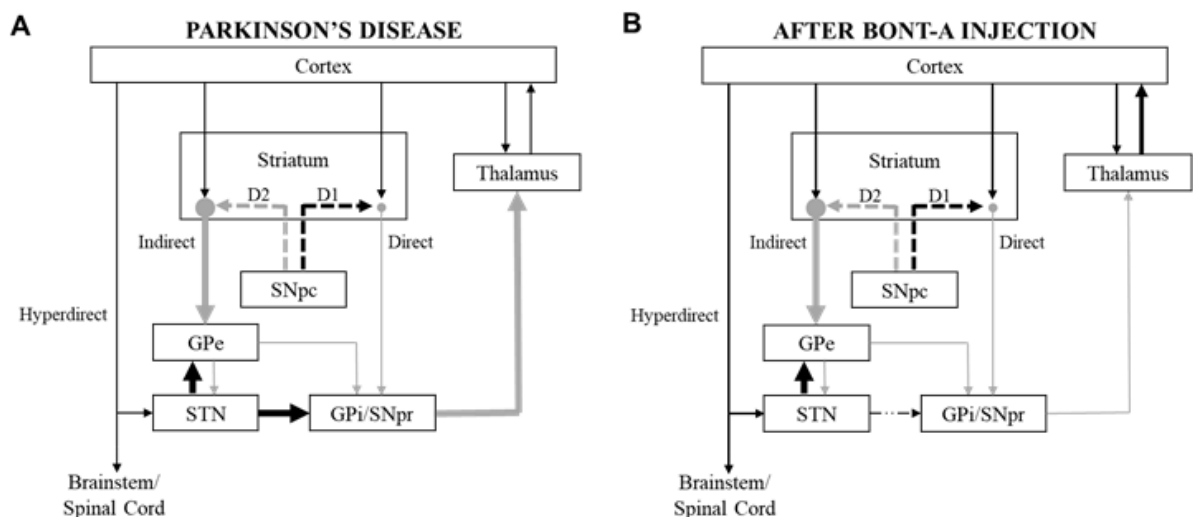


**Figure 24 – BG circuitry in parkinsonian states following BoNT-A injection**

Schematic diagram of the direct and indirect pathways of the BG circuitry in parkinsonian states without intervention (A) and with BoNT-A injection (B). Black arrows represent excitatory projections and grey arrows represent inhibitory projections. The thickness of the arrows indicates changes in activity of specific connections.

## 4.5 Effect of BoNT-A on Specific Gait Parameters

### 4.5.1 Changes in Gait Parameters Following 6-OHDA Lesioning

Numerous CatWalk studies have reported that following 6-OHDA lesioning of the MFB, animals display changes in both dynamic and static gait parameters (previously outlined in detail in Chapter 1.4.3). Amongst these gait parameters, an increase in stand and swing time were reported, which authors suggest reflected a reduction in average speed and cadence (Westin et al., 2012; Zhou et al., 2015). However, no study has yet to directly quantitatively measure these impairments in speed, variation and cadence of the 6-OHDA PD model. This study directly assessed these parameters and observed that 6-OHDA lesioned animals reduced their speed and cadence and increased their body speed variation. This slower and irregular gait is thought to be reflective of an increase in rigidity and bradykinesia. Such differences are seen in clinical manifestations of PD symptoms such as reduced arm swing (Sofuwa et al., 2005; Jankovic, 2008).

Moreover, the changes in static gait parameters (i.e. features independent on time) following 6-OHDA lesioning reported in this study were relatively consistent to findings described by other CatWalk studies (Chuang et al., 2010; Zhou et al., 2015). Significant reductions in max contact area and mean intensity were only seen in the left paws. This asymmetric presentation in the affected side is due to the unilateral depletion of dopamine in the contralateral hemisphere. It is likely that this asymmetry is emphasized by compensation in the unaffected right limbs. These gait disturbances in static parameters are most closely linked to an increase in rigidity and altered use of paw surface. However, not all static gait features displayed this asymmetric presentation and/or were affected by 6-OHDA lesioning of the MFB. Although hemi-PD rodents in our study displayed a minor reduction in stride length across all limbs, no significance was detected. This is different than data directly reported by Zhou et al. (2015) in which stride length was significantly reduced in PD animals, as well as patients with PD who presented with a decreased stride length observed by Sofuwa et al. (2005).

Similarly, the disturbances in dynamic gait parameters (i.e. features dependent on time) following 6-OHDA lesioning described in this study were comparable to findings reported



by other CatWalk studies (Chuang et al., 2010; Zhou et al., 2015). Increases in stand, swing, step cycle, duty cycle, single stance and initial dual stance were observed across all paws. These dynamic impairments are thought to model bradykinesia seen clinically in PD patients. A significant reduction in swing speed of lesioned animals is also thought to be reflective of an increase in muscle rigidity and bradykinesia, as well as a difficulty in the initiation of movements. This difficulty in initiation of movements after 6-OHDA lesioning has been reported by various studies that did not utilize the CatWalk apparatus (Olsson, Nikkhah, Bentlage, & Bjorklund, 1995; Metz, Tse, Ballermann, Smith, & Fouad, 2005; Shi, Luo, Woodward, & Chang, 2006). Furthermore, amongst these dynamic gait parameters, an asymmetrical increase in terminal dual stance of the left paws was observed in PD rodents. It is postulated that terminal dual stance is the most important parameter in mimicking delays by freezing of gait and postural instability (Dibble et al., 2004; Zhou et al., 2015). Disturbances in terminal dual stance in the 6-OHDA lesioned model also reflects a longer double limb support time in PD patients (Ebersbach et al., 1999).

Overall, this study contributes to the current literature that unilateral 6-OHDA lesioning of the MFB induces numerous impairments in both static and dynamic gait parameters, which are assessed by the CatWalk apparatus and can be reproduced with a high degree of fidelity.

#### **4.5.2 Dynamic Gait Parameters Affected by BoNT-A**

Administration of 0.5 ng of BoNT-A at the EPN recovered all impaired dynamic gait parameters in lesioned animals within a week of infusion, and these improvements persisted for a month post-infusion. Reductions in stand and swing across all limbs are linked directly to an overall reduction in step cycle, which suggest that BoNT-A mediated effects at the BG contribute to an overall reduction in bradykinesia. Moreover, the improvement in step cycle of each limb contributes to the observed increase in average speed. Hence, lesioned animals with BoNT-A treatment are once again able to traverse the walkway more rapidly because each paw is spending less contact on the glass plate and in the air. Additionally, the reduction in body speed variation signifies that the timing of each contact and non-contact amongst affected and unaffected paws is remaining more consistent after treatment. Thus, it is postulated that the unaffected right paws must be

compensating for the affected left paws in order to maintain a straight and steady path down the narrow walkway. Furthermore, the increase in swing speed across all limbs, and especially in the hind paws, suggests that initiation of movements is facilitated by BoNT-A administration. In quadrupeds, slower movements of the hindlimbs is more directly related to disturbances in balance and thus, amelioration of swing speed in the hindlimbs by BoNT-A also likely contributes to the ability of treated animals to maintain a straighter path down the walkway (Vlamings et al., 2007). Lastly, the asymmetric impairment in terminal dual stance was also significantly improved by BoNT-A, which suggests that freezing of gait could be minimized by BoNT-A.

Thus, overall, hemiparkinsonian animals treated with BoNT-A are able to spontaneously walk at a more consistent and rapid pace. These alterations in dynamic gait parameters are postulated to reflect a reduction in bradykinesia, facilitation of motor initiation and minimization of freezing. Amongst dynamic gait parameters, there is also compensation by unaffected paws which contribute to and maintain these improvements.

#### **4.5.3 Static Gait Parameters Unaffected by BoNT-A**

On the contrary, infusion of 0.5 ng of BoNT-A at the EPN failed to ameliorate most dysfunctional static gait parameters of 6-OHDA lesioned rodents. The asymmetric impairments in max contact area and mean intensity in the left paws persisted following BoNT-A administration. Gait disturbances in max contact area and mean intensity are most likely associated to an increase in rigidity and an altered use of the paw surface, and thus unilateral injection of BoNT-A unsuccessfully reduces asymmetric rigidity and/or relieves an imbalanced paw use.

Interestingly, although 6-OHDA lesioning of the MFB did not significantly impair stride length, administration of BoNT-A did significantly increase stride length across all paws. In the right paws, this increase was observed as early as 1 week and in the left paws, it emerged at 1 month. This change in stride length most likely reflects an altered walking pattern and the ability of animals to take larger and further steps to cross the walkway.

Thus, as patients with PD present with smaller shuffling steps, it is postulated that BoNT-A administration could ameliorate a reduced stride length.

#### **4.5.4 BoNT-A versus Other Interventions in 6-OHDA Rodents**

Although this project is the first to investigate the role of BoNT-A at the EPN of 6-OHDA lesioned animals with an automated gait analysis tool, other studies have examined the effect of other common therapies in parkinsonian rodents with the CatWalk apparatus.

A study by Westin et al. (2012) reported that administration of a single dose of L-DOPA in bilaterally lesioned animals restored most impaired dynamic gait parameters including a reduced swing speed, impaired stance and prolonged step cycle. L-DOPA also completely restored the impaired stride length of parkinsonian animals. Although authors did not directly report on other static gait parameters such as max contact area or mean intensity, it was observed that base of support was not affected by L-DOPA. Compared to the improvements induced by BoNT-A at the EPN, there are many parallels between the beneficial effects of these two interventions. Both clearly predominantly affect dynamic gait parameters and have a lesser effect on static gait parameters. Thus, it is likely that BoNT-A is exerting its effect by modulating the downstream pathways of the dopaminergic system within the BG. Furthermore, supported by the results presented by Westin et al., it is well-established that there is a limited role of L-DOPA therapy for axial symptoms in PD. However, our project examined more gait parameters, including terminal dual stance which best reflects postural instability, and found that BoNT-A improved the asymmetric postural instability of unilaterally lesioned animals. Thus, by intervening at the level of the EPN and focusing on targeting the glutamatergic system, it is postulated that BoNT-A is exerting a role that extends beyond the dopaminergic motor circuit within the BG.

Similarly, a study by Chuang et al. (2010) investigated the rescuing effect of dopaminergic neuron transplantation on gait function of unilaterally 6-OHDA lesioned animals and found ameliorations in both dynamic and static gait parameters. Following transplantation of dopaminergic neurons derived from embryonic stem cells, 6-OHDA lesioned rodents demonstrated improvements in max contact area, mean intensity and base of support, as

well as swing speed. It is interesting that the effect of L-DOPA versus dopaminergic neuron engraftment lead to benefits in opposing gait parameters. This could be attributed to changes in dopamine uptake (L-DOPA) versus release (stem cells) following these different interventions and their subsequent effect on the corticostriatal motor circuitry.

Furthermore, a study by Vlamings et al. (2007) utilized the CatWalk apparatus to examine the effect of high frequency stimulation of the subthalamic nucleus on bilaterally 6-OHDA lesioned rodents. Bilateral STN electrical stimulation significantly improved overall speed of animals (marked only by a reduction in swing duration) but failed to improve static gait parameters, including max contact area and mean intensity. In fact, it appeared that STN stimulation worsened these static parameters and induced a slowing of forelimb movement (i.e. further reduced swing speed). STN stimulation also failed to have any effect on hindlimb impairments. As authors did not report directly on individual dynamic gait parameters, it is difficult to compare the findings presented in this paper with the results observed in our project. However, as hindlimbs in quadrupeds are mainly involved in the control of balance and postural stability, the findings by Vlamings et al. provide further evidence that electrical stimulation of the STN does not improve deficits in balance and postural instability. This is similar to clinical findings in which bilateral STN stimulation usually fails to restore postural instability and balance impairments in PD patients (Krystkowiak et al., 2003). As our findings suggest that BoNT-A at the EPN does ameliorate many hindlimb deficits of parkinsonian animals and dynamic parameters such as terminal dual stance, there is a clear potential that this intervention could meet some of the shortcomings of DBS. This also indicates that a molecular therapeutic targeting the interaction between the STN-EPN offers different consequences than an electrical intervention. Thus, although the two interventions focus on the same dysregulated sites in PD, the mechanism behind their effect are unique, but possibly overlapping.

#### **4.5.5 Putting It All Together: BG Involvement in Locomotion**

Disorders of the BG network including PD are associated with an inability to initiate voluntary movements, an irregularity in the amount and velocity and amount of movement, and an abnormal muscle tone (Takakusaki, Tomita, & Yano, 2008). Together these contribute to gait failure and locomotor abnormalities. Normal gait is regulated by complex, intricate and overlapping loops involving the BG, cerebral cortex and cerebellum. The control of voluntary movements and automatic execution of learned movements is predominately controlled by BG and intermediate cerebellar loops with motor areas of the cerebral cortex, whereas the programming and planning of visually guided movements is linked to BG and lateral cerebellar loops with the prefrontal cortex (Marsden, 1982; Middleton & Strick, 2000). Additionally, the automaticity and rhythmicity of limb movements during locomotion is most widely associated to the connectivity between the BG and brainstem. Specifically, the GABAergic BG outputs from the SNpr and the GPi to the PPN within the mesencephalic locomotor region (MLR) play a key role in the maintenance of muscle tone and the rhythmicity of locomotion (Woolf & Butcher, 1986; Inglis & Winn, 1995; Pahapill & Lazano, 2000; Takakusaki et al., 2008). A study by Takakusaki et al. (2008) explored the connectivity between the SNpr and PPN/MLR, and found that GABAergic antagonists to the PPN altered locomotion in decerebrated cats with nigral and/or PPN stimulation. The authors found that dorsolateral SNpr and mid to medial SNpr projections to the PPN are required for a basal level of muscle tone. However, this study did not examine the specificity and role of the GPi projections to the PPN.

Combined with the results of our study, in which dynamic aspects of gait were altered by BoNT-A injections at the EPN, it is thus postulated that dynamic aspects of locomotion, such as speed and velocity could be more heavily influenced by the GPi/EPN output to thalamocortical centres. In contrast, the static aspects of gait unaffected by BoNT-A injections at the EPN, such as max contact area and mean intensity are linked more closely to alterations in muscle tone, and more likely associated to the SNpr output to the brainstem via the PPN. Hence, in the parkinsonian state, excessive GABAergic inhibition from the GPi/EPN to thalamocortical centres leads to bradykinesia and overall impairment in locomotion, which is reflected by reductions in average speed, stance, swing, step cycle

and duty cycle. Thus, BoNT-A injections at the EPN lead to recovery of these dynamic parameters. Concurrently, increased GABAergic inhibition from the SNpr to the PPN in the parkinsonian state consequently results in dysregulation of muscle tone. However, BoNT-A injections at the EPN failed to improve impairments in static gait parameters, such as asymmetric paw pressure and max contact area.

## 4.6 Conclusion

### 4.6.1 Significance

Neuromodulation at the scale of the neuron remains a challenge. Interventions such as lesion surgery or brain stimulation offer a limited therapeutic benefit and due to the aggressive nature, these treatment options are restricted to a small population that meets very specific criteria. There is still a clear unmet need for exploring interventions that offer novel neuromodulatory effects, target multiple sites within the brain, be potentially less invasive and less restrictive to patients. Central BoNT-A is a safe and viable option (Chapter 4.1) for targeted chemical neuromodulation with a well-established mechanism of action. Our study directly explored the re-purposing of BoNT-A, an already accepted therapeutic agent in PD, in a novel and innovative manner. This is the first study to conclude a significant preferential effect by BoNT-A on glutamatergic terminals at the site of injection in an animal model (Chapter 4.2). Central administration of 0.5 ng of BoNT-A has an immediate and transient behavioural effect on apomorphine-induced rotations and spontaneous locomotion. Despite a significant dopaminergic lesion, motor and gait impairments can be significantly restored by modulation of the BG network with the use of BoNT-A (Chapters 4.3 and 4.4). Specifically, the ability of BoNT-A to significantly improve impaired dynamic gait parameters offers insight to its potential as a novel intervention for PD, as well as the role of the STN-EPN connectivity in locomotion (Chapters 4.5).

#### **4.6.2 Limitations**

Despite the significant findings of this project, there are several limitations which must be considered. First, interpretation of data from experimental quadrupedal hemiparkinsonian rodents and extrapolation of this data to bipedal PD patients must be taken with careful consideration. In general, bipedal human locomotion is less stable than quadrupedal animal locomotion and is hypothesized to require additional descending cerebral cortical control involving the cerebellum (Takakusaki et al., 2008). As discussed in Chapter 1.3, although the unilateral 6-OHDA model of PD was cautiously chosen as the most well-suited animal model for this project, there are inherent limitations to this rodent model. The 6-OHDA unilateral model allowed for the performance of drug-induced rotational testing, but does not reflect the accurate clinical bilateral degeneration of PD patients. Likewise, successful 6-OHDA lesioning of the MFB lead to a sudden and drastic loss of dopaminergic terminals at the striatum (>95%), which does not reflect the true progressive nature of this disease. Ultimately, all research involving experimental animals will have associated limitations which must be considered, yet they remain vital in the development of novel therapeutics.

Another limitation of this study was the use of sucrose pellets in the CatWalk testing as it places emphasis on reward and motivational behaviour, rather than solely spontaneous locomotion. The dopaminergic system is crucially involved in motivation and reward-seeking behaviour and thus, the loss of dopamine in PD contributes to apathy, impulsiveness and other non-motor behavioural impairments (Schultz, 2002; Bromberg-Martin, Matsumoto, & Hikosaka, 2010). Furthermore, 6-OHDA lesioning of the MFB in rodents does not selectively target the nigrostriatal pathway as it also impairs the mesolimbic dopaminergic system, therefore affecting reward and motivation (Ma et al., 2014). Thus, the gait impairments following 6-OHDA lesioning and subsequent improvement following BoNT-A treatment may not be solely linked to changes in motor pathways within the basal ganglia, but also affected by other dopaminergic pathways.

A third limitation of this study was the lack of behavioural testing at a 2-month experimental timepoint. This oversight was due to an original experimental timeline of a year, in which animals were to be tested at 1 week/1 month/3 months/6 months/1 year post-treatment. This timeline was initially set based on other studies involving behavioural

testing of animals injected centrally with BoNT-A. However, as our findings diverged from the planned timeline and experimental groups were already underway, the crucial 2-month timepoint was missed. Nonetheless, current and future studies in our lab involving central BoNT-A injections in experimental animals are and will be performed with the inclusion of this timepoint.

Furthermore, another limitation of this project was the inconclusiveness of the spread of BoNT-A by staining either directly for BoNT-A or indirectly for cleaved SNAP-25. Commercially available antibodies for BoNT-A (anti-BoNT-A; Meridian Life Science; C01372M; Monoclonal; Mouse: 1:50-1:200) and cleaved SNAP-25 (anti-cSNAP25; Meridian Life Science; Q01235M; Monoclonal; Mouse: 1:200-1:500) failed to demonstrate any specificity for the substrate of interest. In other words, positive immunoreactive staining for these markers was detected in both sham and lesioned brains with vehicle injection (data not shown). Moreover, there have been many published studies in which the antibodies used to detect cleaved SNAP-25 by western blots and immunohistochemical assays have been questioned for their reliability and specificity (Antonucci et al., 2008; Matak, Riederer, & Lacković, 2012). In 2017, a recent paper by Cai et al. (2017) claimed to have developed a highly selective antibody for the cleaved substrate of BoNT-A, SNAP25<sub>197</sub>, but this antibody is proprietary to Allergan plc. Thus, there is a need for commercially available antibodies for either cleaved SNAP-25 and/or BoNT-A to be developed and validated for immunohistochemical studies.

Lastly, a final limitation of this study was the lack of consideration for cholinergic inputs to the EPN. As the PPN is implicated to play a key role in gait, there is a possibility that the behavioural changes induced by BoNT-A injections could be mediated by a reduction of cholinergic transmission from the PPN to the EPN (Woolf & Butcher, 1986). Along with the analysis of glutamatergic and GABAergic terminals in the EPN, immunostaining for cholinergic terminals (i.e. choline acetyltransferase (ChAT) labeling) could be performed to identify any potential changes in this pathway.



### **4.6.3 Future Directions**

The findings of this study offered deeper insight into the therapeutic application of BoNT-A in the CNS to treat neurological disorders including PD. Higher doses and/or repeated cycles of injection at the EPN may be promising for a longer and sustained duration of improvement. Expansion into other and multiple sites affected in PD, such as the SNpr, STN and PPN, could also be beneficial for impairments in specific gait parameters. Respective trials in the parkinsonian animal model are currently under way to target other hyperactive and dysregulated sites.

Furthermore, no previous studies have yet examined the effects of BoNT-A in the CNS from an electrophysiological perspective. Electrophysiological recordings in BoNT-A treated hemiparkinsonian rodents can enhance our current understanding of STN-EPN overactivity in PD and its implications in gait and motor control. Simultaneous BoNT-A administration and electrophysiological recording by means of injectrodes could also be used to compare and understand current data from other therapeutics focusing on the STN, such as DBS. This data would provide us with invaluable information in regards to changes in firing pattern and connectivity between the cortex and BG.

Overall, our study offers tremendous potential for a variety of translational studies in the future. A similar approach can be used in other rodent models of neurodegenerative diseases linked to glutamate excitotoxicity, such as amyotrophic lateral sclerosis and Alzheimer's disease. This study serves as a launching platform for the translation from rodents to primates and ultimately, to humans in the future. As BoNT-A is safe, commercially available and could be readily paired with established delivery systems, the opportunity for delivery of BoNT-A to specific CNS targets is immense. With many industry partners currently developing stable room temperature pre-mixed toxins, the path to market is rapid and thus, the possibility of delivering BoNT-A chronically in human PD is a real possibility.

## References

- Akaike, N., Ito, Y., Shin, M. C., Nonaka, K., Torii, Y., Harakawa, T., ... & Kaji, R. (2010). Effects of A2 type botulinum toxin on spontaneous miniature and evoked transmitter release from the rat spinal excitatory and inhibitory synapses. *Toxicon*, *56*(8), 1315-1326.
- Albin, R. L., Young, A. B., & Penney, J. B. (1989). The functional anatomy of basal ganglia disorders. *Trends in Neurosciences*, *12*(10), 366-375.
- Antipova, V., Hawlitschka, A., Mix, E., Schmitt, O., Dräger, D., Benecke, R., & Wree, A. (2013). Behavioral and structural effects of unilateral intrastriatal injections of botulinum neurotoxin a in the rat model of Parkinson's disease. *Journal of Neuroscience Research*, *91*(6), 838-847.
- Antonucci, F., Di Garbo, A., Novelli, E., Manno, I., Sartucci, F., Bozzi, Y., & Caleo, M. (2008). Botulinum neurotoxin E (BoNT/E) reduces CA1 neuron loss and granule cell dispersion, with no effects on chronic seizures, in a mouse model of temporal lobe epilepsy. *Experimental Neurology*, *210*(2), 388-401.
- Aschner, M., Erikson, K. M., Hernández, E. H., & Tjalkens, R. (2009). Manganese and its role in Parkinson's disease: from transport to neuropathology. *Neuromolecular Medicine*, *11*(4), 252-266.
- Ashour, R., & Jankovic, J. (2006). Joint and skeletal deformities in Parkinson's disease, multiple system atrophy, and progressive supranuclear palsy. *Movement Disorders*, *21*(11), 1856-1863.
- Ashton, A. C., & Dolly, J. O. (1988). Characterization of the inhibitory action of botulinum neurotoxin type A on the release of several transmitters from rat cerebrocortical synaptosomes. *Journal of Neurochemistry*, *50*(6), 1808-1816.
- Baba, M., Nakajo, S., Tu, P. H., Tomita, T., Nakaya, K., Lee, V. M., ... & Iwatsubo, T. (1998). Aggregation of alpha-synuclein in Lewy bodies of sporadic Parkinson's

- disease and dementia with Lewy bodies. *The American Journal of Pathology*, 152(4), 879.
- Bamford, N. S., Robinson, S., Palmiter, R. D., Joyce, J. A., Moore, C., & Meshul, C. K. (2004). Dopamine modulates release from corticostriatal terminals. *Journal of Neuroscience*, 24(43), 9541-9552.
- Bankiewicz, K. S., Oldfield, E. H., Chiueh, C. C., Doppman, J. L., Jacobowitz, D. M., & Kopin, I. J. (1986). Hemiparkinsonism in monkeys after unilateral internal carotid artery infusion of 1-methyl-4-phenyl-1, 2, 3, 6-tetrahydropyridine (MPTP). *Life Sciences*, 39(1), 7-16.
- Beckstead, R. M., Domesick, V. B., & Nauta, W. J. (1993). Efferent connections of the substantia nigra and ventral tegmental area in the rat. In *Neuroanatomy* (pp. 449-475). Birkhäuser Boston.
- Benabid, A. L., Pollak, P., Louveau, A., Henry, S., & De Rougemont, J. (1987). Combined (thalamotomy and stimulation) stereotactic surgery of the VIM thalamic nucleus for bilateral Parkinson disease. *Stereotactic and Functional Neurosurgery*, 50(1-6), 344-346.
- Berardelli, A., Rothwell, J. C., Thompson, P. D., & Hallett, M. (2001). Pathophysiology of bradykinesia in Parkinson's disease. *Brain*, 124(11), 2131-2146.
- Bernheimer, H., Birkmayer, W., Hornykiewicz, O., Jellinger, K., & Seitelberger, F. (1973). Brain dopamine and the syndromes of Parkinson and Huntington: clinical, morphological and neurochemical correlations. *Journal of the Neurological Sciences*, 20(4), 415-455.
- Betarbet, R., Sherer, T. B., MacKenzie, G., Garcia-Osuna, M., Panov, A. V., & Greenamyre, J. T. (2000). Chronic systemic pesticide exposure reproduces features of Parkinson's disease. *Nature Neuroscience*, 3(12), 1301-1306.
- Bigalke, H., Heller, I., Bizzini, B., & Habermann, E. (1981). Tetanus toxin and botulinum A toxin inhibit release and uptake of various transmitters, as studied with

- particulate preparations from rat brain and spinal cord. *Naunyn-Schmiedeberg's Archives of Pharmacology*, 316(3), 244-251.
- Biousse, V., Skibell, B. C., Watts, R. L., Loupe, D. N., Drews-Botsch, C., & Newman, N. J. (2004). Ophthalmologic features of Parkinson's disease. *Neurology*, 62(2), 177-180.
- Blandini, F., Nappi, G., Tassorelli, C., & Martignoni, E. (2000). Functional changes of the basal ganglia circuitry in Parkinson's disease. *Progress in Neurobiology*, 62(1), 63-88.
- Blasi, J., Chapman, E. R., Link, E., Binz, T., Yamasaki, S., De Camilli, P., ... & Jahn, R. (1993). Botulinum neurotoxin A selectively cleaves the synaptic protein SNAP-25. *Nature*, 365(6442), 160-163.
- Blesa, J., & Przedborski, S. (2014). Parkinson's disease: animal models and dopaminergic cell vulnerability. *Frontiers in Neuroanatomy*, 8.
- Blesa, J., Phani, S., Jackson-Lewis, V., & Przedborski, S. (2012). Classic and new animal models of Parkinson's disease. *BioMed Research International*, 2012.
- Blin, O., Ferrandez, A. M., Pailhous, J., & Serratrice, G. (1991). Dopa-sensitive and dopa-resistant gait parameters in Parkinson's disease. *Journal of the Neurological Sciences*, 103(1), 51-54.
- Bloem, B. R., Hausdorff, J. M., Visser, J. E., & Giladi, N. (2004). Falls and freezing of gait in Parkinson's disease: a review of two interconnected, episodic phenomena. *Movement Disorders*, 19(8), 871-884.
- Blum, D., Torch, S., Lambeng, N., Nissou, M. F., Benabid, A. L., Sadoul, R., & Verna, J. M. (2001). Molecular pathways involved in the neurotoxicity of 6-OHDA, dopamine and MPTP: contribution to the apoptotic theory in Parkinson's disease. *Progress in Neurobiology*, 65(2), 135-172.

- Braak, H., Bohl, J. R., Müller, C. M., Rüb, U., de Vos, R. A., & Del Tredici, K. (2006). Stanley Fahn Lecture 2005: The staging procedure for the inclusion body pathology associated with sporadic Parkinson's disease reconsidered. *Movement Disorders, 21*(12), 2042-2051.
- Braak, H., Del Tredici, K., Rüb, U., de Vos, R. A., Steur, E. N. J., & Braak, E. (2003). Staging of brain pathology related to sporadic Parkinson's disease. *Neurobiology of Aging, 24*(2), 197-211.
- Bragina, L., Fattorini, G., Giovedì, S., Melone, M., Bosco, F., Benfenati, F., & Conti, F. (2012). Analysis of synaptotagmin, SV2, and Rab3 expression in cortical glutamatergic and GABAergic axon terminals. *Frontiers in Cellular Neuroscience, 5*, 32.
- Breese, G. R., & Traylor, T. D. (1971). Depletion of brain noradrenaline and dopamine by 6-hydroxydopamine. *British Journal of Pharmacology, 42*(1), 88-99.
- Bromberg-Martin, E. S., Matsumoto, M., & Hikosaka, O. (2010). Dopamine in motivational control: rewarding, aversive, and alerting. *Neuron, 68*(5), 815-834.
- Bronstein, J. M., Tagliati, M., Alterman, R. L., Lozano, A. M., Volkmann, J., Stefani, A., ... & Pahwa, R. (2011). Deep brain stimulation for Parkinson disease: an expert consensus and review of key issues. *Archives of Neurology, 68*(2), 165-165.
- Brooks, A. I., Chadwick, C. A., Gelbard, H. A., Cory-Slechta, D. A., & Federoff, H. J. (1999). Paraquat elicited neurobehavioral syndrome caused by dopaminergic neuron loss. *Brain Research, 823*(1), 1-10.
- Bruchelt, G., Schraufstatter, I. U., Niethammer, D., & Cochrane, C. G. (1991). Ascorbic acid enhances the effects of 6-hydroxydopamine and H<sub>2</sub>O<sub>2</sub> on iron-dependent DNA strand breaks and related processes in the neuroblastoma cell line SK-N-SH. *Cancer Research, 51*(22), 6066-6072.
- Burgen, A. S. V., Dickens, F., & Zatman, L. J. (1949). The action of botulinum toxin on the neuro-muscular junction. *The Journal of Physiology, 109*(1-2), 10-24.

- Cai, B. B., Francis, J., Brin, M. F., & Broide, R. S. (2017). Botulinum neurotoxin type A-cleaved SNAP25 is confined to primary motor neurons and localized on the plasma membrane following intramuscular toxin injection. *Neuroscience*, *352*, 155-169.
- Calderón-Garcidueñas, L., Solt, A. C., Henríquez-Roldán, C., Torres-Jardón, R., Nuse, B., Herritt, L., ... & Brooks, D. M. (2008). Long-term air pollution exposure is associated with neuroinflammation, an altered innate immune response, disruption of the blood-brain barrier, ultrafine particulate deposition, and accumulation of amyloid  $\beta$ -42 and  $\alpha$ -synuclein in children and young adults. *Toxicologic Pathology*, *36*(2), 289-310.
- Cannon, J. R., Tapias, V., Na, H. M., Honick, A. S., Drolet, R. E., & Greenamyre, J. T. (2009). A highly reproducible rotenone model of Parkinson's disease. *Neurobiology of Disease*, *34*(2), 279-290.
- Canteras, N. S., Shammah-Lagnado, S. J., Silva, B. A., & Ricardo, J. A. (1990). Afferent connections of the subthalamic nucleus: a combined retrograde and anterograde horseradish peroxidase study in the rat. *Brain Research*, *513*(1), 43-59.
- Cantinioux, S., Vaugoyeau, M., Robert, D., Horrelou-Pitek, C., Mancini, J., Witjas, T., & Azulay, J. P. (2010). Comparative analysis of gait and speech in Parkinson's disease: hypokinetic or dysrhythmic disorders? *Journal of Neurology, Neurosurgery & Psychiatry*, *81*(2), 177-184.
- Carvalho, M. M., Campos, F. L., Coimbra, B., Pêgo, J. M., Rodrigues, C., Lima, R., ... & Salgado, A. J. (2013). Behavioral characterization of the 6-hydroxidopamine model of Parkinson's disease and pharmacological rescuing of non-motor deficits. *Molecular Neurodegeneration*, *8*(1), 14.
- Chaddock, J. A., Purkiss, J. R., Alexander, F. C., Doward, S., Fooks, S. J., Friis, L. M., ... & Dickenson, A. (2004). Retargeted clostridial endopeptidases: inhibition of nociceptive neurotransmitter release in vitro, and antinociceptive activity in in vivo models of pain. *Movement Disorders*, *19*(S8), S42-S47.

- Chiueh, C. C., Markey, S. P., Burns, R. S., Johannessen, J. N., Pert, A., & Kopin, I. J. (1984). Neurochemical and behavioral effects of systematic and intranigral administration of N-methyl-4-phenyl-1, 2, 3, 6-tetrahydropyridine in the rat. *European Journal of Pharmacology*, *100*(2), 189-194.
- Chuang, C. S., Su, H. L., Cheng, F. C., Hsu, S. H., Chuang, C. F., & Liu, C. S. (2010). Quantitative evaluation of motor function before and after engraftment of dopaminergic neurons in a rat model of Parkinson's disease. *Journal of Biomedical Science*, *17*(1), 9.
- Coon, S., Stark, A., Peterson, E., Gloi, A., Kortsha, G., Pounds, J., ... & Gorell, J. (2006). Whole-body lifetime occupational lead exposure and risk of Parkinson's disease. *Environmental Health Perspectives*, *114*(12), 1872.
- Cooper, J. A., Sagar, H. J., Tidswell, P., & Jordan, N. (1994). Slowed central processing in simple and go/no-go reaction time tasks in Parkinson's disease. *Brain*, *117*(3), 517-529.
- Davison, A. J., Legault, N. A., & Steele, D. W. (1986). Effect of 6-hydroxydopamine on polymerization of tubulin protection by superoxide dismutase, catalase, or anaerobic conditions. *Biochemical Pharmacology*, *35*(9), 1411-1417.
- De Lau, L. M., & Breteler, M. M. (2006). Epidemiology of Parkinson's disease. *The Lancet Neurology*, *5*(6), 525-535.
- De Medinaceli, L., Freed, W. J., & Wyatt, R. J. (1982). An index of the functional condition of rat sciatic nerve based on measurements made from walking tracks. *Experimental Neurology*, *77*(3), 634-643.
- Deep-Brain Stimulation for Parkinson's Disease Study Group. (2001). Deep-brain stimulation of the subthalamic nucleus or the pars interna of the globus pallidus in Parkinson's disease. *New England Journal of Medicine*, *345*(13), 956-963.
- DeLong, M. R., & Wichmann, T. (2007). Circuits and circuit disorders of the basal ganglia. *Archives of Neurology*, *64*(1), 20-24.

- Deumens, R., Blokland, A., & Prickaerts, J. (2002). Modeling Parkinson's disease in rats: an evaluation of 6-OHDA lesions of the nigrostriatal pathway. *Experimental Neurology*, *175*(2), 303-317.
- Dexter, D. T., Wells, F. R., Lee, A. J., Agid, F., Agid, Y., Jenner, P., & Marsden, C. D. (1989). Increased nigral iron content and alterations in other metal ions occurring in brain in Parkinson's disease. *Journal of Neurochemistry*, *52*(6), 1830-1836.
- Dibble, L. E., Nicholson, D. E., Shultz, B., MacWilliams, B. A., Marcus, R. L., & Moncur, C. (2004). Sensory cueing effects on maximal speed gait initiation in persons with Parkinson's disease and healthy elders. *Gait & posture*, *19*(3), 215-225.
- Dong, M., Yeh, F., Tepp, W. H., Dean, C., Johnson, E. A., Janz, R., & Chapman, E. R. (2006). SV2 is the protein receptor for botulinum neurotoxin A. *Science*, *312*(5773), 592-596.
- Dorsey, E., Constantinescu, R., Thompson, J. P., Biglan, K. M., Holloway, R. G., Kieburtz, K., ... & Tanner, C. M. (2007). Projected number of people with Parkinson disease in the most populous nations, 2005 through 2030. *Neurology*, *68*(5), 384-386.
- Ebersbach, G., Sojer, M., Valldeoriola, F., Wissel, J., Müller, J., Tolosa, E., & Poewe, W. (1999). Comparative analysis of gait in Parkinson's disease, cerebellar ataxia and subcortical arteriosclerotic encephalopathy. *Brain*, *122*(7), 1349-1355.
- Ermengem, E. V. (1897). Ueber einen neuen anaeroben Bacillus und seine Beziehungen zum Botulismus. *Medical Microbiology and Immunology*, *26*(1), 1-56.
- Fearnley, J. M., & Lees, A. J. (1991). Ageing and Parkinson's disease: substantia nigra regional selectivity. *Brain*, *114*(5), 2283-2301.
- Ferrante, R. J., Schulz, J. B., Kowall, N. W., & Beal, M. F. (1997). Systemic administration of rotenone produces selective damage in the striatum and globus pallidus, but not in the substantia nigra. *Brain Research*, *753*(1), 157-162.



- Findley, L. J. (2007). The economic impact of Parkinson's disease. *Parkinsonism & Related Disorders*, *13*, S8-S12.
- Forno, L. S., DeLanney, L. E., Irwin, I., & Langston, J. W. (1992). Similarities and differences between MPTP-induced parkinsonism and Parkinson's disease. Neuropathologic considerations. *Advances in Neurology*, *60*, 600-608.
- Galna, B., Lord, S., Burn, D. J., & Rochester, L. (2015). Progression of gait dysfunction in incident Parkinson's disease: impact of medication and phenotype. *Movement Disorders*, *30*(3), 359-367.
- Gerfen, C. R., Keefe, K. A., & Gauda, E. B. (1995). D1 and D2 dopamine receptor function in the striatum: coactivation of D1-and D2-dopamine receptors on separate populations of neurons results in potentiated immediate early gene response in D1-containing neurons. *Journal of Neuroscience*, *15*(12), 8167-8176.
- Gibb, W. R., & Lees, A. J. (1988). The relevance of the Lewy body to the pathogenesis of idiopathic Parkinson's disease. *Journal of Neurology, Neurosurgery & Psychiatry*, *51*(6), 745-752.
- Gispert, S., Ricciardi, F., Kurz, A., Azizov, M., Hoepken, H. H., Becker, D., ... & Kunz, W. S. (2009). Parkinson phenotype in aged PINK1-deficient mice is accompanied by progressive mitochondrial dysfunction in absence of neurodegeneration. *PloS One*, *4*(6), e5777.
- Glass, C. K., Saijo, K., Winner, B., Marchetto, M. C., & Gage, F. H. (2010). Mechanisms underlying inflammation in neurodegeneration. *Cell*, *140*(6), 918-934.
- Glinka, Y. Y., & Youdim, M. B. (1995). Inhibition of mitochondrial complexes I and IV by 6-hydroxydopamine. *European Journal of Pharmacology: Environmental Toxicology and Pharmacology*, *292*(3-4), 329-332.
- Goetz, C. G. (2011). The history of Parkinson's disease: early clinical descriptions and neurological therapies. *Cold Spring Harbor Perspectives in Medicine*, *1*(1), a008862.

- Goldberg, M. S., Pisani, A., Haburcak, M., Vortherms, T. A., Kitada, T., Costa, C., ... & Bernardi, G. (2005). Nigrostriatal dopaminergic deficits and hypokinesia caused by inactivation of the familial Parkinsonism-linked gene DJ-1. *Neuron*, *45*(4), 489-496.
- Goldman, S. M. (2014). Environmental toxins and Parkinson's disease. *Annual Review of Pharmacology and Toxicology*, *54*, 141-164.
- Grumelli, C., Corradini, I., Matteoli, M., & Verderio, C. (2010). Intrinsic calcium dynamics control botulinum toxin A susceptibility in distinct neuronal populations. *Cell Calcium*, *47*(5), 419-424.
- Hamers, F. P., Lankhorst, A. J., van Laar, T. J., Veldhuis, W. B., & Gispen, W. H. (2001). Automated quantitative gait analysis during overground locomotion in the rat: its application to spinal cord contusion and transection injuries. *Journal of Neurotrauma*, *18*(2), 187-201.
- Hariz, M. I. (2000). Complications of movement disorder surgery and how to avoid them. In *Movement Disorder Surgery* (Vol. 15, pp. 246-265). Karger Publishers.
- Hass, C. J., Malczak, P., Nocera, J., Stegemöller, E. L., Shukala, A., Malaty, I., ... & McFarland, N. (2012). Quantitative normative gait data in a large cohort of ambulatory persons with Parkinson's disease. *PloS One*, *7*(8), e42337.
- Hatheway, C. L. (1989). Bacterial sources of clostridial neurotoxins. *Botulinum Neurotoxin and Tetanus Toxin*, 3-24.
- Hawlitshka, A., Antipova, V., Schmitt, O., Witt, M., Benecke, R., Mix, E., & Wree, A. (2013). Intracerebrally applied botulinum neurotoxin in experimental neuroscience. *Current Pharmaceutical Biotechnology*, *14*(1), 124-130.
- Heikkila, R. E., Manzino, L., Cabbat, F. S., & Duvoisin, R. C. (1984). Protection against the dopaminergic neurotoxicity of 1-methyl-4-phenyl-1, 2, 5, 6-tetrahydropyridine by monoamine oxidase inhibitors. *Nature*, *311*(5985), 467-469.

- Heikkila, R., & Cohen, G. (1972). Further studies on the generation of hydrogen peroxide by 6-hydroxydopamine. *Molecular Pharmacology*, 8(2), 241-248.
- Hinkle, K. M., Yue, M., Behrouz, B., Dächsel, J. C., Lincoln, S. J., Bowles, E. E., ... & Kent, C. B. (2012). LRRK2 knockout mice have an intact dopaminergic system but display alterations in exploratory and motor co-ordination behaviors. *Molecular Neurodegeneration*, 7(1), 25.
- Hollman, J. H., McDade, E. M., & Petersen, R. C. (2011). Normative spatiotemporal gait parameters in older adults. *Gait & Posture*, 34(1), 111-118.
- Hudson, J. L., van Horne, C. G., Strömberg, I., Brock, S., Clayton, J., Masserano, J., ... & Gerhardt, G. A. (1993). Correlation of apomorphine- and amphetamine-induced turning with nigrostriatal dopamine content in unilateral 6-hydroxydopamine lesioned rats. *Brain Research*, 626(1), 167-174.
- Hughes, A. J., Daniel, S. E., Blankson, S., & Lees, A. J. (1993). A clinicopathologic study of 100 cases of Parkinson's disease. *Archives of Neurology*, 50(2), 140-148.
- Hunker, C. J., Abbs, J. H., & Barlow, S. M. (1982). The relationship between parkinsonian rigidity and hypokinesia in the orofacial system: A quantitative analysis. *Neurology*, 32(7), 749-749.
- Iancu, R., Mohapel, P., Brundin, P., & Paul, G. (2005). Behavioral characterization of a unilateral 6-OHDA-lesion model of Parkinson's disease in mice. *Behavioural Brain Research*, 162(1), 1-10.
- Inglis, W. L., & Winn, P. (1995). The pedunculopontine tegmental nucleus: where the striatum meets the reticular formation. *Progress in neurobiology*, 47(1), 1-29.
- Itier, J. M., Ibáñez, P., Mena, M. A., Abbas, N., Cohen-Salmon, C., Bohme, G. A., ... & Ret, G. (2003). Parkin gene inactivation alters behaviour and dopamine neurotransmission in the mouse. *Human Molecular Genetics*, 12(18), 2277-2291.

- Jackson-Lewis, V., & Przedborski, S. (2007). Protocol for the MPTP mouse model of Parkinson's disease. *Nature Protocols*, 2(1), 141-151.
- Jankovic, J. (2008). Parkinson's disease: clinical features and diagnosis. *Journal of Neurology, Neurosurgery & Psychiatry*, 79(4), 368-376.
- Javitch, J. A., D'Amato, R. J., Strittmatter, S. M., & Snyder, S. H. (1985). Parkinsonism-inducing neurotoxin, N-methyl-4-phenyl-1, 2, 3, 6-tetrahydropyridine: uptake of the metabolite N-methyl-4-phenylpyridine by dopamine neurons explains selective toxicity. *Proceedings of the National Academy of Sciences*, 82(7), 2173-2177.
- Kelly, V. E., Israel, S. M., Samii, A., Slimp, J. C., Goodkin, R., & Shumway-Cook, A. (2010). Assessing the effects of subthalamic nucleus stimulation on gait and mobility in people with Parkinson disease. *Disability and rehabilitation*, 32(11), 929-936.
- Kelly, V. E., Samii, A., Slimp, J. C., Price, R., Goodkin, R., & Shumway-Cook, A. (2006). Gait changes in response to subthalamic nucleus stimulation in people with Parkinson disease: a case series report. *Journal of Neurologic Physical Therapy*, 30(4), 184-194.
- Kemp, J. M., & Powell, T. P. S. (1971). The structure of the caudate nucleus of the cat: light and electron microscopy. *Philosophical Transactions of the Royal Society of London B: Biological sciences*, 262(845), 383-401.
- Kim, S. D., Yiannikas, C., Mahant, N., Vucic, S., & Fung, V. S. (2014). Treatment of proximal upper limb tremor with botulinum toxin therapy. *Movement Disorders*, 29(6), 835-838.
- Kita, H., & Kitai, S. T. (1987). Efferent projections of the subthalamic nucleus in the rat: light and electron microscopic analysis with the PHA-L method. *Journal of Comparative Neurology*, 260(3), 435-452.

- Korizova, L. K., & Montal, M. (2003). Translocation of botulinum neurotoxin light chain protease through the heavy chain channel. *Nature Structural & Molecular Biology*, *10*(1), 13-18.
- Kostrzewa, R. M., & Jacobowitz, D. M. (1974). Pharmacological actions of 6-hydroxydopamine. *Pharmacological Reviews*, *26*(3), 199-288.
- Kozaki, S., Kamata, Y., Watarai, S., Nishiki, T. I., & Mochida, S. (1998). Ganglioside GT1b as a complementary receptor component for Clostridium botulinum neurotoxins. *Microbial Pathogenesis*, *25*(2), 91-99.
- Krack, P., Batir, A., Van Blercom, N., Chabardes, S., Fraix, V., Ardouin, C., ... & Benabid, A. L. (2003). Five-year follow-up of bilateral stimulation of the subthalamic nucleus in advanced Parkinson's disease. *New England Journal of Medicine*, *349*(20), 1925-1934.
- Krystkowiak, P., Blatt, J. L., Bourriez, J. L., Duhamel, A., Perina, M., Blond, S., ... & Defebvre, L. (2003). Effects of subthalamic nucleus stimulation and levodopa treatment on gait abnormalities in Parkinson disease. *Archives of neurology*, *60*(1), 80-84.
- Kumar, R., Agarwal, A. K., & Seth, P. K. (1995). Free radical-generated neurotoxicity of 6-hydroxydopamine. *Journal of Neurochemistry*, *64*(4), 1703-1707.
- Lacy, D. B., & Stevens, R. C. (1999). Sequence homology and structural analysis of the clostridial neurotoxins. *Journal of Molecular Biology*, *291*(5), 1091-1104.
- Langston, J. W., Langston, E. B., & Irwin, I. (1983). MPTP-induced parkinsonism in human and non-human primates--clinical and experimental aspects. *Acta Neurologica Scandinavica. Supplementum*, *100*, 49-54.
- Lee, H. Y., Hsieh, T. H., Liang, J. I., Yeh, M. L., & Chen, J. J. J. (2012). Quantitative video-based gait pattern analysis for hemiparkinsonian rats. *Medical & Biological Engineering & Computing*, *50*(9), 937-946.

- Lei, W., Jiao, Y., Del Mar, N., & Reiner, A. (2004). Evidence for differential cortical input to direct pathway versus indirect pathway striatal projection neurons in rats. *Journal of Neuroscience*, *24*(38), 8289-8299.
- Lesage, S., & Brice, A. (2009). Parkinson's disease: from monogenic forms to genetic susceptibility factors. *Human Molecular Genetics*, *18*(R1), R48-R59.
- Lewis, S. J., & Barker, R. A. (2009). A pathophysiological model of freezing of gait in Parkinson's disease. *Parkinsonism & Related Disorders*, *15*(5), 333-338.
- Lin, M. T., & Beal, M. F. (2006). Mitochondrial dysfunction and oxidative stress in neurodegenerative diseases. *Nature*, *443*(7113), 787-795.
- Lord, S., Galna, B., & Rochester, L. (2013). Moving forward on gait measurement: toward a more refined approach. *Movement Disorders*, *28*(11), 1534-1543.
- Ma, Y., Zhan, M., OuYang, L., Li, Y., Chen, S., Wu, J., ... & Lei, W. (2014). The effects of unilateral 6-OHDA lesion in medial forebrain bundle on the motor, cognitive dysfunctions and vulnerability of different striatal interneuron types in rats. *Behavioural Brain Research*, *266*, 37-45.
- Manning-Bog, A. B., McCormack, A. L., Li, J., Uversky, V. N., Fink, A. L., & Di Monte, D. A. (2002). The Herbicide Paraquat Causes Up-regulation and Aggregation of  $\alpha$ -Synuclein in Mice PARAQUAT AND  $\alpha$ -SYNUCLEIN. *Journal of Biological Chemistry*, *277*(3), 1641-1644.
- Marder, E., & Calabrese, R. L. (1996). Principles of rhythmic motor pattern generation. *Physiological Reviews*, *76*(3), 687-717.
- Marsden, C. D. (1982). The mysterious motor function of the basal ganglia: the Robert Wartenberg Lecture. *Neurology*.
- Marsden, C. D., & Parkes, J. D. (1977). Success and problems of long-term levodopa therapy in Parkinson's disease. *The Lancet*, *309*(8007), 345-349.

- Matak, I., Riederer, P., & Lacković, Z. (2012). Botulinum toxin's axonal transport from periphery to the spinal cord. *Neurochemistry international*, *61*(2), 236-239.
- Mazzocchio, R., & Caleo, M. (2015). More than at the neuromuscular synapse: actions of botulinum neurotoxin A in the central nervous system. *The Neuroscientist*, *21*(1), 44-61.
- McCormack, A. L., Thiruchelvam, M., Manning-Bog, A. B., Thiffault, C., Langston, J. W., Cory-Slechta, D. A., & Di Monte, D. A. (2002). Environmental risk factors and Parkinson's disease: selective degeneration of nigral dopaminergic neurons caused by the herbicide paraquat. *Neurobiology of Disease*, *10*(2), 119-127.
- McMahon, H. T., Foran, P., Dolly, J. O., Verhage, M., Wiegant, V. M., & Nicholls, D. G. (1992). Tetanus toxin and botulinum toxins type A and B inhibit glutamate, gamma-aminobutyric acid, aspartate, and met-enkephalin release from synaptosomes. Clues to the locus of action. *Journal of Biological Chemistry*, *267*(30), 21338-21343.
- Mehlan, J., Brosig, H., Schmitt, O., Mix, E., Wree, A., & Hawlitschka, A. (2016). Intrastratial injection of botulinum neurotoxin-A is not cytotoxic in rat brain—A histological and stereological analysis. *Brain Research*, *1630*, 18-24.
- Metz, G. A., Tse, A., Ballermann, M., Smith, L. K., & Fouad, K. (2005). The unilateral 6-OHDA rat model of Parkinson's disease revisited: an electromyographic and behavioural analysis. *European Journal of Neuroscience*, *22*(3), 735-744.
- Middleton, F. A., & Strick, P. L. (2000). Basal ganglia and cerebellar loops: motor and cognitive circuits. *Brain research reviews*, *31*(2-3), 236-250.
- Montecucco, C., & Schiavo, G. (1995). Structure and function of tetanus and botulinum neurotoxins. *Quarterly Reviews of Biophysics*, *28*(04), 423-472.
- Montecucco, C., Papini, E., & Schiavo, G. (1994). Bacterial protein toxins penetrate cells via a four-step mechanism. *Febs Letters*, *346*(1), 92-98.

- Monville, C., Torres, E. M., & Dunnett, S. B. (2006). Comparison of incremental and accelerating protocols of the rotarod test for the assessment of motor deficits in the 6-OHDA model. *Journal of Neuroscience Methods*, *158*(2), 219-223.
- Narendra, D., Tanaka, A., Suen, D. F., & Youle, R. J. (2008). Parkin is recruited selectively to impaired mitochondria and promotes their autophagy. *The Journal of Cell Biology*, *183*(5), 795-803.
- National Collaborating Centre for Chronic Conditions (Great Britain). (2006). Parkinson's disease: national clinical guideline for diagnosis and management in primary and secondary care. Royal College of Physicians.
- Nutt, J. G., Marsden, C. D., & Thompson, P. D. (1993). Human walking and higher-level gait disorders, particularly in the elderly. *Neurology*, *43*(2), 268-268.
- Oaks, A. W., Frankfurt, M., Finkelstein, D. I., & Sidhu, A. (2013). Age-dependent effects of A53T alpha-synuclein on behavior and dopaminergic function. *PLoS One*, *8*(4), e60378.
- Obeso, J. A., Marin, C., Rodriguez-Oroz, C., Blesa, J., Benitez-Temiño, B., Mena-Segovia, J., ... & Olanow, C. W. (2008). The basal ganglia in Parkinson's disease: current concepts and unexplained observations. *Annals of Neurology*, *64*(S2), S30-S46.
- Olsson, M., Nikkhah, G., Bentlage, C., & Bjorklund, A. (1995). Forelimb akinesia in the rat Parkinson model: differential effects of dopamine agonists and nigral transplants as assessed by a new stepping test. *Journal of Neuroscience*, *15*(5), 3863-3875.
- Oyler, G. A., Higgins, G. A., Hart, R. A., Battenberg, E., Billingsley, M., Bloom, F. E., & Wilson, M. C. (1989). The identification of a novel synaptosomal-associated protein, SNAP-25, differentially expressed by neuronal subpopulations. *The Journal of Cell Biology*, *109*(6), 3039-3052.
- Pahapill, P. A., & Lozano, A. M. (2000). The pedunculopontine nucleus and Parkinson's disease. *Brain*, *123*(9), 1767-1783.



- Parent, A., & Hazrati, L. N. (1995). Functional anatomy of the basal ganglia. I. The cortico-basal ganglia-thalamo-cortical loop. *Brain Research Reviews*, 20(1), 91-127.
- Parkinson Society Canada. (2003). Parkinson's Disease: Social and Economic Impact. Retrieved April 27, 2017, from [http://www.parkinson.ca/atf/cf/%7B9ebd08a9-7886-4b2d-a1c4-a131e7096bf8%7D/PARKINSONSDISEASE\\_EN.PDF](http://www.parkinson.ca/atf/cf/%7B9ebd08a9-7886-4b2d-a1c4-a131e7096bf8%7D/PARKINSONSDISEASE_EN.PDF)
- Parkinson Study Group. (2004). Levodopa and the progression of Parkinson's disease. *New England Journal of Medicine*, 351(24), 2498-2508.
- Parkinson, J. (2002). An essay on the shaking palsy. *The Journal of Neuropsychiatry and Clinical Neurosciences*, 14(2), 223-236.
- Perese, D. A., Ulman, J., Viola, J., Ewing, S. E., & Bankiewicz, K. S. (1989). A 6-hydroxydopamine-induced selective parkinsonian rat model. *Brain Research*, 494(2), 285-293.
- Poewe, W. (2008). Non-motor symptoms in Parkinson's disease. *European Journal of Neurology*, 15(s1), 14-20.
- Polymeropoulos, M. H., Lavedan, C., Leroy, E., Ide, S. E., Dehejia, A., Dutra, A., ... & Stenroos, E. S. (1997). Mutation in the  $\alpha$ -synuclein gene identified in families with Parkinson's disease. *Science*, 276(5321), 2045-2047.
- Porter, C. C., Totaro, J. A., & Stone, C. A. (1963). Effect of 6-hydroxydopamine and some other compounds on the concentration of norepinephrine in the hearts of mice. *Journal of Pharmacology and Experimental Therapeutics*, 140(3), 308-316.
- Rahman, M. K., Toshiharu, N., & Takeshi, K. (1981). Aromatic L-amino acid decarboxylase activity in central and peripheral tissues and serum of rats with L-DOPA and L-5-hydroxytryptophan as substrates. *Biochemical Pharmacology*, 30(6), 645-649.

- Ramonet, D., Daher, J. P. L., Lin, B. M., Stafa, K., Kim, J., Banerjee, R., ... & Liu, Y. (2011). Dopaminergic neuronal loss, reduced neurite complexity and autophagic abnormalities in transgenic mice expressing G2019S mutant LRRK2. *PloS One*, *6*(4), e18568.
- Rascol, O., Brooks, D. J., Korczyn, A. D., De Deyn, P. P., Clarke, C. E., & Lang, A. E. (2000). A five-year study of the incidence of dyskinesia in patients with early Parkinson's disease who were treated with ropinirole or levodopa. *New England Journal of Medicine*, *342*(20), 1484-1491.
- Rodriguez, M. C., Obeso, J. A., & Olanow, C. W. (1998). Subthalamic nucleus-mediated excitotoxicity in parkinson's disease: A target for neuroprotection. *Annals of Neurology*, *44*(S1).
- Rossetto, O., & Montecucco, C. (2008). Presynaptic neurotoxins with enzymatic activities. In *Pharmacology of Neurotransmitter Release* (pp. 129-170). Springer Berlin Heidelberg.
- Sakaguchi, G. (1982). Clostridium botulinum toxins. *Pharmacology & Therapeutics*, *19*(2), 165-194.
- Samotus, O., Rahimi, F., Lee, J., & Jog, M. (2016). Functional Ability Improved in Essential Tremor by IncobotulinumtoxinA Injections Using Kinematically Determined Biomechanical Patterns—A New Future. *PloS one*, *11*(4), e0153739
- Sanchez-Prieto, J., Sihra, T. S., Evans, D., Ashton, A., Dolly, J. O., & Nicholls, D. G. (1987). Botulinum toxin A blocks glutamate exocytosis from guinea-pig cerebral cortical synaptosomes. *The FEBS Journal*, *165*(3), 675-681.
- Schiavo, G., Matteoli, M., & Montecucco, C. (2000). Neurotoxins affecting neuroexocytosis. *Physiological Reviews*, *80*(2), 717-766.
- Schiavo, G., Santucci, A., Dasgupta, B. R., Mehta, P. P., Jontes, J., Benfenati, F., ... & Montecucco, C. (1993). Botulinum neurotoxins serotypes A and E cleave SNAP-25 at distinct COOH-terminal peptide bonds. *FEBS Letters*, *335*(1), 99-103.

- Schober, A. (2004). Classic toxin-induced animal models of Parkinson's disease: 6-OHDA and MPTP. *Cell and Tissue Research*, 318(1), 215-224.
- Schultz, W. (2002). Getting formal with dopamine and reward. *Neuron*, 36(2), 241-263.
- Senoh, S., & Witkop, B. (1959). Non-enzymatic Conversions of Dopamine to Norepinephrine and Trihydroxyphenethylamines<sup>1</sup>. *Journal of the American Chemical Society*, 81(23), 6222-6231.
- Sherer, T. B., Kim, J. H., Betarbet, R., & Greenamyre, J. T. (2003). Subcutaneous rotenone exposure causes highly selective dopaminergic degeneration and  $\alpha$ -synuclein aggregation. *Experimental Neurology*, 179(1), 9-16.
- Shi, L. H., Luo, F., Woodward, D. J., & Chang, J. Y. (2006). Basal ganglia neural responses during behaviorally effective deep brain stimulation of the subthalamic nucleus in rats performing a treadmill locomotion test. *Synapse*, 59(7), 445-457.
- Shiosaka, S., Tohyama, M., Takagi, H., Takahashi, Y., Saitoh, Y., Sakumoto, T., ... & Shimizu, N. (1980). Ascending and descending components of the medial forebrain bundle in the rat as demonstrated by the horseradish peroxidase-blue reaction. *Experimental Brain Research*, 39(4), 377-388.
- Shiraga, H., Pfeiffer, R. F., & Ebadi, M. (1993). The effects of 6-hydroxydopamine and oxidative stress on the level of brain metallothionein. *Neurochemistry International*, 23(6), 561-566.
- Simon-Sanchez, J., Schulte, C., Bras, J. M., Sharma, M., Gibbs, J. R., Berg, D., ... & Krüger, R. (2009). Genome-wide association study reveals genetic risk underlying Parkinson's disease. *Nature Genetics*, 41(12), 1308-1312.
- Simpson, L. L. (1981). The origin, structure, and pharmacological activity of botulinum toxin. *Pharmacological Reviews*, 33(3), 155-188.
- Simpson, L. L. (2004). Identification of the major steps in botulinum toxin action. *Annual Review of Pharmacology and Toxicology*, 44, 167-193.

- Sofuwa, O., Nieuwboer, A., Desloovere, K., Willems, A. M., Chavret, F., & Jonkers, I. (2005). Quantitative gait analysis in Parkinson's disease: comparison with a healthy control group. *Archives of Physical Medicine and Rehabilitation*, 86(5), 1007-1013.
- Spillantini, M. G., Schmidt, M. L., Lee, V. M. Y., Trojanowski, J. Q., Jakes, R., & Goedert, M. (1997).  $\alpha$ -Synuclein in Lewy bodies. *Nature*, 388(6645), 839-840.
- Storch, A., Ludolph, A. C., & Schwarz, J. (2004). Dopamine transporter: involvement in selective dopaminergic neurotoxicity and degeneration. *Journal of Neural Transmission*, 111(10), 1267-1286.
- Takakusaki, K. (2017). Functional neuroanatomy for posture and gait control. *Journal of movement disorders*, 10(1), 1.
- Takakusaki, K., Tomita, N., & Yano, M. (2008). Substrates for normal gait and pathophysiology of gait disturbances with respect to the basal ganglia dysfunction. *Journal of neurology*, 255(4), 19-29.
- Tanner, C. M., Kamel, F., Ross, G. W., Hoppin, J. A., Goldman, S. M., Korell, M., ... & Comyns, K. (2011). Rotenone, paraquat, and Parkinson's disease. *Environmental Health Perspectives*, 119(6), 866.
- Tillerson, J. L., Cohen, A. D., Philhower, J., Miller, G. W., Zigmond, M. J., & Schallert, T. (2001). Forced limb-use effects on the behavioral and neurochemical effects of 6-hydroxydopamine. *Journal of Neuroscience*, 21(12), 4427-4435.
- Tipton, K. F., & Singer, T. P. (1993). Advances in our understanding of the mechanisms of the neurotoxicity of MPTP and related compounds. *Journal of Neurochemistry*, 61(4), 1191-1206.
- Tong, Y., Pisani, A., Martella, G., Karouani, M., Yamaguchi, H., Pothos, E. N., & Shen, J. (2009). R1441C mutation in LRRK2 impairs dopaminergic neurotransmission in mice. *Proceedings of the National Academy of Sciences*, 106(34), 14622-14627.

- Torres, E. M., & Dunnett, S. B. (2012). 6-OHDA lesion models of Parkinson's disease in the rat. *Animal Models of Movement Disorders: Volume I*, 267-279.
- Ungerstedt, U. (1968). 6-Hydroxy-dopamine induced degeneration of central monoamine neurons. *European Journal of Pharmacology*, 5(1), 107-110.
- Ungerstedt, U. (1971). Postsynaptic supersensitivity after 6-hydroxy-dopamine induced degeneration of the nigro-striatal dopamine system. *Acta Physiologica*, 82(S367), 69-93.
- Van der Putten, H., Wiederhold, K. H., Probst, A., Barbieri, S., Mistl, C., Danner, S., ... & Lin, S. (2000). Neuropathology in mice expressing human  $\alpha$ -synuclein. *Journal of Neuroscience*, 20(16), 6021-6029.
- Vandeputte, C., Taymans, J. M., Casteels, C., Coun, F., Ni, Y., Van Laere, K., & Baekelandt, V. (2010). Automated quantitative gait analysis in animal models of movement disorders. *BMC Neuroscience*, 11(1), 92.
- Verderio, C., Grumelli, C., Raiteri, L., Coco, S., Paluzzi, S., Caccin, P., ... & Matteoli, M. (2007). Traffic of botulinum toxins A and E in excitatory and inhibitory neurons. *Traffic*, 8(2), 142-153.
- Verderio, C., Pozzi, D., Pravettoni, E., Inverardi, F., Schenk, U., Coco, S., ... & Matteoli, M. (2004). SNAP-25 modulation of calcium dynamics underlies differences in GABAergic and glutamatergic responsiveness to depolarization. *Neuron*, 41(4), 599-610.
- Verderio, C., Rossetto, O., Grumelli, C., Frassoni, C., Montecucco, C., & Matteoli, M. (2006). Entering neurons: botulinum toxins and synaptic vesicle recycling. *EMBO Reports*, 7(10), 995-999.
- Verghese, J., Holtzer, R., Lipton, R. B., & Wang, C. (2009). Quantitative gait markers and incident fall risk in older adults. *The Journals of Gerontology: Series A*, 64(8), 896-901.

- Vlamings, R., Visser-Vandewalle, V., Koopmans, G., Joosten, E. A. J., Kozan, R., Kaplan, S., ... & Temel, Y. (2007). High frequency stimulation of the subthalamic nucleus improves speed of locomotion but impairs forelimb movement in Parkinsonian rats. *Neuroscience*, *148*(3), 815-823.
- Westin, J. E., Janssen, M. L. F., Sager, T. N., & Temel, Y. (2012). Automated gait analysis in bilateral Parkinsonian rats and the role of L-DOPA therapy. *Behavioural Brain Research*, *226*(2), 519-528.
- Whetten-Goldstein, K., Sloan, F., Kulas, E., Cutson, T., & Schenkman, M. (1997). The burden of Parkinson's disease on society, family, and the individual. *Journal of the American Geriatrics Society*, *45*(7), 844-849.
- Williams, D. R., Watt, H. C., & Lees, A. J. (2006). Predictors of falls and fractures in bradykinetic rigid syndromes: a retrospective study. *Journal of Neurology, Neurosurgery & Psychiatry*, *77*(4), 468-473.
- Woolf, N. J., & Butcher, L. L. (1986). Cholinergic systems in the rat brain: III. Projections from the pontomesencephalic tegmentum to the thalamus, tectum, basal ganglia, and basal forebrain. *Brain research bulletin*, *16*(5), 603-637.
- Wree, A., Mix, E., Hawlitschka, A., Antipova, V., Witt, M., Schmitt, O., & Benecke, R. (2011). Intra-striatal botulinum toxin abolishes pathologic rotational behaviour and induces axonal varicosities in the 6-OHDA rat model of Parkinson's disease. *Neurobiology of Disease*, *41*(2), 291-298.
- Wu, Y. N., & Johnson, S. W. (2011). Dopamine oxidation facilitates rotenone-dependent potentiation of N-methyl-d-aspartate currents in rat substantia nigra dopamine neurons. *Neuroscience*, *195*, 138-144.
- Yuan, H., Sarre, S., Ebinger, G., & Michotte, Y. (2005). Histological, behavioural and neurochemical evaluation of medial forebrain bundle and striatal 6-OHDA lesions as rat models of Parkinson's disease. *Journal of Neuroscience Methods*, *144*(1), 35-45.

- Yung, K. K. L., Bolam, J. P., Smith, A. D., Hersch, S. M., Ciliax, B. J., & Levey, A. I. (1995). Immunocytochemical localization of D 1 and D 2 dopamine receptors in the basal ganglia of the rat: light and electron microscopy. *Neuroscience*, *65*(3), 709-730.
- Zakin, E., & Simpson, D. (2017). Botulinum Toxin in Management of Limb Tremor. *Toxins*, *9*(11), 365.
- Zhou, M., Zhang, W., Chang, J., Wang, J., Zheng, W., Yang, Y., ... & Xiao, H. (2015). Gait analysis in three different 6-hydroxydopamine rat models of Parkinson's disease. *Neuroscience Letters*, *584*, 184-189.
- Zibetti, M., Merola, A., Rizzi, L., Ricchi, V., Angrisano, S., Azzaro, C., ... & Rizzone, M. (2011). Beyond nine years of continuous subthalamic nucleus deep brain stimulation in Parkinson's disease. *Movement Disorders*, *26*(13), 2327-2334.
- Zigmond, M. J., & Stricker, E. M. (1973). Recovery of feeding and drinking by rats after intraventricular 6-hydroxydopamine or lateral hypothalamic lesions. *Science*, *182*(4113), 717-720.

# Appendices

## Appendix 1 – Animal Use Protocol Approval



**AUP Number:** 2015-087

**PI Name:** Jog, Mandar S

**AUP Title:** Understanding The Effects Of Botulinum Toxin On The Basal Ganglia In A Rodent Model Of Parkinson Disease By Behavioural Studies And Multi-neuronal Recordings

**Approval Date:** 03/04/2016

**Official Notice of Animal Use Subcommittee (AUS) Approval:** Your new Animal Use Protocol (AUP) entitled "Understanding The Effects Of Botulinum Toxin On The Basal Ganglia In A Rodent Model Of Parkinson Disease By Behavioural Studies And Multi-neuronal Recordings" has been APPROVED by the Animal Use Subcommittee of the University Council on Animal Care. This approval, although valid for four years, and is subject to annual Protocol Renewal.2015-087::1

1. This AUP number must be indicated when ordering animals for this project.
2. Animals for other projects may not be ordered under this AUP number.
3. Purchases of animals other than through this system must be cleared through the ACVS office. Health certificates will be required.

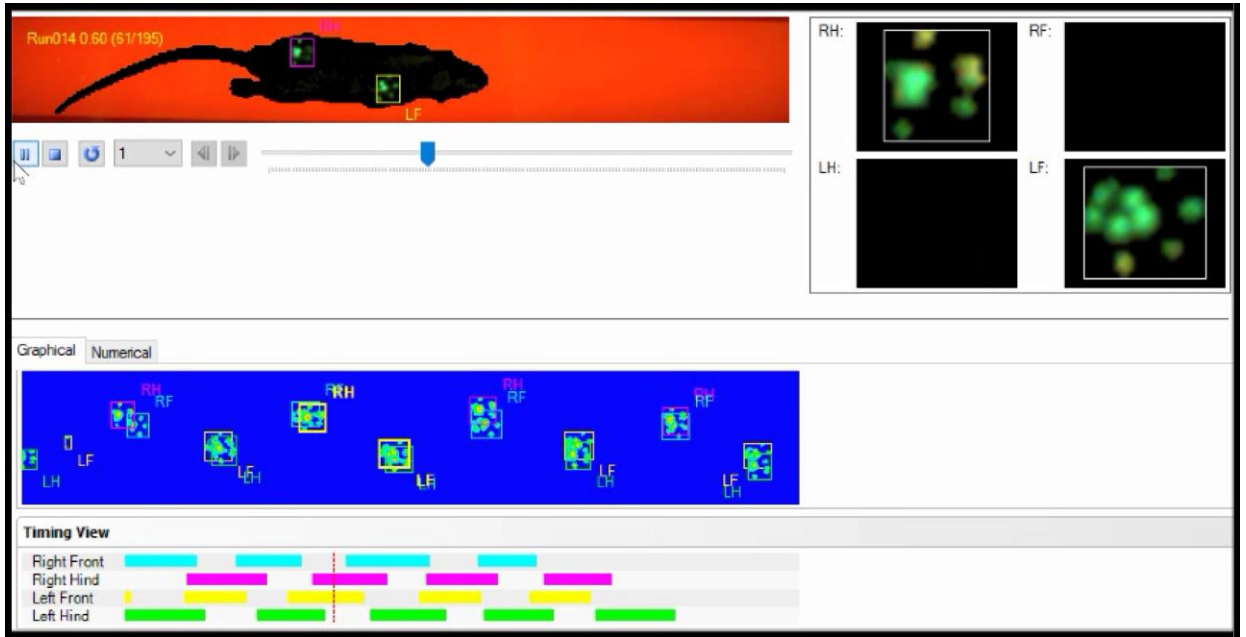
The holder of this Animal Use Protocol is responsible to ensure that all associated safety components (biosafety, radiation safety, general laboratory safety) comply with institutional safety standards and have received all necessary approvals. Please consult directly with your institutional safety officers.

Submitted by: Copeman, Laura  
on behalf of the Animal Use Subcommittee  
University Council on Animal Care

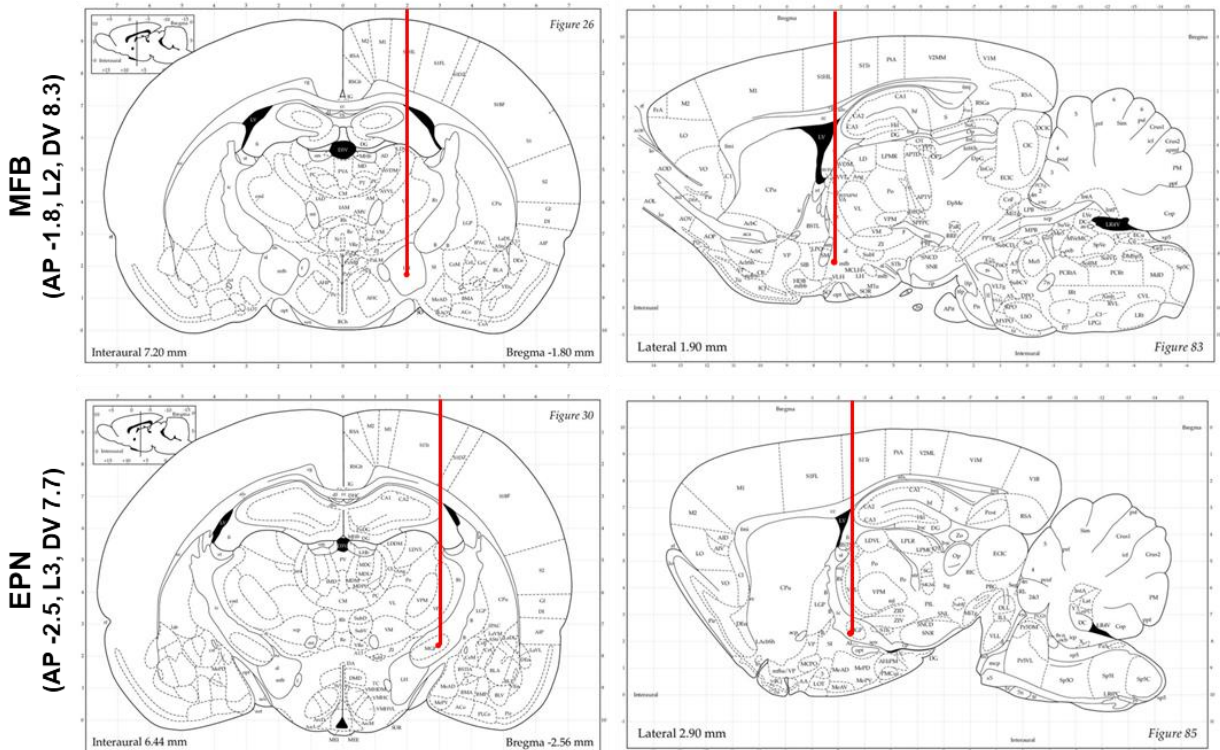
*The University of Western Ontario*  
Animal Use Subcommittee / University Council on Animal Care  
Health Sciences Centre, • London, Ontario • CANADA – N6A 5C1  
PH: 519-661-2111 ext. 86768 • FL 519-661-2028  
Email: [auspc@uwo.ca](mailto:auspc@uwo.ca) • <http://www.uwo.ca/animal/website/>



Appendix 2 – Sample of Raw CatWalk Data



Appendix 3 – Stereotaxic Surgery Coordinates



## Curriculum Vitae

**Name:** Adrianna Tsang

**Post-secondary Education and Degrees:** McGill University  
Montreal, Quebec, Canada  
2010-2014 B.Sc.

**Honours and Awards:** Mitacs Graduate Research Internship  
2016-2017

**Related Work Experience**

Teaching Assistant  
Western University  
Physiology 1021  
2015-2017

Teaching Assistant  
McGill University  
ANAT 214  
2013-2014